An evaluation of geographical information systems for surface water studies in the Badia region of Jordan

Rafe S. Abu Ashour

AN EVALUATION OF GEOGRAPHICAL INFORMATION SYSTEMS FOR SURFACE WATER STUDIES IN THE BADIA REGION OF JORDAN

A thesis presented for the degree of
Master of Science

By

Rafe S. Abu Ashour

University of Durham

Department of Geography

March, 1998

An evaluation of Geographical Information Systems for surface water studies in the Badia region of Jordan

Rafe S. Abu Ashour

Abstract

Three applications of Geographical Information Systems for surface water studies in the Badia region of Jordan are presented. In the first application, a Digital Elevation Model (DEM) of the study area was generated from the available contour maps. The channel drainage network was enforced into the created DEM to ensure accurate emplacement of the extracted drainage network. The channel drainage network was extracted from the DEM at a threshold value of 250 pixels. At this threshold, the drainage density of the extracted channel network is equivalent to the wadis network on the topographic maps

In the second application, a hydrologically-oriented GIS database was developed. The database aimed to provide detailed description of the watershed characteristics and the hydrological processes relevant to surface water studies. A menu-driven application was built on the database to extract and analyse the database information at the sub-watershed level.

The third application involved building a spatial model for generating surface runoff hydrographs from the rainfall data. The model applies GIS data structure and the raster processing techniques to simulate the rainfall-excess generation and flow routing processes. The distributed structure of the model allows for representing the hydrological processes and modelling the watershed response at the level of details that fits the resolution of the available data.

Statement of copyright

Declaration

The work contained in this thesis has not been submitted elsewhere for any other degree or qualification and that unless otherwise referenced is the authors own work.

Acknowledgement

I wish to express my sincere appreciation and thanks to my supervisor, Dr. Danny Donoghue, for his help, constant guidance, patience and encouragement during the writing of this thesis. My thanks also go to Dr Roderic Dutton for all the help he provided to me during my study.

I wish particularly to thank the British Council for support and assistance during my study programme. Thanks also goes to all the friends in the University of Durham who offered help and encouragement when needed. In particular, I wish to thank Dr Salem al-Oun, Mohammad Fattah, Dr. Musa Abu Dalbuh, Dr. Mohammad Shra'a Rida al-Adamat. Shahin Serhan and Raed Al tubaini.

I would like to thank the staff of the University of Durham, particularly the staff of the ITS, for their constant help and advice.

In Jordan, special thanks are extended to the Director General of the Royal Jordanian Geographic Centre for his support and encouragement, and the staff of the Department of Modern Applications for their help with the digital maps used in the study. Thanks also go to Mr. Mohammad Shahbaz, the Director of the Jordan Badia Research and Development Programme, for his support and assistance during the field work.

Thanks also go to my brother, Dr Jamal Ashour, for the academic help he provided to me during my field study. I wish also to thank Dr. fayez abdulla from the Jordan University of Science and Technology, Dr. Rakad Ayed from the Ministry of Water and Irrigation, Dr Radwan Wishah from the University of Jordan and my colleagues, Omar Malkawi and Salim Hussain for their help with technical notes or data.

Last but not least I would like to express my gratitude to my wife, my children, my brother Jihad, and my family in Jordan for all the support they provided to me during my study.

Table of contents

CHAPTER 5

DESCRIPTION OF WADI RAJIL

HYDROLOGICAL DATABASE

CHAPTER 7

RUNNING THE MODEL AND

DISCUSSION OF RESULTS

CHAPTER 8

CONCLUSIONS AND RECOMMENDATIONS

List of tables

List of figures

CHAPTER 1

INTRODUCTION

1.1 Background

The scarcity of water in Jordan places a strong emphasis on the need for monitoring and management of the resources. With the rapid depletion of groundwater resources, surface water flood flows in the winter appear to be a potential source of water that could be developed. The National Water Master Plan of Jordan (Agrar, 1977) has estimated that 50 Mm^3 (million cubic metres) of winter flow in the eastern ephemeral desert wadis runs unused into the many closed *qa'* areas where it remains until it evaporates. This has justified the need to construct desert dams at a number of selected sites as water harvesting schemes that can be used for irrigation and to satisfy the needs of local people (Hydrosult, 1990).

Since the emergence of the Jordan Badia Research and Development Programme (JBRD) in 1992, surface water studies have been recognised as a priority research topic. The JBRD report on the priority research themes for the period 1996-1998 has identified several surface water studies aiming at "maximising the available water resources by optimising use of surface flows which, today, are mostly lost as evaporation from the *qa'*s" (JBRD, 1995).

Information regarding wadi flows is essential for the design and management of any project based on these flows. This information is usually derived from long term flow records, or, when such records are not available, from empirical approaches based on rainfall-runoff

relationships. Since no wadi gauges exist in the study area, Jolly (1996) has recommended establishing a short term and long term surface water monitoring programme to provide data for water resources study. The programme consists of a number of wadi stage recorders and rainfall recorders and totalizers. Runoff simulation in the area has been carried out using the SCS curve number method (Jolly, 1996). This approach does not fully consider the specific characteristics of the hydrological processes that are active in the watershed area. To improve the estimates of the empirical method Jolly (1996) suggests studying the active hydrological processes at the micro-catchment level. On the other hand, Wheater *et al* (1995) stated the need to build local hydrological models for arid catchments that consider the specific conditions of the catchment and maximise the use of the available data.

The specific characteristics of arid catchments are the spatial and temporal variability of rainfall and surface processes (Wheater *et al*, 1995). Therefore, it is important to collect as much information as possible about catchment area characteristics to help build high quality hydrological models. This is where geographical information systems (GIS) help to integrate spatial data sets that describe the distributed characteristics of the catchment processes.

1.2 GIS applications in hydrology

A comprehensive and widely accepted definition of the Geographical Information System (GIS) is given by Burrough (1990) as "a powerful set of tools for collecting, storing, retrieving, and displaying spatial data from the real world for a particular purpose". Over the last twenty years GIS has emerged as a powerful computer system for handling and analysing spatial data. GIS capabilities have found many applications especially in the

resources management and environment-related studies. The involvement of GIS in hydrology has developed from the traditional use of GIS systems for storing, managing and visualising distributed catchment parameters and hydrological processes (Kemp, 1993) to "rethinking hydrological modelling in spatial terms so that better GIS-based hydrological models can be created" (Maidment, 1993). Between these two views, others have suggested that GIS can serve as an extension to distributed parameter hydrological models for data preparation and presentation (Grayson *et al*, 1993), or for multi-layer overlay processing to determine the hydrologically similar units (Schultz, 1993).

For the Badia area, the integration of DEM and hydrological data in a GIS database has been identified as a priority research topic (JBRD, 1995). Other useful applications of GIS and DEM for hydrological studies in the area include defining the hydrologically similar units (Dr. R. Wishah, personal communication, 1997) and extending the digitised drainage lines over the mud pan areas (Francis, 1995). The present research will look at the use of GIS management and analysis tools to build a spatial hydrological model for generating hydrographs from the input rainfall data.

1.3 Research objectives

The main goal of the research is to apply GIS techniques for the study of surface water in the Jordan Badia region, in particular the Wadi Rajil watershed area. The focus is first on the digital description of the hydrological processes and the watershed characteristics relevant to surface water applications and then on the development of a spatial hydrological model that fits the available data.

The specific objectives of this research are:

1. To build a hydrologically correct digital elevation model (DEM) from the available contour line maps. The DEM should be free of sinks to enable extraction of hydrological information.
2. To use the DEM and GIS techniques to extract the channel drainage network to solve the problem of disconnected drainage links through the *qa'* areas that appear on the topographic maps. The drainage density of the extracted network should be equivalent to the density of the topographic wadi network.
3. To use digital techniques of watershed delineation to define the sub-watersheds in a scaled manner.
4. To define, collect, and evaluate the available data on the hydrological processes known to be active in the area. The collected data are to be stored and managed in a GIS database.
5. To develop a distributed hydrological model that simulates the runoff generation and transport on the watershed area. The model will be based on the available data and will make use of the ARC/INFO data structures and surface water analysis functions.
6. Since no flow records are available for the study area, the model performance will be tested using simulated events. The same events will be used to perform sensitivity analysis to study the influence of the model parameters on the watershed hydrological response.

1.4 Thesis structure

Chapter 2 provides a description of the study area and the physical environment relevant to surface water hydrology. The spatial and temporal variations of rainfall, evaporation and infiltration are described in chapter 3. Section (3-6) presents a quantitative assessment of

the effect of transmission losses on the transported flows. The runoff characteristics and previous works on the estimation of runoff using empirical approaches are described in section (3-7).

Chapter 4 is concerned with the creation of a digital elevation model and discussion of the methodology to extract the channel drainage network and to delineate sub-watersheds. Chapter 5 provides a description of the structure of a GIS database for hydrological applications as well as the data structures and the automation processes used to establish the database layers.

The main subject in chapters 6 and 7 is hydrological modelling. A general description of the components of hydrological models as well as brief descriptions of some of the widely known hydrological models are given in chapter 6. In section (6-5) the focus is put on a proposed spatial hydrological model for the study area. A description of the structure of the model and its components is given. The emphasis in chapter 7 is on the computer formulation of the model processes. The model performance is investigated in section (7-3). The section involves a sensitivity analysis of the influence of selected model parameters on the overall hydrological response of the watershed.

Finally, the research conclusions and recommendations are given in chapter 8.

CHAPTER 2

DESCRIPTION OF THE STUDY AREA

2.1 Introduction

The physical environment of the watershed area plays an important role in defining its response to the active hydrological processes within it. The topographical, geomorphological, geological and soil factors exert controlling effects on most of the hydrological processes. The topography, for instance, defines the shape and structure of the drainage network and thus controls the surface flow patterns over the catchment. The soil hydraulic properties are the key factors that determine the infiltration characteristics and the subsurface flows. On the other hand, the geological factors like the hydraulic properties of the bedrock (Viessman *et al*, 1989) and the distribution of the subsurface lineaments (Noble, 1994) have significant effects on the recharge to the groundwater aquifers.

This chapter provides brief description of the physical environment in the Jordan Badia area. The description provided here is based on the available surveys and maps of the area.

2.2 Location

The Jordan Badia Research and Development Programme area occupies an area of 11,110 km^2 that covers most of the basalt field in the eastern part of Jordan. The area borders Syria and Saudi Arabia and comprises parts of the three major drainage basins in the area: the Azraq, Hamad, and Sirhan basins (figure 2-1). The population of the area is about

15,000 people living mainly around the foothill of Jabal al-Arab where the annual average of rainfall exceeds 150 mm. Figure (2-2) shows a general locational map of the area. The focus in this study will be on the watershed area of Wadi Rajil. The area of the watershed in Jordan is 2,812 km^2. The upper northern part of the watershed extends into the Syrian territories over an area of about 200 km^2. The watershed drains most of the ephemeral wadis in the central and northern parts of the Badia area. Wadi Rajil is the main wadi in the watershed with a length of about 150 km. The Wadi Rajil watershed occupies about 30% of the JBRD area and covers most of the central and northern parts of the Badia Programme area (figure 2-1).

2.3 Soil

This section is mainly derived from the reports of level 1 of the National Soil Map and Land Use Project conducted by Hunting Technical Services Ltd in association with the Ministry of Agriculture of Jordan. The project aimed to establish an accurate soil database based on interpretation of aerial photographs and satellite images and complemented by field observations. The project activities were carried out at three levels as follows:

1- Level 1 included a broad reconnaissance of the soils of Jordan based on analysis of Landsat images and aerial photographs. The survey was complemented by field observations at an overall density of one observation every 7.6 km^2. The level 1 survey resulted in grouping broad soil types into mapping units which were depicted on 1/250,000 scale maps covering the whole country.

2- Level 2 consisted of semi-detailed surveying of 5,000 km^2 of lands identified from the level 1 surveying as having some agricultural potential. The level 2 survey was based

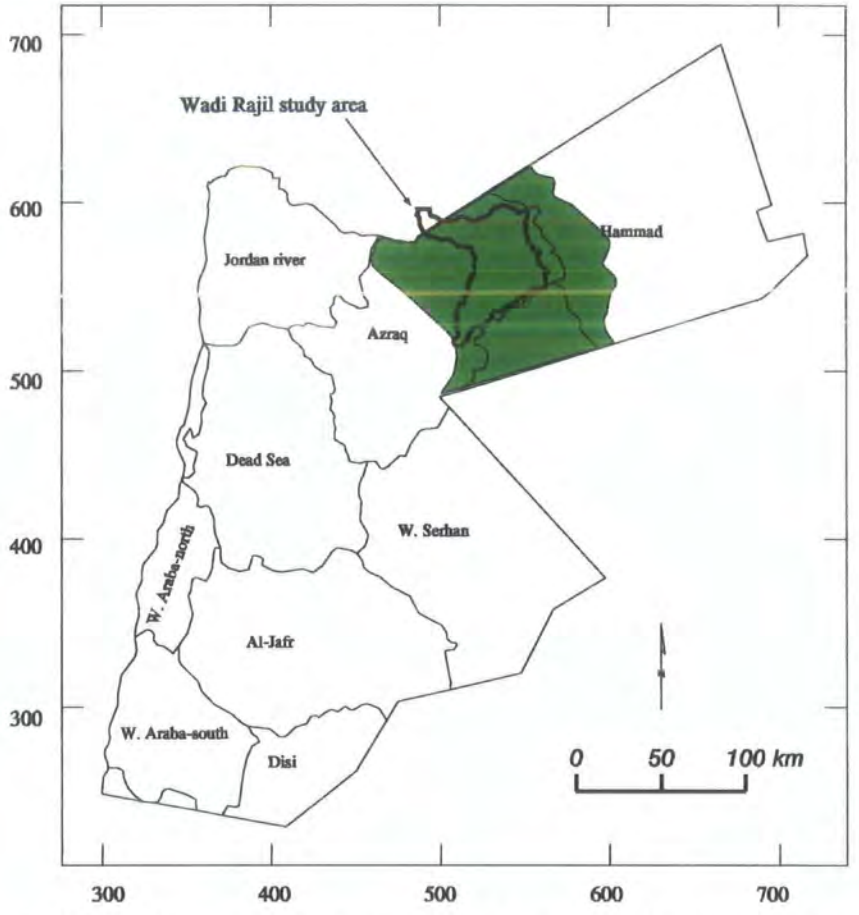

Figure (2 - 1) Location of the Badia Programme area and the major drainage basins

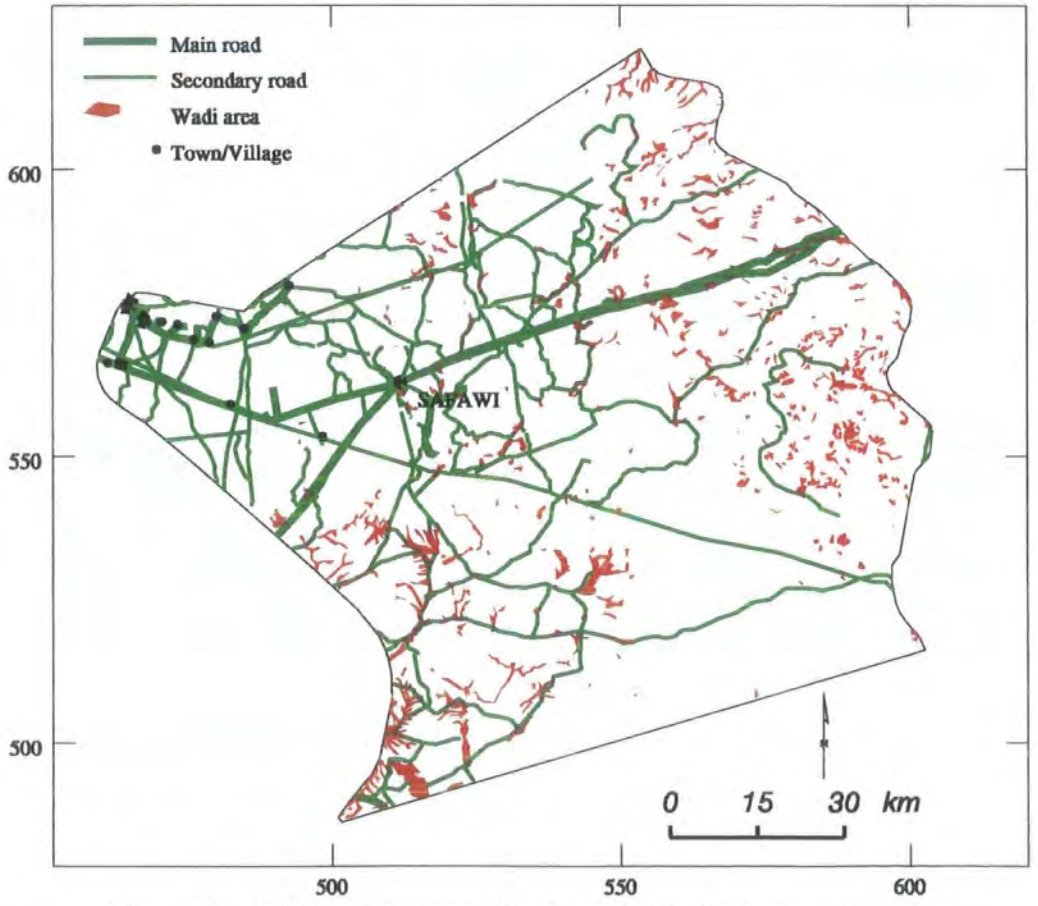

Figure (2 - 2) General locational map of the Badia Programme area

on analysis of Landsat TM images and field surveying at an overall density of 3.5 observation every km^2.

3. Level 3 involved detailed land suitability mapping for some 1000 km^2 of priority areas.

All soil maps and observations were geo-coded in SPANS-GIS system.

In the frame of this project the soil of the whole Badia area was surveyed at level 1. At level 2 only 613 km^2 of the area including qa' Shubayka, qa' Buqayawi and the Wadi Rajil course were surveyed.

2.3.1 Soil genesis and classification

The surface soil in the majority of the area is of depositional origin. This tends to be a general characteristic of soils of arid lands where sedimentation processes of aeolian, alluvial, and colluvial types are dominant (Cooke *et al*, 1993). Residual soils on rocks occur only in areas subject to active erosion such as steep slopes and at the top of hills and mountains.

The dominant soils of the area are classified in the USDA system as either Aridisols or Entisols. These are mineral soils of low organic matter content and occur typically in arid zones. Aridisols subsurface horizons are enriched with calcium carbonates or gypsum. Soils enriched with gypsum develop gypsic horizons and are classified in the USDA system as Gypsiorthids. When enriched with calcium carbonates they usually develop calcic horizons and are classified as Calciorthids. If the amounts of calcium carbonate in the soil are not sufficient to develop calcic horizons the soil is classified as Camborthid.

Entisols are mineral soils that have no distinct pedogenic horizons within 1 metre of the soil surface (Foth, 1984). The major Entisols great groups identified in the area are Toriorthents and torrifluvents.

The broad reconnaissance surveying of the soils of Jordan conducted in the frame of the National Soil Map and Land Use Project has shown that soils from five great groups of the USDA's Soil Taxonomy classification were recognised in the area. Table (2-1) shows the groups and subgroups of soils in the area.

Table (2-1) The major soil orders, groups and subgroups.

Soil order	Great groups	Subgroups
Aridisols	Calciorthids	Xerochreptic Calciorthids
		Ustochreptic Calciorthids
		Typic Calciorthids
		Lithic Xerochreptic Calc.
	Camborthids	Lithic Camborthids
		Xeretic Camborthids
		Xerochreptic Camborthids
		Typic Camborthids
	Gyypsiorthids	Petrogypsic Gypsiorthids
		Cambic Gypsiorthids
		Typic Gypsiorthids
		Lithic Gypsiorthids
	Paleorthids	Xerochreptic Paleorthids
		Typic Paliorthids
Entisols	Torrifluvents	Xeric Torrifluvents
		Typic Torrifluvents
	Toriorthents	Lithic Xeric Torriorthents
		Lithic Torriorthents
		Xeric Torriorthens
		Typic Torriorthents

In a broad categorisation of landscape characteristics in terms of climate, land use, topography, hydrology, geology and geomorphology the whole country was divided into 18 regions. Each land region was further sub-divided into soil units of similar physiographic properties. Soil associations for each map unit were then described and depicted into soil maps of 1/250,000 (figure 2-3).

Two soil moisture regimes are recognised in the area. These are defined as follows;

-Aridic: moisture control section is dry in all parts more than half the time that the soil temperature is above 5° C at 50 cm depth, or the section is never moist in some or all parts for 90 consecutive days when soil temperature at 50 cm exceeds 8° C.

-Xeric-Aridic: moisture regime intermediate between Xeric and Aridic moisture regimes. The Xeric regime is defined as: moisture control section is moist in some part more than half the time the soil temperature is higher than 5° C, or is moist in some part for at least 90 consecutive days in six years out of ten when soil temperature is higher than 8° C.

The Aridic soil moisture regime prevails in the whole area except for the area situated at the foothills of Jabal al Arab (Jabal ed Druz) where the Xeric Aridic soil moisture regime dominates (fig 2-4). This area lies in the transitional zone between the arid soils to the east and the more fertile Mediterranean soils to the west.

In terms of soil temperature, the majority of the soils in the area belong to the Thermic soil temperature regime (fig 2-5). The average annual temperature of the soils of this regime ranges between 15°C and 22°C. Soils of the area around the Azraq basin are of the Hyper thermic soil temperature regime where the average annual temperature of the soil can exceed 22°C.

2.4 Geology (mainly based on the 1/50000 scale geologic maps, 1990)

Igneous rocks are the dominant rock types in the area. Basalt lava flows cover an area of 11,000 km^2 spreading over an area from the Syrian borders in the north to the Saudi Arabian borders in the south.

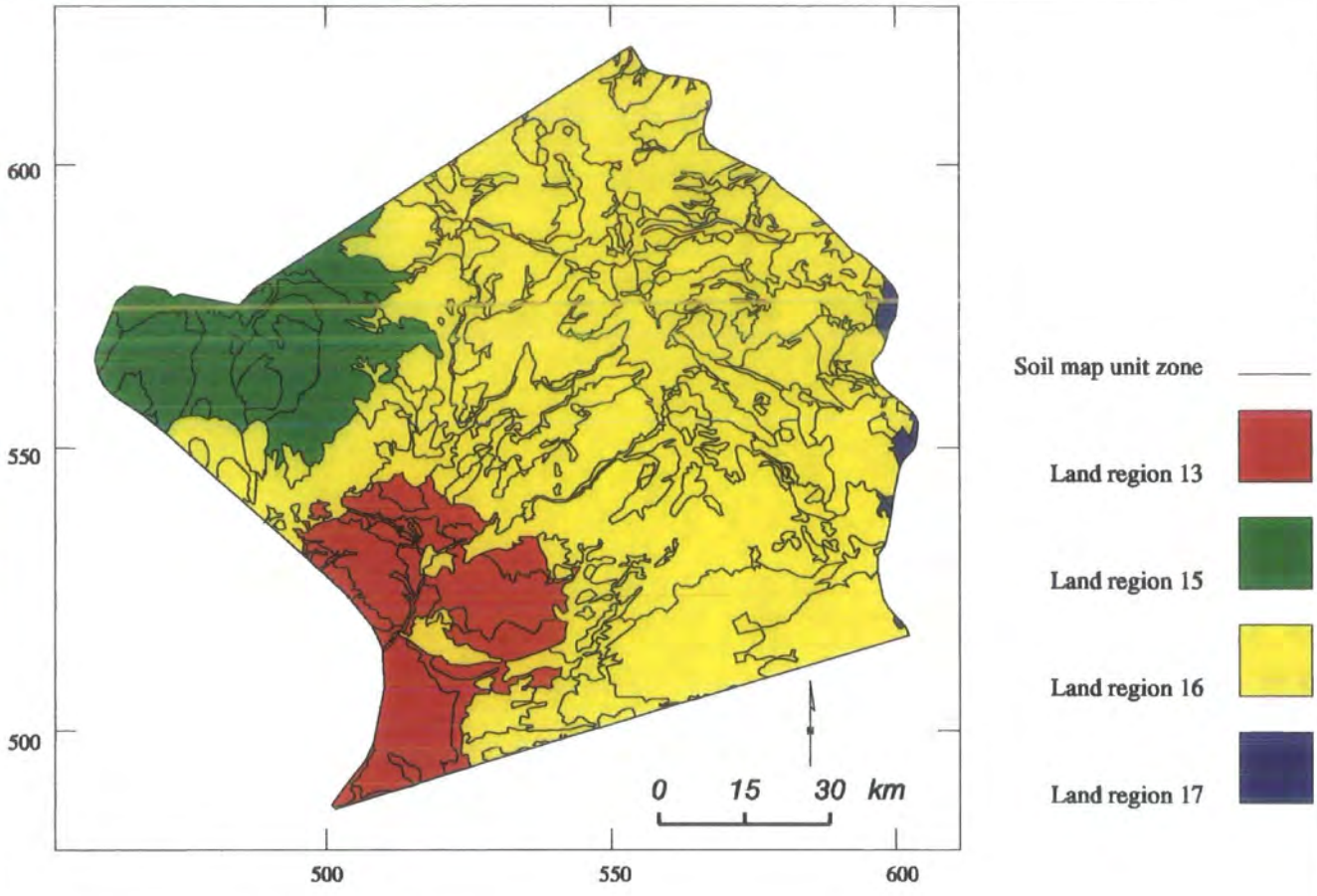

Figure (2 - 3) Soil map units and land regions
(Source: Soil maps,1/250,000 produced by Hunting Technical Services)

Figure (2 - 4) Soil moisture regimes
(Source: Hunting, 1993)

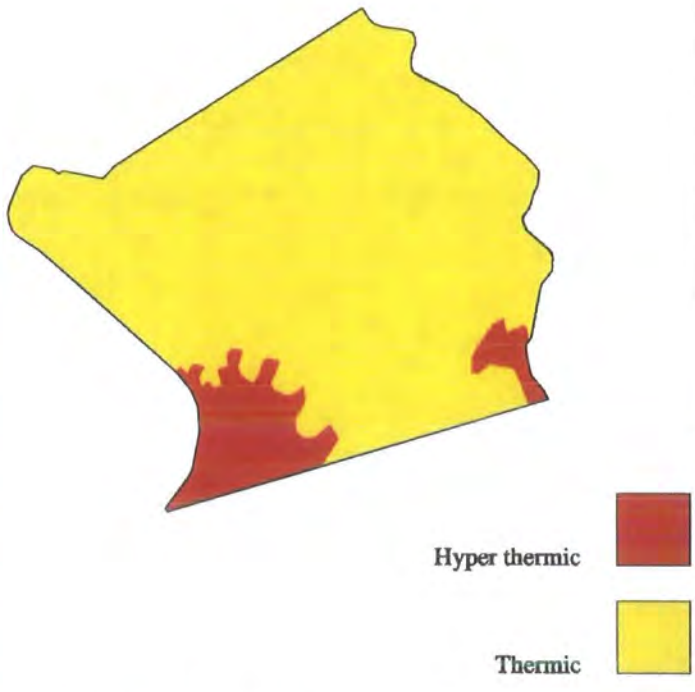

Figure (2-5) Soil temperature regimes
(Source: Hunting, 1993)

The basalts of the area originate from magmatic sources of the upper earth mantle. They are part of the Harrat Ash Sham basaltic super group of the alkali olivine basalt series belonging to the family of intraplate continental basalt.

The basalt outcrops in the area are of Neogene age. They are composed of the Miocene-Pliocene basalt plateau, the Pleistocene basalt lava flows, and the Holocene shield volcanics (Schaffer, 1995).

Plateau basalt and shield basalt are generated from fissure effusions from a system of dike feeders that have a NW-SE trending direction. Basaltic lava flows occur as wadi-filling lava flows around their point source feeders.

Only the youngest three basalt types outcrop in the area (Abed, 1982). Basalt generated from the oldest of these three emissions outcrop in the eastern and southern parts of the basalt plateau and in scattered places through the basalt of the middle and most abundant emission (fig 2-6). The Holocene basalt in the area, the basalt from the third emission, outcrop at the north east of the basalt field and run in a N-S direction (Hunting, 1993). Figure (2-7) shows the classification of the basalt groups and formations according to a geological-age scale.

The basalts are classified according to age and chemical and physical properties into five groups and twelve formations. Table (2-2) shows a brief description of these formations.

The bedrocks of the Southwest corner of the area are mainly composed of limestone of the Upper Cretaceous Belqa group. The rocks of this formation consist mainly of massive chalk layers interbedded by an alteration of thin layers of chert, chalk, porcellanite, and crystalline limestone.

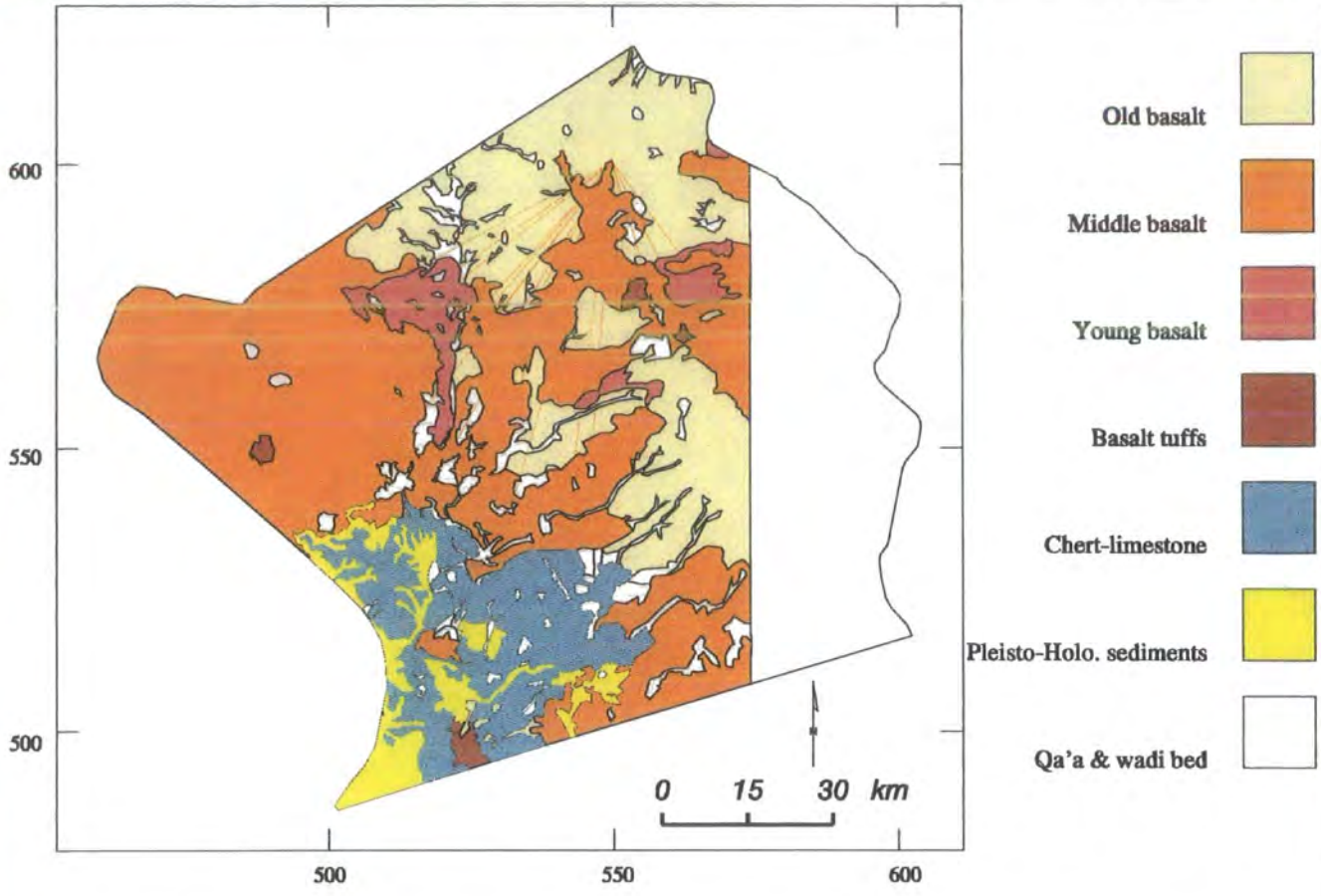

Figure (2 - 6) Generalised geology map (based on the geological map of Al-Azraq, scale 1/250,000)

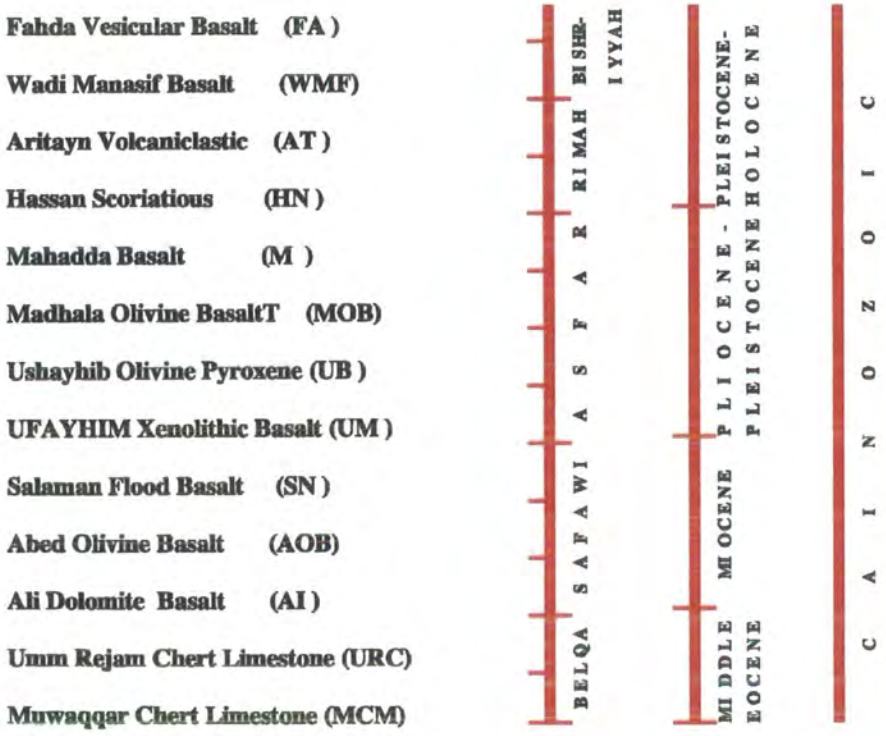

Figure (2 - 7) Geological ages of the basalt formations (based on the geological maps at scale 1/50,000)

Table (2-2) The basalt groups and formations

Group	Formation	Description
Safawi	Ali Doleritic Trachytic basalt (AI)	Massive flow, medium to coarse grained, rugged and hard.
	Abed Olivine basalt (AOB)	Generated from feeder dykes, medium to fine grained.
	Salaman Flood basalt (SN)	Small boulders on flat areas and black soil, darkish to redish brown.
Asfar	Ufayhim Xenolithic basalt (UM)	Erupted from Aritayn valcano, wadi-filling basalt, fine to very fine-grained.
	Ushayhib Olivine Pyroxene Pheric basalt(UB)	Generated from the central vent of Ushayhib shield volcano, dark grey to light grey, very fine grained.
	Hashemiyyah Aphanitic basalt (HAB)	Bluesh grey to medium grey, very fine grained.
	Madhala Olivine basalt (MOB)	Of central volcanism, dark brown to black, smooth, fine to medium grained.
	Mahadda (M)	Wadi-fill lava flows, dark brown, fine grained.
Rimah	Hassan Scoriatious basalt (HN)	Erupted from Hassan volcanic centre, composed of volcanic bombs and scoriatious blocks, very coarse grained agglomerates.
	Aritayn Volcaniclastic (AT)	Stratified fine-grained ash and bombs.
Bishriyyah	Wadi Manasif (WMF) & Fahda (FA)	Fresh and unweathered lava flow basalt, dark grey, fine grained, dense and hard basalt.

2.5 Geomorphology

The main surface features in the area are produced by volcanism. The major volcanic landforms are as follows:

1- The basalt plateau produced from fissure eruptions of basalt floods from the fault system dissecting the plateau in a NW-SE trending direction. The basalt plateau appears as a large undulating plain of low relief and gentle slopes of less than 5% in general and extends over large areas in the east and south of Safawi (region 5 in figure 2-8). Figure (2-9) shows a slope map generated from the DEM of the area. The stepped appearance of slopes results from the influence of the contours on the DEM. In fact, the interpolation process used to generate the DEM considers the source elevation data as fixed data and therefore, data points along the contour lines are not subject to the interpolation process.

2- Shield basalt areas resulted from eruptions of shield volcanoes that build up masses with gentle sloping sides and represent basalts of the last emissions (Schaffer, 1995). Shield basalts occur around their source feeders (regions 1 and 2 in figure 2-8).

3- Wadi filling lava flows, which appear in the wadis near the strato volcanoes in the central eastern part of the area (region 6 in figure 2-8). Volcanic cinder cones in this region form local relief with significant slopes.

The area is also characterised by the presence of many mud pans of different sizes. Mud pans (locally known as *Qa's*) are morphological depressions filled with alluvium clay rich sediments (Schaffer, 1995). They appear as internal drainage basins that do not have, in general, an outflow. Water drained into these basins remains until it evaporates or slowly infiltrates into the subsurface layers. Mud pans represent local barriers to the surface flow and create important discontinuities in the drainage system network. The general flow direction of the drainage network is from north to south and Southeast (Al-Homoud *et al*, 1992). However, flow directions are poorly identified in the flat areas of the basalt plateau where the wadis emerge into mud pan areas.

The drainage pattern is of radial type in general under the influence of local relief and slopes. In the Northwest hilly area the drainage pattern is of centrifugal type, a subtype of the radial pattern, where "the drainage area radiates outward from a central topographic height" (Vann, 1971, p 173). Desert pavement composed of basalt boulders of different sizes and different weathering conditions covers most of the area. The Southwest corner pavement is composed of small chert fragments (Al-Homoud *et al*, 1992).

As shown in the report on "Geomorphology and Physical Resources " by (Al-Homoud *et al*, 1992) 12 major geomorphologic zones were identified from interpretation of one Landsat TM scene of the area. The following brief description of the 10 regions within the Badia Programme area is derived from this report:

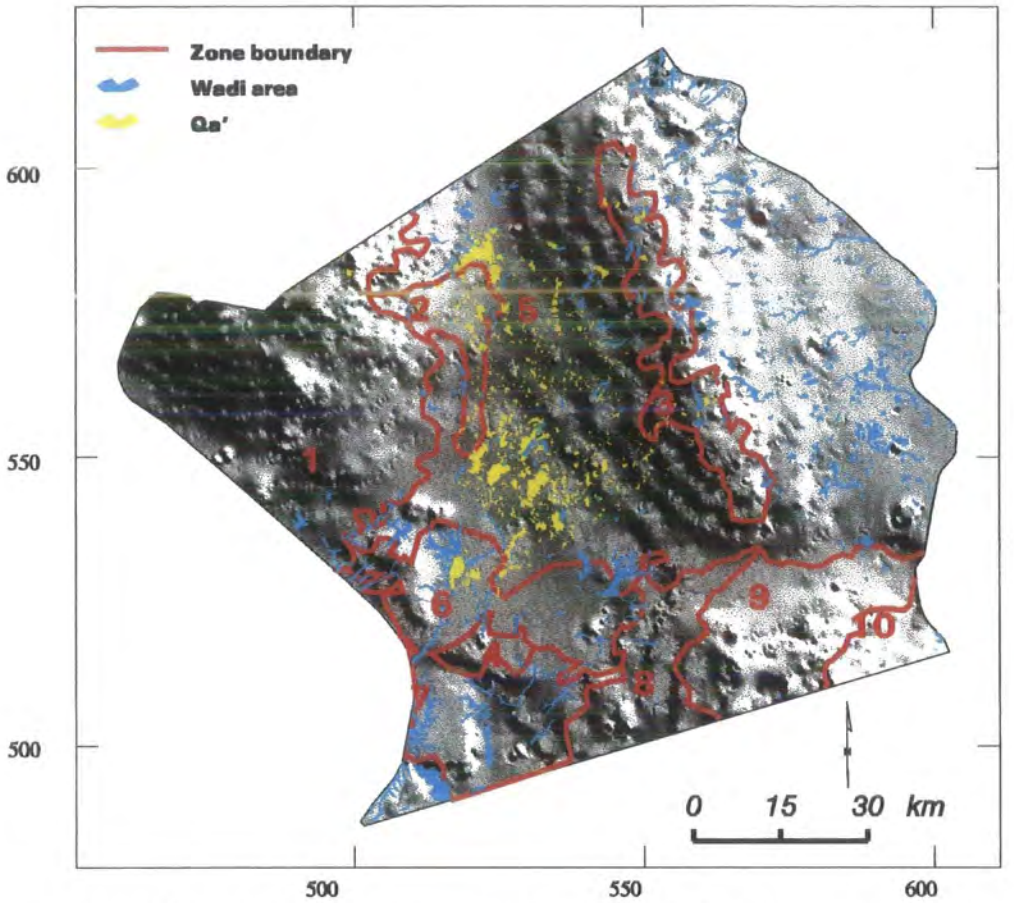

Figure (2 - 8) The major geomorphological zones of the Badia Programme area
(Based on Al-Homoud et al, 1992)

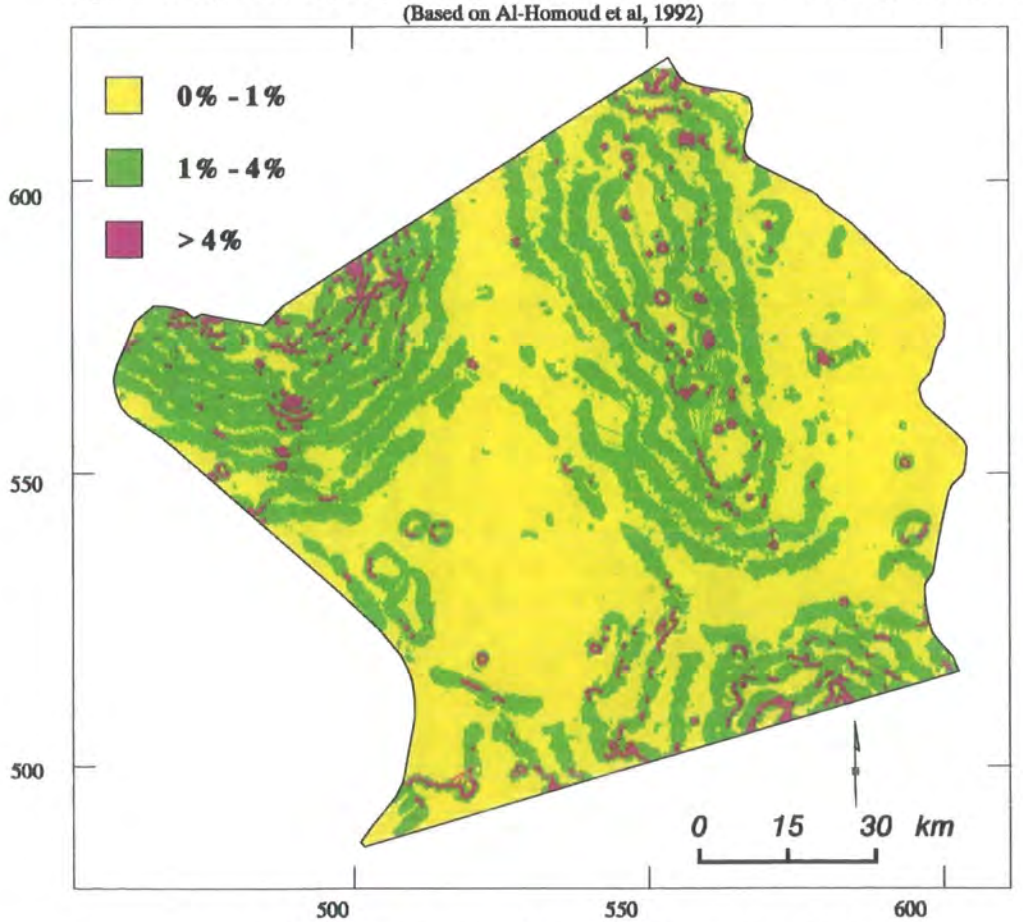

Figure (2 - 9) Slope map of the Badia Programme area

Zone 1: a region with high density of outward drainage wadis and small mudpans. Lichen appears on the ground surface basalt.

Zone 2: An area of the youngest Fahda basalt formation containing many *qa's*.

Zone 3: An area of lighter colour basalt and small number of *qa's*. The zone is slightly higher than the surrounding areas and thus divides the drainage to east and west.

Zone 4: A basalt area.

Zone 5: The main basalt area with many *qa's*. The area forms a plateau with very gentle slopes.

Zone 6: A limestone bedrock area with gypsum crusts in much of the zone. The surface is covered by chert fragments.

Zone 7: A low lying limestone area with gypsiferous soils and surface covered chert fragments.

Zones 8,9 and 10: Areas of aeolian sediment cover.

2.6 Climate

Except for the hilly areas in the Northwest the whole programme area lies in the arid climatological zone. The climate is characterised by hot and dry summers and cold and low rainfall winters.

The network of climate stations covering the area consists of 8 daily rainfall recording stations and two totalizer stations. Two of the daily recording stations (Azraq evaporation station and Safawi station) provide measurements of pan evaporation, humidity, radiation, wind speed and direction, and temperature (Ayed, 1996). Table (2-3) gives a brief description of the climate stations of the area. The density of rainfall gauges varies from

one gauge for every 700 km^2 in the western part to one gauge for more than 2,000 km^2 in the central and eastern parts. Although this density complies with the standards of the World Meteorological Organisation (Agrar, 1977), it is however, not sufficient for rainfall-runoff modelling purposes where accurate representation of the spatial and temporal distribution of rainfall events is an essential requirement.

Table (2-3) Climate stations within the Badia area
(source: Ayed, 1996)

Station name	Code	X-coord. (km)	Y-coord. (km)	Altitude (m)	Annual average mm/y	Period of record
Um el-Quttein	F1	464.9	576.5	986	153.2	1947-1995
Safawi	F2	509.6	563.3	715	69.9	1942-1995
Deir el-Kahf	F4	486.2	568.7	1025	113.2	1963-1995
El-Aritayn	F6	491.0	553.6	800	95.4	1963-1995
Azraq	F9	480.5	525.3	533	65.6	1963-1995
El-umari	F11	502.0	490.7	525	44.1	1963-1995
Wadi Salahib	F13	542.3	542.4	700	65	1967-1995
Qa' Samika	F16	463.8	569.9	760	69	1967-1995
Ghadeer el Mallah	F17	519.1	546.7	630	65	1967-1995
Jabal Aseikhim	F18	495.4	535.1	640	65	1967-1995
Tulul al-Ashqaf	H4	550.5	575.6	900	69.8	1967-1995
Al-Ruayshid	H1	612.8	597.3	686	75.8	1945-1975

The annual average of rainfall varies from more than 150 mm in the Northwest to less than 45 mm in the South. The annual area average is around 71 mm. The characteristics of the rainfall in the region will be considered further in chapter 3.

Evaporation rates are in general very high and the average daily potential evaporation varies from a maximum of about 17 mm/day in July to a minimum of 3 mm/day in January (more details on the characteristics of rainfall and evaporation will be provided in chapter 3).

The annual mean temperature in the area is 15° C. The monthly average temperature varies between 28° C in July to 8° C in January. An absolute maximum of 46.6° C was recorded

in Safawi station in July 1978. The absolute minimum is -6° C was recorded in January 1973 (Ayyash, 1993).

The annual relative humidity varies between 40% to 50%. The mean monthly humidity varies from 60% in January to 30% in June (Ayed, 1996).

2.7 Summary

A brief description of the physical environment of the study area has been presented. The large number of possible combinations of bedrock types, soil groups and topography suggests a heterogeneous catchment in terms of its hydrological response. This indicates the need for detailed description of the physical environment if an accurate assessment of the surface water resources in the area is required.

CHAPTER 3

CHARACTERISTICS OF THE HYDROLOGICAL PROCESSES IN THE JORDAN BADIA AREA

3.1 Introduction

The hydrometeorological processes of concern for the study of surface water in the Jordan Badia area are rainfall, evaporation, infiltration, transmission losses, and runoff. The characteristics of these processes in arid zones are not very well understood (Wheater *et al*, 1995). The situation in the Badia area is not an exception to this for the following reasons. First, there are no hydrological records of the discharge of the wadis in the area and all the available data are based on empirical approaches. Secondly, the studies on infiltration and transmission losses have been based on a limited number of infiltrometer tests. The validity of extrapolating these results to the whole catchment area is uncertain. Thirdly, the density of rainfall stations and the daily recording time step may not be sufficient to describe the spatial and temporal distribution of rainfall in the area.

This chapter describes the hydrometeorological processes in the study area. In view of the limited number of local studies on these processes reference shall be made to relevant studies in other areas of similar arid conditions.

3.2 Rainfall

Rainfall in deserts, in general, is caused by cyclonic storms commonly associated with convective thunderstorms that produce high intensity, short duration rainfall events (Cooke *et al* 1993). The typical characteristic of arid region rainfall is its variability both in time and space. In a study on the spatial and temporal structure of rainfall in Saudi Arabia, Wheater *et al* (1990) demonstrated that the probability of occurrence of rainfall drops down to close to zero at distances more than 20 kilometres from a station where rainfall has occurred. Similar observation on the localised nature of rainfall in the Jordan Badia area was reported by Noble (1994) where an intense storm that occurred at *Qa' Saut* was not registered at the *Safawi* station 30 kilometres away.

3.2.1 Characteristics of annual rainfall

The annual rainy season in Jordan starts in October and lasts until early May. However, the number of rainy days and the duration of the rainy season vary from year to year and from one place to another. In terms of the area average annual rainfall, the hydrological years in the Badia area can be classified into three categories; wet years, with annual rainfall exceeding 100 mm; dry years, with annual rainfall less than 80 mm and normal years, with annual rainfalls between the other two categories (Ayed, personal communication, 1996).

3.2.1.1 Distribution of annual rainfall

The long term average annual rainfall amounts registered at the gauging stations in the area are shown in table (3-2). Based on these values a three dimensional surface representing the distribution of the average annual rainfall in the area is generated using the ARC/INFO KRIGING surface interpolation technique. An isohyetal contour map of the average annual

rainfall is then extracted from the interpolated surface (figure 3-1). The accuracy of this representation, however, depends on the density of rainfall stations involved in the interpolation process.

The spatial distribution of annual rainfall can be better illustrated using the spot representation shown in figure (3-2). In this figure, spots of size proportional to the annual average represent the average annual rainfall for each rainfall stations. Each spot represents the annual rainfall average for the Thiessen polygon constructed around the rainfall station. The distribution of the spots suggests three distinct zones: the hilly area zone in the north west with relatively high average annual rainfall, the small area to the south west with very low annual average, and the central and eastern parts with low rainfall.

3.2.1.2 Temporal variations in annual rainfall

Fluctuations of annual rainfall are illustrated by the graphs of annual rainfalls at three stations; F1 station situated in the area of high rainfall; F2 station in the area of low rainfall; and F11 station in the area of very low rainfall (figure 3-3). A least square trend analysis of the annual rainfall for twenty-seven years of record (1967 - 1994) at the three stations indicates a decreasing trend for stations F1, F2 and an increasing trend for station F11. However, an assessment of long term rainfall trend conducted by Agrar (1977), based on comparisons with historical records of a rainfall station in Jerusalem, suggests that "there is no distinct trend or recognisable periodicity of rainfall in any part of Jordan".

The temporal variability of annual rainfall can be quantified using the coefficient of variability defined by the following equation

$$C_v = \frac{s}{\bar{x}}$$

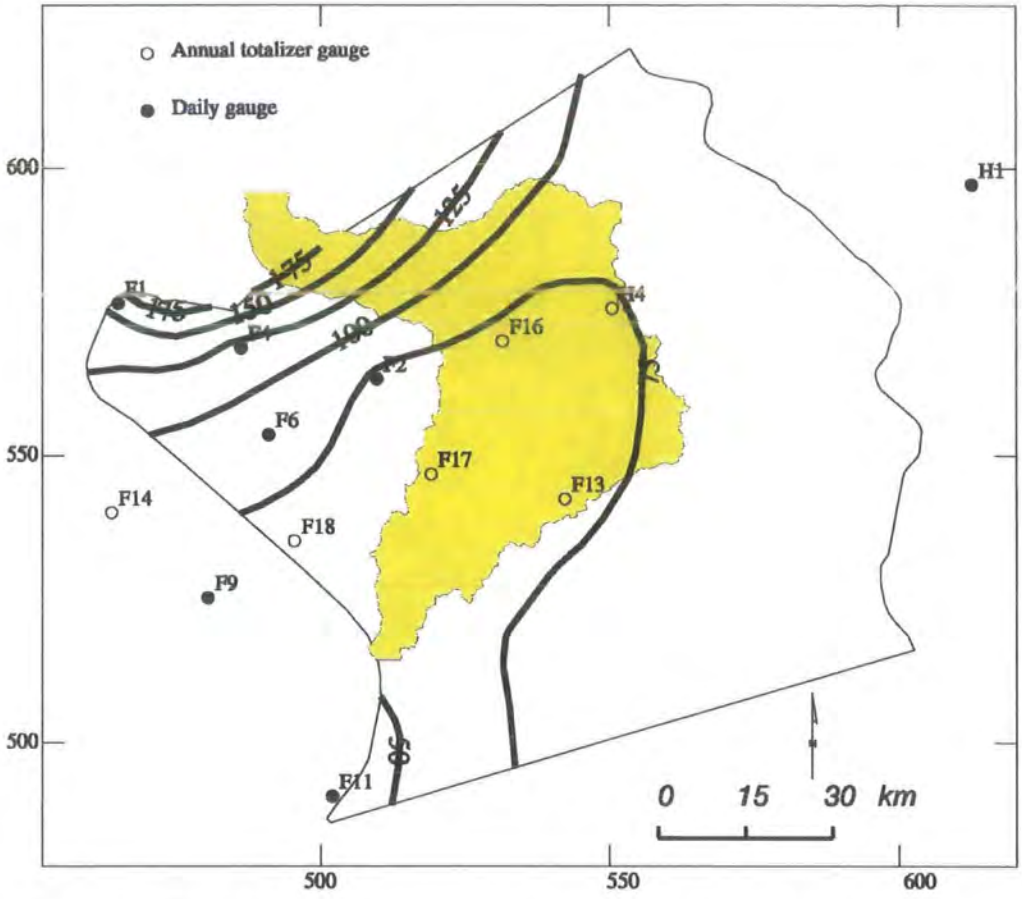

Figure (3 - 1) Isohyetal contour repesentation of the annual average rainfall

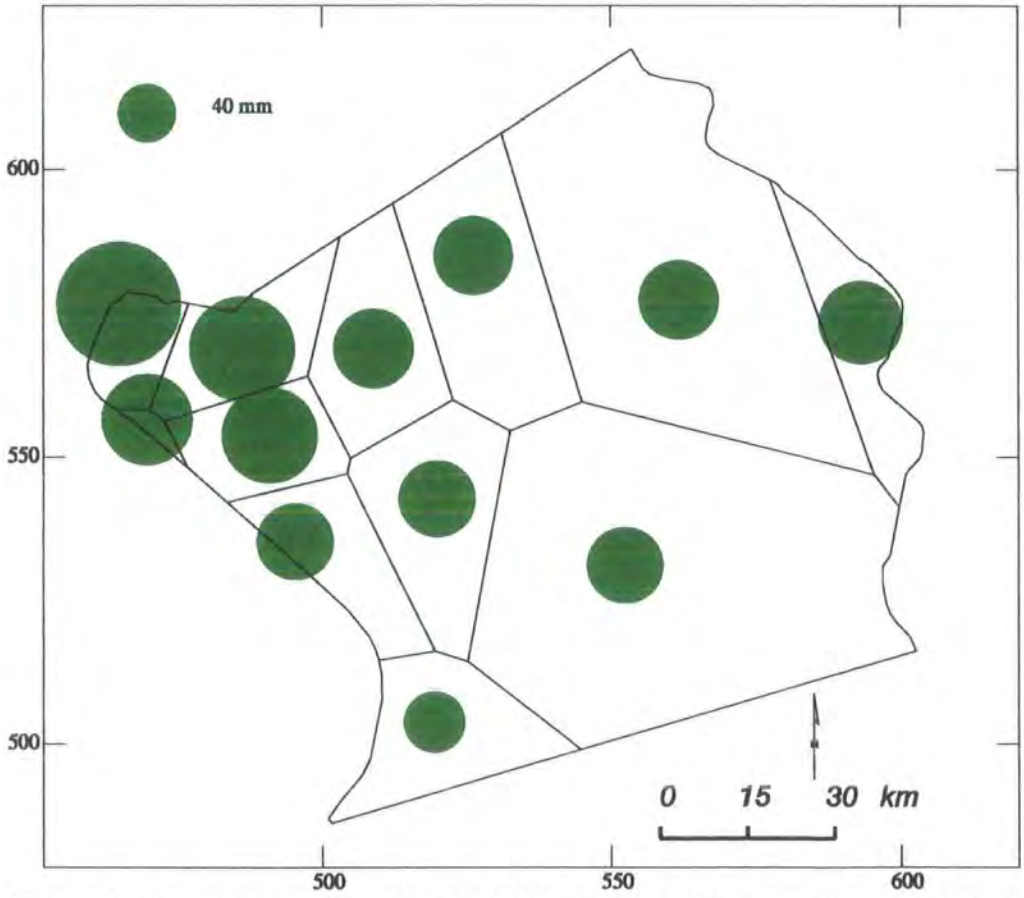

Figure (3 - 2) Spot representation of the distribution of the annual average rainfall

where,
C_v : coefficient of variability,
s : the standard deviation,
$\bar{x}$: the average.

Table (3-1) illustrates the coefficient of variability of annual rainfall for the three stations F1, F2, and F11. The table shows lower fluctuations in the hilly area represented by station F1 compared to the other areas.

Table (3-1) The coefficient of variability of annual rainfall

Station	Mean ($\bar{x}$)	Standard deviation s	C_v
F1	153.207	57.612	.376
F2	69.893	42.800	.612
F11	44.082	26.395	.598

3.2.2 Calculation of area annual rainfall

Calculation of the volume of annual rainfall over an area is usually performed using the Thiessen method. The method consists of generating polygons around the rainfall stations. The polygons are formed from the intersections of the perpendicular bisectors of the lines connecting the rainfall stations (ESRI, 1996). The rainfall amount recorded at each station is assumed to represent the rainfall within the Thiessen polygon comprising the station. The average area rainfall can be expressed as,

$$\bar{p} = \sum_{i=1}^{n} w_i p_i$$

$$w_i = A_i / A$$

where,
$\bar{p}$: Average annual area rainfall,
w_i : Weighted area,
A_i : Area of Thiessen polygon,
A : Total area (11,110 km^2),
n : Total number of stations.

Table (3-2) shows the results of the computation.

Table (3-2) Computation of average annual area rainfall

Station code i	Period of record	Av. annual rainfall p_i (mm)	Area of influence km^2	w_i	$p_i w_i$ (mm)
F1	1947 - 1995	153.2	243.5	0.022	3.37
F2	1967 - 1995	69.9	668.7	0.060	4.19
F4	1963 - 1995	113.2	494.6	0.045	5.09
F6	1963 - 1995	95.4	437.5	0.039	3.72
F11	1963 - 1995	44.1	630.4	0.057	2.51
F13	1967 - 1995	65.0	3287.4	0.296	19.24
F14	1967 - 1995	88.0	32.3	0.003	0.26
F16	1967 - 1995	69.0	964.5	0.086	6.00
F17	1967 - 1995	65.0	745.2	0.067	4.36
F18	1967 - 1995	65.0	463.3	0.042	2.73
H1	1967 - 1995	75.8	497.5	0.045	3.38
H4	1967 - 1995	69.8	2645.6	0.238	16.61
Total			11110	1.000	71.46 (mm)

The average annual area rainfall calculated by the Thiessen method (71.46 mm) complies with the mean height of the Kriging interpolated surface computed by dividing the volume of the Kriging surface by the surface area. Using this approach the average annual area rainfall is 71.30 mm.

3.2.3 Characteristics of monthly rainfall

The variability in monthly rainfall is illustrated by the distribution of long-term average of monthly rainfall for the three stations F1, F2, and F11 shown in figure (3-4). The figure shows that the highest monthly rainfalls occur during winter (from December to March) and very little rainfall is expected after April.

3.2.4 Characteristics of daily rainfall

The concentrated nature of rainfall in arid regions may result in having single storm events with rainfall amounts exceeding the annual average (Cooke *et al* 1989). Traces of heavy storm events can be detected from the daily rainfall records. The graphs in figures (3-5)

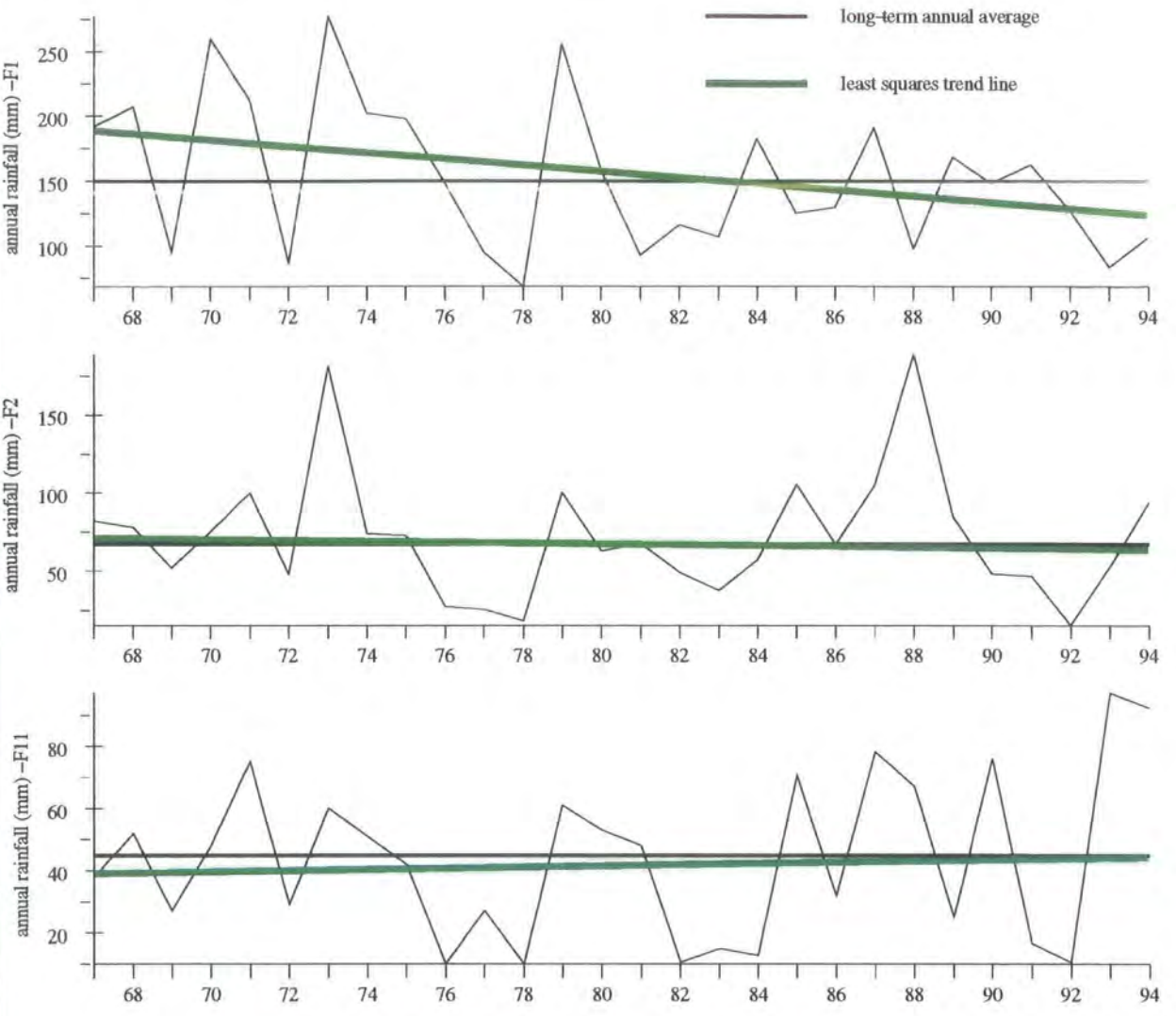

Figure (3 - 3) Fluctuations of annual rainfall for stations F1,F2,F11

(source of data : Ayed (1996))

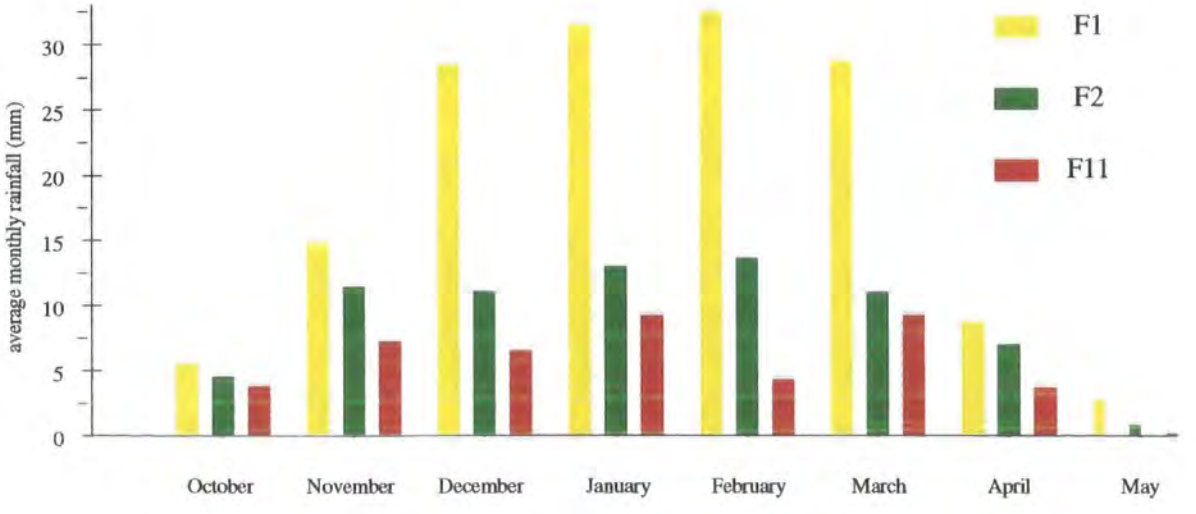

Figure (3 - 4) The long-term average monthly rainfall for stations F1, F2, F11

(source of data : Ayed (1996))

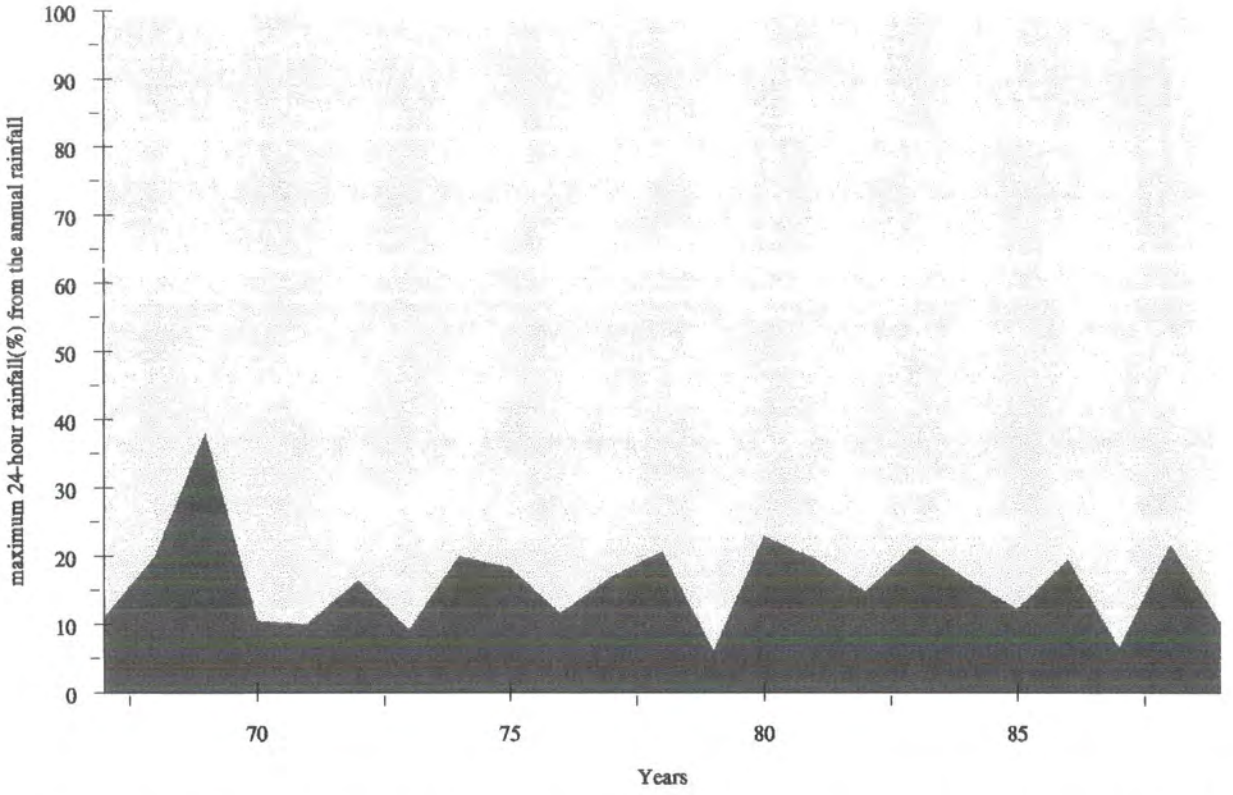

Figure (3 - 5) The maximum 24-hour rainfall for station F1 as a percentage of the annual rainfall
(Sources of data : Ayed (1996), Ayyash (1993))

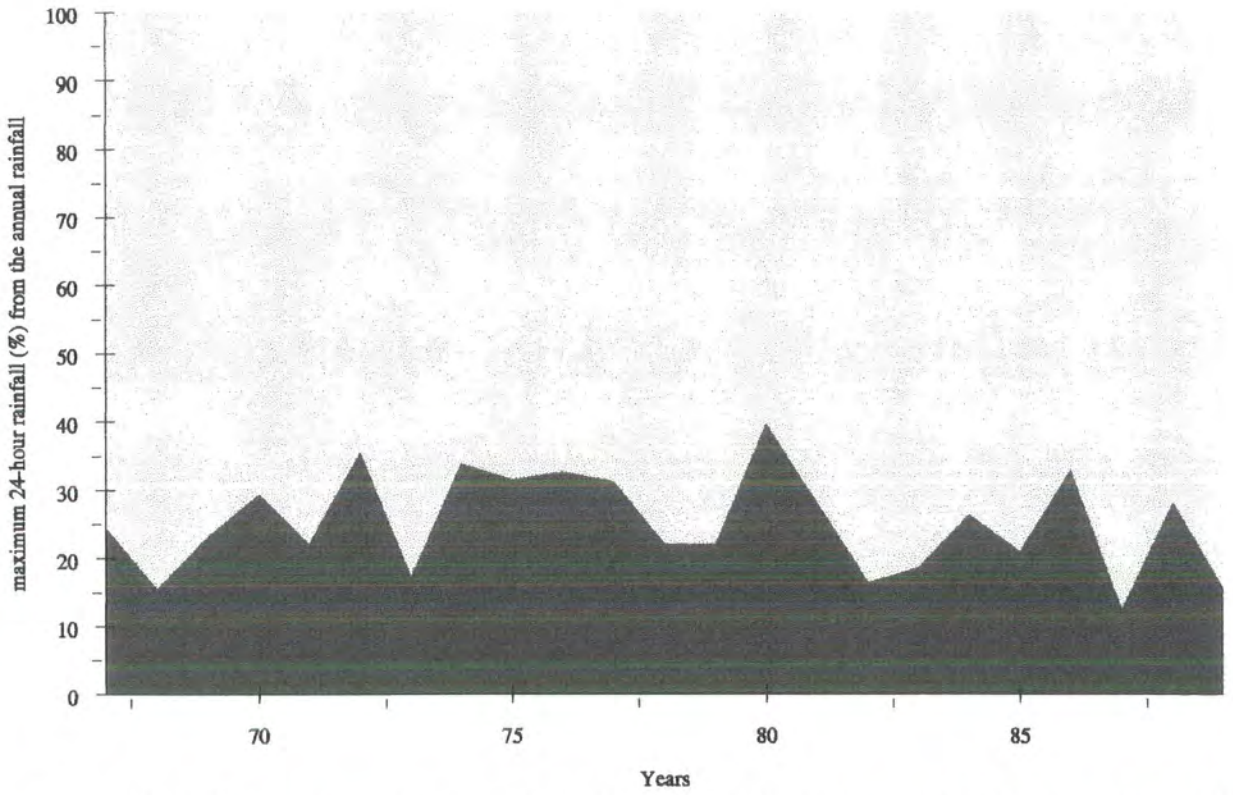

Figure (3 - 6) The maximum 24-hour rainfall for station F2 as a percentage of the annual rainfall

(Sources of data : Ayed (1996), Ayyash (1993))

and (3-6) illustrate the significant effect that single storm events may have on the total annual rainfall. The graphs show the maximum 24-hour rainfall recorded at stations F1 and F2 during each year for the period (1967-1990) computed as a percentage value of the annual amount.

The distribution of rainfall within a day appears also to be of concentrated nature. Wheater *et al* (1990) has shown that the majority of rainfall events on a study area in Saudi Arabia are composed of one hour duration storms and practically no rainfall is expected after six hours from the start of rainfall (figure 3-8). Hourly distribution of rainfall in the Badia area can be extracted from the average mass curve of the cumulative 24-hour rainfall at station F2 (figure 3-7). The average mass curve for the station is produced from the mass curves of a group of continuously recorded rainfall events of different return periods. Each mass curve represents the cumulative rainfall amounts recorded every hour over a 24-hour period. If we consider the hourly rainfall increments of the mass curve as probabilities of occurrence we obtain the probability distribution of hourly rainfall shown in figure (3-8). The distribution shows that the probability of rainfall occurrence decreases exponentially with the increase in rainfall duration.

3.3 Evaporation

Evaporation is the process by which water returns to the atmosphere from open water bodies and soil surfaces. In arid regions the annual potential evaporation rate usually exceeds the annual rainfall. This fact poses serious problems to projects for surface water storage in these areas (Christiaan, 1979). The determination of evaporation rates in the study area is based on the Class A Pan evaporation data measured at two climatic stations:

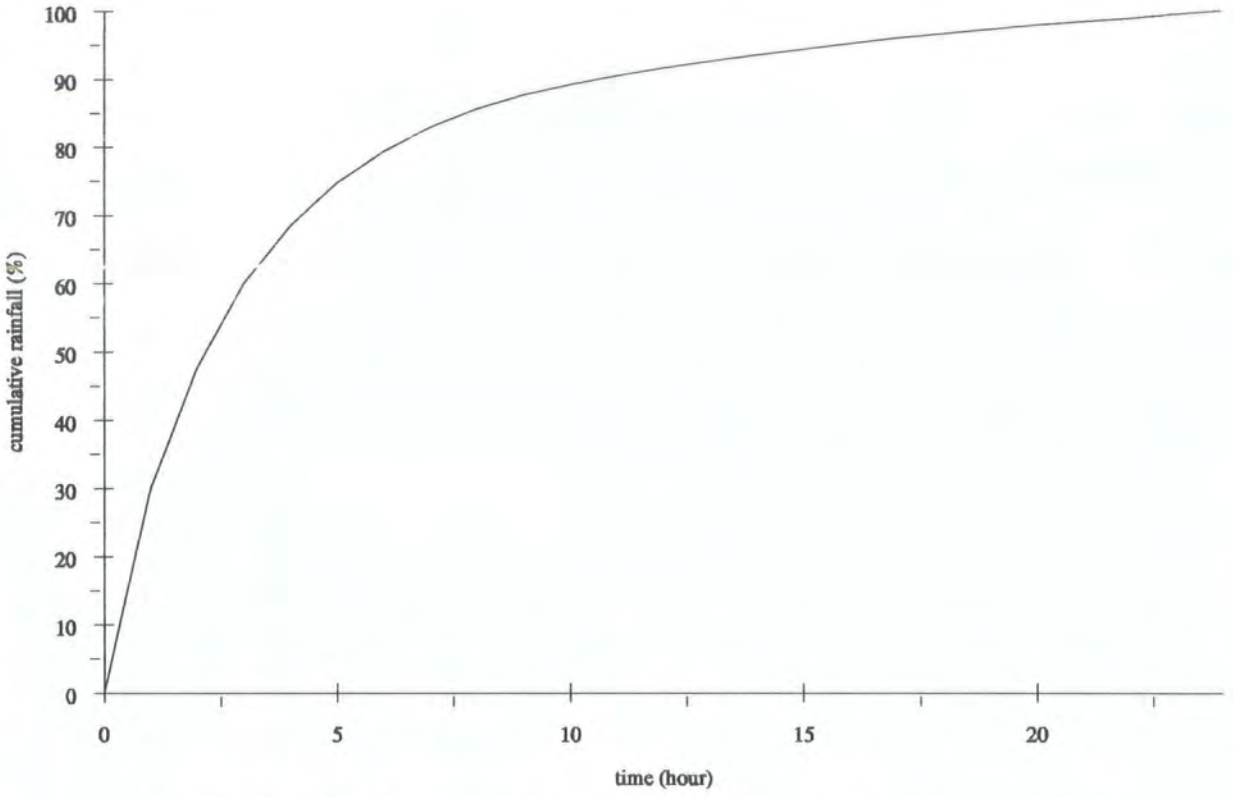

Figure (3 - 7) The average mass curve of 24 - hour rainfall of Azraq station

(Source of data : Ayyash (1993))

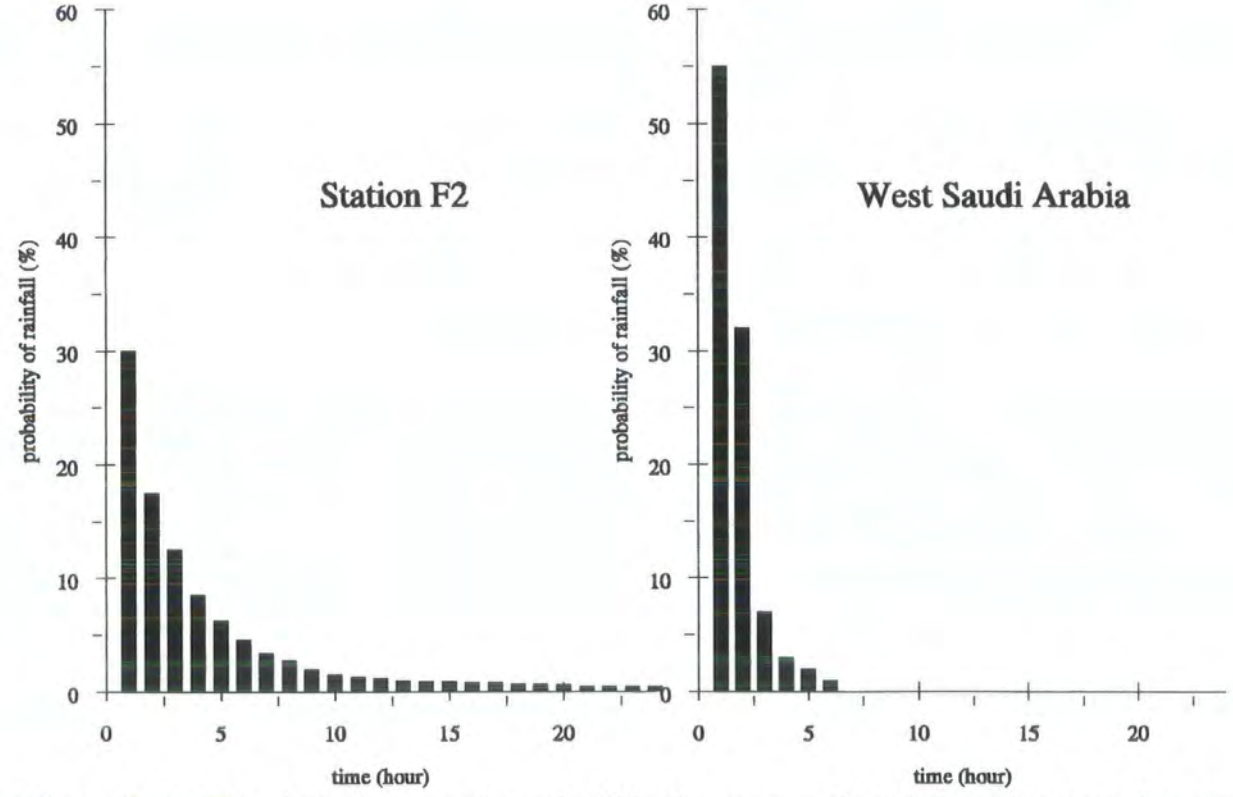

Figure (3 - 8) The relation between the probability of occurence of rainfall and the storm duration

(Sources of data : Wheater et al. (1990), Ayyash (1993))

Azraq (F9) and Safawi (F2).Table (3-3) shows some statistical parameters of pan evaporation data in these stations.

Table (3-3) Pan evaporation data for stations F2 and F9
(source: Ayed, 1996)

Parameter (mm/day)	F2	F9
long-term daily average	9.9	10.1
maximum monthly average (July)	18.1	17.1
minimum monthly average (January)	3	3

By matching the daily pan evaporation data with the potential evaporation computed by the Penman formula, Ayed (1996) has found a pan coefficient of 60% for Azraq station (F9) and 63% for Safawi station (F2). The pan coefficient can be used to estimate the potential evaporation from the measured pan evaporation using the following equation:

$$E_p = E_{pan} * C_{pan}$$

where,
E_p : potential evaporation.
E_{pan} : pan evaporation.
C_{pan} : pan coefficient (%).

While spatial variations of evaporation in the area are not as significant as the precipitation variations, because of the low relief differences, the seasonal variations are relatively high. Table (3-4) shows the monthly average values of pan and potential evaporation for the two climatic stations.

3.4 Infiltration

Infiltration is the process of downward movement of water into the ground. The infiltrating water either percolates through the upper soil layer in a lateral movement or goes into

replenishment of the soil moisture storage. Any excess amounts of infiltration may continue its downward movement to the saturated zone of the soil profile.

Table (3-4) Monthly average values of potential and pan evaporation
(source : Ayed, 1996)

Month	Azraq station (F9)		Safawi station (F2)	
	E_p	E_{pan}	E_p	E_{pan}
October	4.9	7.8	5.2	9.0
November	3.1	4.3	3.3	5.0
December	2.3	3.1	2.2	3.1
January	2.5	3.0	2.3	3.0
February	3.5	5.2	2.9	4.5
March	5.3	8.1	4.3	7.1
April	7.9	12.0	6.4	10.9
May	9.6	15.0	7.8	13.4
June	10.7	17.9	8.9	16.2
July	9.9	18.1	8.9	17.7
August	8.6	15.5	7.5	14.5
September	6.9	12.2	7.0	13.3
Annual Average	6.3	10.1	5.9	9.9

Under initially dry conditions infiltration occurs under the combined action of gravity and pore pressure deficiency (Raudkivi, 1979). If the conditions of ponded supply of water remain, the rate of infiltration decays exponentially with time until it reaches a final low steady rate. The following relation attributed to Horton (Viessman et al 1989) describes this time-dependent characteristic of infiltration

$$f_p = f_c + (f_0 - f_c) * \exp(-kt)$$

where,
f_p : the infiltration capacity rate at time t ,
f_c : final infiltration rate,
f_0 : initial infiltration rate,
k : constant.

The infiltration capacity of the soil depends on many factors including the soil characteristics (texture, structure, and hydraulic conductivity), the surface conditions, and the initial moisture conditions.

3.4.1 Characteristics of infiltration in the Badia area

The infiltration rate in the majority of the area is low. Except for the extremely high rates through the wadi beds infiltration rates are generally of the order of 10 mm/hour (Noble, 1994). The low infiltration rates are caused by the typical arid environment conditions that dominate in the area. These conditions include stone cover, crusted soil, and gentle slopes. A limited number of studies on the infiltration characteristics in the study area have been conducted. The main findings of these studies are discussed in the following sections.

3.4.1.1 Infiltration rate

The different types of rocks and soil groups in the area reflect the heterogeneity of the study area in terms of the infiltration characteristics. The area comprises twelve different formations of bedrock basalt and six different soil groups. This heterogeneity results in high spatial variability of infiltration properties and hence indicates the need for a large number of measurements to describe the spatial distribution of the infiltration. The cost factor involved in such detailed studies may go beyond the budget of many projects. An alternative and more feasible approach would be to subdivide the area into a limited number of units representing the possible combinations of infiltration-related factors. Berndtsson and Larson (1987) have described this lumping approach in a study on the spatial variability of infiltration in semi-arid regions. Berndtsson and Larson suggest dividing the catchment area into three categories: *nose* areas, characterised by crusted soil and low infiltration rates; *slopes,* with smoothly decaying infiltration rates and *hollow*

areas representing the close vicinity of wadi beds and assumed to have saturated soil and very low infiltration rates.

In his study on the infiltration characteristics in the Badia area Warburton (1997) uses a land system approach to classify the area into three zones: wadi beds, mudflat depressions, and side slopes. The infiltration tests that have been carried out in sample areas from each zone have shown high initial infiltration rates for all the three zones. While remaining at a very high rate for the wadi beds, the infiltration rate drops down to its lowest steady rate very rapidly for the side slopes and mud pan areas.

Noble (1994) has also carried out double ring infiltrometer tests and sprinkler tests. The main results of these tests can be summarised as follows:

1. The initial and final infiltration rates are very high in wadi bed areas (more than 1000 mm/hour).
2. The infiltration rate drops down to a lower steady rate of 10 mm/hour for the side slope areas and 3 mm/hour for the mud pan areas as soon as the upper 70 mm of the soil are saturated.
3. The depth of the wetting front after 24 hours of ponded water supply was found to be 100 mm for the uncultivated areas and from 150 to 200 mm for the cultivated areas (Hunting's measurements according to Noble, 1994).

3.4.1.2 Spatial distribution of infiltration

The spatial variability of the soil hydraulic characteristics implies high spatial variability in infiltration (Sharma, 1980). This variability has been shown experimentally to follow the curve illustrated in figure (3-9) (Manley, 1977). Burgin and Lutin (according to Manley, 1977) were the first to suggest using a straight line to simulate the cumulative distribution function of infiltration which seems to be, as shown in the figure, an acceptable

approximation to the experimental results. The linear cumulative distribution function has been used in the Stanford Watershed Model to relate infiltration to runoff. The key point in the application of the linear cumulative distribution function consists in the definition of the point *b* in figure (3-9).

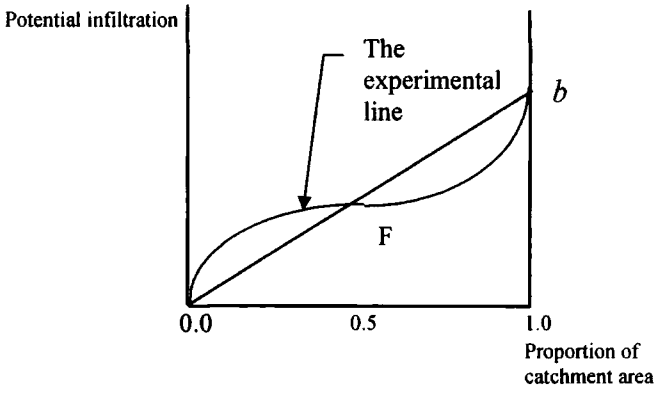

Figure (3-9) The spatial distribution of infiltration over the watershed area

The Stanford Watershed Model defines the value of *b* as the ratio of the moisture level in the soil lower zone storage to the nominal capacity of this zone. Warburton (1997) suggests using the same linear representation to roughly estimate the runoff from side slopes in the Badia area. The value he uses for the point *b* is the initial (or maximum) infiltration rate.

A non-linear representation of the cumulative distribution function of infiltration has been used in the Variable Infiltration Capacity Model VIC-2L (Abdulla, 1995). In this model the distribution function of the infiltration is expressed as

$$i = i_m(1-(1-A)^{1/b})$$

where,
i : the maximum infiltration rate over the area,
A : the fraction area for which the infiltration rate is less than or equal to i ,
b : the infiltration factor.

The value of i_m can be determined by assuming that the cumulative infiltration over the area is equal to the maximum soil storage capacity averaged over the area (Abdulla, 1995).

3.4.2 Infiltration and runoff

It is generally believed that runoff in deserts occurs when the rainfall intensity exceeds the infiltration rate (Cooke *et al*, 1989). In the case of bare soils, as in the Badia area, the tendency of the soil to form a crusted layer presents a major factor influencing the infiltration rate. The soil crust is formed when the fine materials, resulting from the direct impact of rainfall drops on the surface soil, are washed into the surface pores (Cooke *et al*, 1989). Morin and Benyamini (1977) described a quantitative assessment of the effect of soil crust on the infiltration rate. Their experimental studies on bare soils under field conditions have shown that the effect of soil crust on the infiltration rate can be illustrated by the following equation

$$I_t = (I_i - I_f) * e^{-\gamma p t} + I_t$$

where,

I_i : the initial infiltration rate,

I_f : the final infiltration rate,

p : rainfall intensity,

t : time from beginning of rainfall (hours),

γ : given by the equation $\gamma = a/V_m$ where

a : average size of the area sealed by the impact of one median raindrop, causing the infiltration rate of this area to drop from I_t to I_f (mm^2),

V_m : the median drop volume(mm^3).

For the Badia area, it has been observed by Noble (1994) and Kirk (personal communication, 1998) that soil crust is formed shortly after the start of rainfall. This results in significant decrease in the infiltration rate and rapid generation of runoff. Kirk (personal communication, 1998) has observed that runoff occurs very soon after the start of rainfall irrelevant of the moisture content of the soil profile. On the other hand, Noble (1994) has noticed that the application of the Hortonian assumption implies that runoff from side slope areas is only expected once every 10 years whereas observation has shown more frequent occurrence of runoff. Noble has concluded that runoff is promoted as soon as the upper 70 mm of the soil is saturated. These studies however, did not result in a quantification of the effect of soil crust on the infiltration rate.

Noble (1994) and Ayed (1996) documented the available estimates of the runoff and infiltration volumes in the area, based on the SCS curve number method. Their estimates of the infiltration volume that appears as a recharge to the Azraq basin are 37.5 $M m^3$ (million cubic meters) and 34 $M m^3$ respectively.

3.5 Transmission losses

Transmission losses are the amounts of stream flow that infiltrate into the channel bed during transmission (Jordan, 1977). In the absence of any contribution to the channel flow between two stations along the channel, the effect of transmission losses appears as a significant drop in the runoff volume at the downstream station.

The rate of transmission loss decreases with the increase of soil moisture content (Walters, 1990). In the Badia area factors like the depth of water table under the wadi beds (100 metres on average) (Al-Homoud *et al* 1992), the high evaporation rates and the relatively long duration between consecutive rainfall events make it unlikely for conditions of high

soil moisture content to occur. In addition, the coincidence between the channel network and the underlying system of lineaments may indicate possible passages of the infiltrated water to the groundwater aquifers and thus enhances the rate of transmission loss (Noble, 1994).

Experiments on transmission loss in semi-arid environments in the United States has shown a linear regression between transmission losses per unit distance and the upstream flow volume (Jordan, 1977). Jordan (1977) described this relationship as the following transmission loss equation,

$$V_x = V_A * R^x$$

where,
V_x : the flow volume at distance x from the upstream station (A),
V_A : the flow volume at station A,
R : the ratio of the flow volume at any location to the volume at a location one mile away in the upstream direction.

The study of Walters (1990) on transmission losses in Saudi Arabia has shown comparable results. Besides the upstream flow volume, the Walters (1990) study included testing the correlation between transmission losses and several other factors like the channel active width, channel slope, antecedent moisture conditions and duration of flow. The results of this study can be summarised as follows:

1. Using a linear regression model, only the upstream flow volume was found to be related to transmission losses and the regression equation can be expressed as

$$V_1 = 0.05 * V_A$$

where V_1 represents transmission loss at 1 mile from the upstream station.

2. Using an exponential regression model, both the flow volume and the active channel width are related to transmission loss by the following regression equation

$$V_1 = 0.0006225 * W^{1.216} * V_A^{0.507}$$

where W is the active channel width.

The linear regression equation of Walters (1990) appears suitable for application to transmission losses in the Jordan Badia area. This is first, because of the similarity in watershed conditions in the two areas in terms of watershed area, slopes of channels and rainfall amount. Secondly, the transferability of the equation since transmission losses are estimated per mile of channel distance and thirdly, because no data on transmission losses in the Badia area are currently available.

3.6 Runoff

Surface runoff occurs when the rainfall excess generated within a catchment starts moving towards the catchment outlet. These amounts of rainfall excess are generally produced when the rainfall intensity, after satisfying the interception and depression storage requirements, exceeds the infiltration rate. The movement of water across the catchment takes place as overland flow that merges into the network of streams where the water continues its flow as channel flow to the catchment outlet.

3.6.1 Characteristics of runoff in the Badia area

In arid regions, the runoff generated within the catchment may not reach the outlet. This is mainly due to the losses that take place during transmission and the fact that many channel segments drain into closed depression areas where water remains until it evaporates (Cooke *et al* 1989). Since both high rates of transmission loss and an abundance of mud

pan depressions are seen in the Wadi Rajil watershed, only runoff from major storm events is expected to survive until it reaches the watershed outlet. Under the assumption of linear cumulative distribution of infiltration, Warburton (1997) estimates that 10% of the side slope areas are expected to generate runoff following a rainfall event of 20-mm/hr intensity. Such intensities occur for short duration during events of five years return period (Sa'ad, 1986).

3.6.2 Estimation of the annual runoff of Wadi Rajil watershed

Since no stream flow records are available, empirical approaches have been used to estimate the annual runoff of the Wadi Rajil watershed. As part of a feasibility study on the potential yield of Wadi Rajil, the following rainfall-runoff relationship was applied to generate long-term runoff records (Hydrosult, 1990),

$$Q = C * P$$

where,
Q : the annual flow volume,
C : the runoff coefficient,
P : the annual precipitation volume.

A runoff coefficient of 2% was adopted. This value was selected based on an assessment of several estimates of the runoff coefficient for similar desert regions. Using the above formula the annual runoff volume of Wadi Rajil watershed was computed for the period 1963 - 1985. Based on this sample the 95% confidence interval for the annual average runoff is 4.1 ± 0.82 M m^3 (Hydrosult, 1990).

Another empirical approach was applied by Ayed (1996) using the unit hydrograph method. In this approach, a curve number of 75 was applied to estimate the rainfall excess

volume. The resulting rainfall excess amounts were convoluted using a synthetic unit hydrograph to produce the runoff at the watershed outlet. Using this approach Ayed (1996) estimates the average annual runoff of Wadi Rajil watershed to be 12.82 M m^3

3.6.3 Estimation of flood peaks and volumes for different return periods

Both Hydrosult (1990) and Ayed (1996) have given estimates of flood peaks and volumes. The Hydrosult (1990) estimates were based on using regional flood indexes and mean annual flood peak and volume. The mean annual flood peak and mean annual flood volume were estimated using the following regression equations,

$$\overline{Q} = b * A^a$$
$$\overline{V} = c * A^d$$

where,
$\overline{Q}$: mean annual flood peak,
$\overline{V}$: mean annual flood volume,
A : the watershed area,
a, b, c, d : regression coefficients.

The computed mean annual flood peak (95 $m^3 s^{-1}$) and annual flood volume (11.4 M m^3) were used in the calculation of daily peak flows and flood volumes using the following equations,

$$Q_t = r_t * \overline{Q}$$
$$V_t = i_t * \overline{V}$$

where,
Q_t : maximum daily peak flow for the return period t,
V_t : flood volume for the return period t,
r, i : regional flood indexes.

Ayed (1996) used the SCS curve number and the unit hydrograph method to estimate the flood peak and flood volume for simulated storms of different return periods. The following tables summarise the results of both studies.

Table (3-5) Estimates of peak daily flows for different return periods (values given in m^3s^{-1})

Return period	5 years	10 years	25 years	50 years	100 years
Hydrosult (1990)	136	229	-	535	664
Ayed	-	18.0	185.6	440.0	681.2

Table (3-6) Estimates of flood volumes for different return periods (values given in $M m^3$)

Return period	5 years	10 years	25 years	50 years	100 years
Hydrosult (1990)	16.8	28.2	-	54.7	62.8
Ayed	-	1.6	16.5	39.5	61.9

3.7 Runoff hydrographs

A hydrograph is a graphical or tabular representation of the flow rates out of the catchment outlet versus time. The flow rates reflected by the hydrograph usually result from the compound contributions of the groundwater flow and the surface flow.

Hydrographs of ephemeral streams, like Wadi Rajil, are characterised by steep rising and falling limbs. The rising limb indicates a rapid response of the catchment to water input mainly due to the low infiltration rates, while the steep falling limb indicates the absence of ground flow contribution.

3.7.1 The unit hydrograph

The concept of unit hydrograph has long been recognised as a simple empirical method for estimating the runoff produced from a given rainfall excess hyetogram. A T-unit hydrograph (TUH) is defined as the hydrograph "resulting from a unit depth of effective rainfall falling in T hours over the catchment" (Shaw, 1988).

The application of the unit hydrograph method involves the gross assumption of uniform rainfall distribution over the whole catchment area. Moreover, it is assumed that the rainfall intensity remains constant over the time base of the unit hydrograph. These assumptions are very unlikely to occur especially in arid areas characterised by variable rainfall over time and space.

In this section two approaches for synthesising a unit hydrograph for Wadi Rajil will be discussed. The first approach is based on the SCS synthetic unit hydrograph method. The second approach applies GIS techniques in the derivation of the unit hydrograph. The depth of rainfall assumed in the derivation of the unit hydrographs is 1 mm.

3.7.1.1 The SCS synthetic unit hydrograph

The SCS synthetic unit hydrograph method consists of estimating the unit hydrograph parameters from the catchment geometric characteristics. The curvilinear shape of the unit hydrograph can then be defined using the unitless hydrograph that was developed for the application of the SCS method (Appendix 1). The unit hydrograph parameters like the time to peak, peak discharge and the time base of the unit hydrograph are usually estimated using empirical formulas. Ayed (1996) and Ayyash (1993) use this approach to generate unit hydrographs for several wadi catchments in the Badia area. The SCS synthetic unit hydrograph method is applied here to generate the unit hydrograph resulting from 1 mm depth of rainfall excess for Wadi Rajil watershed using the following empirical equations (Ayyash, 1993),

$$T_c = (0.871 * L^3 / H)^{0.385}$$
$$D = 0.133 * T_c$$
$$T_p = D/2 + 0.6 * T_c$$
$$Q_p = 0.208 * A / T_p$$

where,

T_c : the time of concentration (hour),

T_p : the time to peak (hour),

D : the time base of the hydrograph (hour),

Q_p : the peak discharge ($m^3 s^{-1}$),

L : the length of the longest stream in the watershed area (km),

H : the drop in elevation along the longest stream (m),

A : the watershed area (km^2).

The watershed parameters, derived from the digital database of this study, are shown in figure (3-10). The resulting unit hydrograph parameters are as follows

T_c = 24.6 hours

D = 3.27 hours

T_p = 16.26 hours

Q_p = 36 $m^3 s^{-1}$

By approximating the unit hydrograph duration to 3 hours and using the unitless table (appendix 1) a 3-hour unit hydrograph is generated for the Wadi Rajil watershed (figure 3-11). An S-curve is generated from the 3-hour unit hydrograph and used to obtain the 1-hour unit hydrograph (figure 3-12).

Ayed (1996) estimated the unit hydrograph parameters for Wadi Rajil watershed as follows,

T_p = 18.3 hours

D = 1 hour

Q_p = 45.11 $m^3 s^{-1}$

A comparison between the SCS unit hydrograph of this study and that of the study of Ayed (1996) (figure 3-13) shows slight differences. These differences are mainly due to the difference in the watershed parameters used in generating each hydrograph. For example, in this research, the available maps does not cover the whole watershed area inside the Syrian borders while an estimate of that area was considered in the study of Ayed (1996).

3.7.1.2 The spatially distributed unit hydrograph

Maidment (1993) described this method as an application of GIS techniques for deriving a unit hydrograph using the time-area approach. The method consists of using GIS raster processing capabilities to define the flow pathways from each cell element in the watershed area to the outlet. Given the flow direction is determined, GIS functions enable calculating the flow length from each cell to the outlet. If the flow velocity within the watershed can be estimated, the time of travel required for the rainfall excess generated at each cell to reach the watershed outlet can be easily calculated.

By dividing the watershed area into zones of equal time of concentration, the time-area diagram for the watershed is produced and hence the unit hydrograph can be generated.

To apply this method for Wadi Rajil the flow lengths and the flow velocities have to be estimated. Chapter four discusses the procedure for defining the flow directions through the watershed area, while the estimation of the flow length and velocity will be discussed in chapter six. The use of the method to derive a unit hydrograph for Wadi Rajil is illustrated in chapter seven.

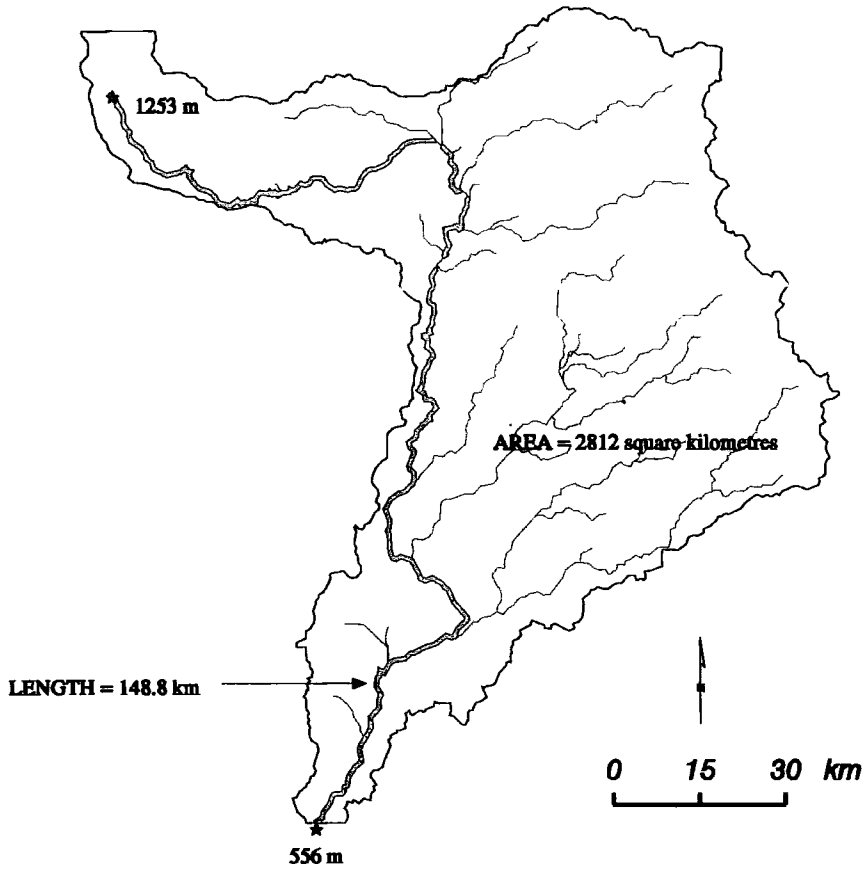

Figure (3 - 10) The watershed parameters used in the derivation of the SCS-synthetic unit hydrograph

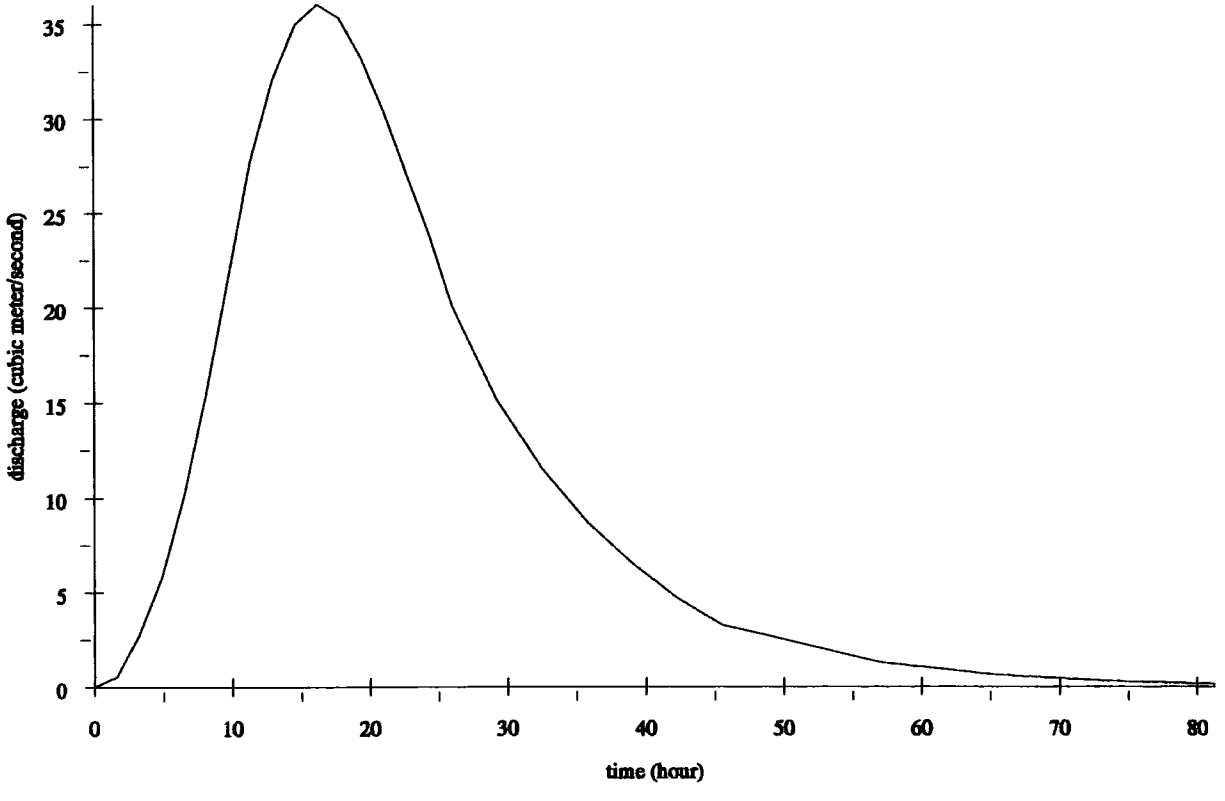

Figure (3 - 11) The SCS-synthetic 3-hour unit hydrograph of wadi Rajil

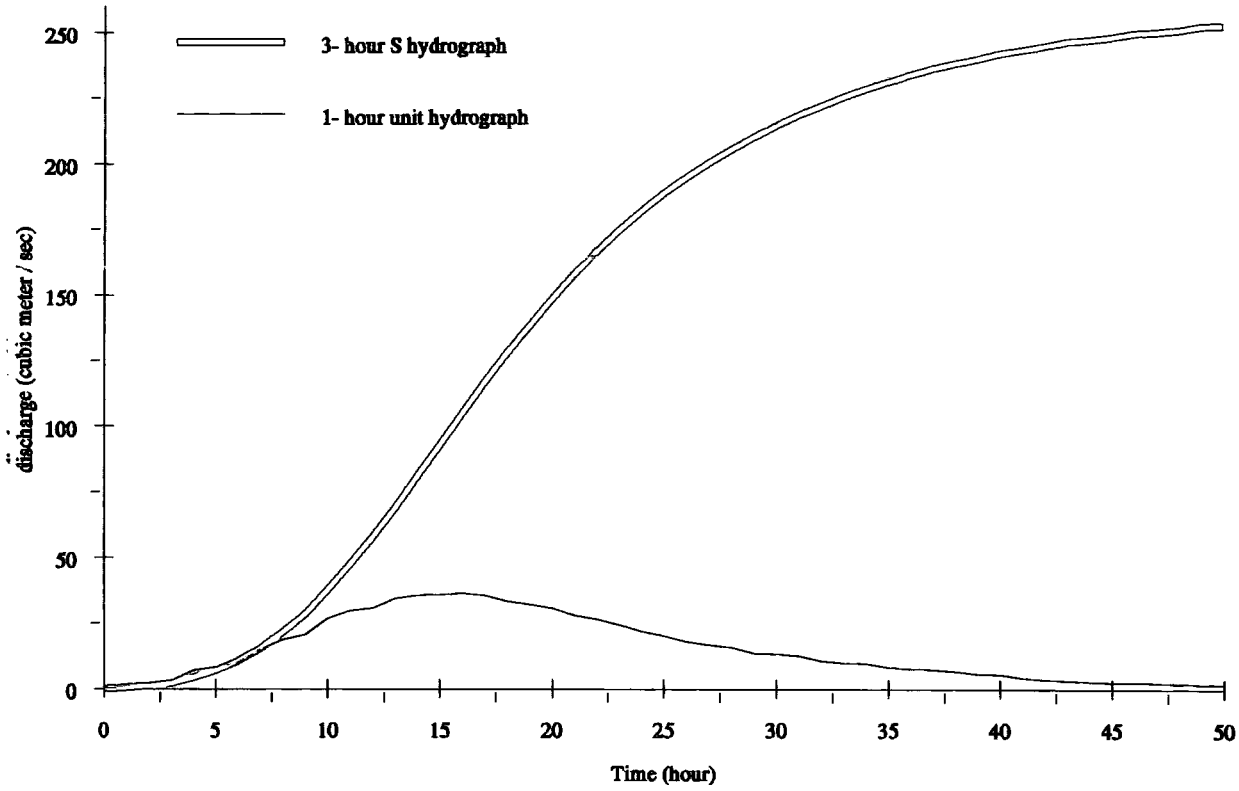

Figure (3 - 12) The 1- hour hydrograph constructed from the 3- hour S hydrograph

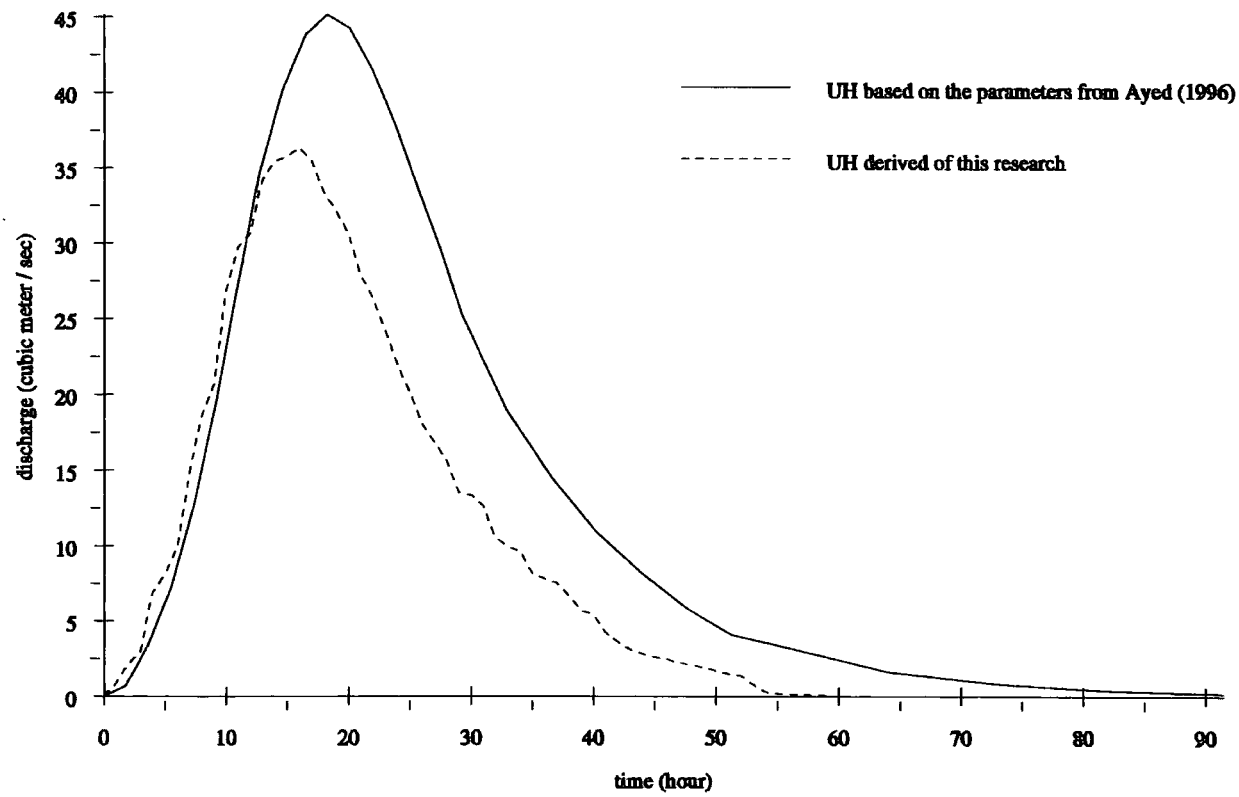

Figure (3 - 13) Comparaison between the UH of Ayed (1996) and the synthetic UH of this research

3.8 Summary

The typical characteristics of arid zone hydrometeorological processes dominate in the study area. These characteristics include variable distribution of rainfall both in time and space, high potential evaporation rates that exceed the annual rainfall, low infiltration rates in the slope areas; high transmission losses through the wadi beds; and rapid response to the surface runoff. A quantitative description of the characteristics of these processes in the study area has been presented. The description was based on previous works conducted in the study area and on the literature of studies conducted on similar arid zones hydrological processes.

CHAPTER 4

EXTRACTION OF THE CHANNEL NETWORK FROM THE DIGITAL ELEVATION MODEL

4.1 Introduction

The advent of digital elevation models (DEM) has found many uses in scientific disciplines where a three-dimensional analysis of the terrain features is required. The numerical structure of DEMs has enabled developing automatic procedures for extracting important topographic indices like slope, aspect, ridges and valleys.

An important application of DEMs in hydrology is the automatic extraction of the channel drainage network and the delineation of the watershed boundaries. The automatic procedures are more efficient than the laborious manual methods and are less subject to errors especially in flat areas where it is difficult to define accurately the watershed boundaries and the channel networks from maps (Burrough, 1990).

For the Wadi Rajil watershed, the automatic extraction of the channel network provides an automatic procedure to overcome the problem of discontinuity of the wadi lines through the flat *qa'* areas as it appears on the topographic maps. The extracted drainage network, particularly in the flat areas, is highly sensitive to errors in the DEM and requires field investigation.

The process of automatic extraction of the channel network relies on the flow direction, calculated from the DEM, to define the flow pathways through the *qa'* areas. In this chapter

a hydrologically correct DEM for the Wadi Rajil watershed area will be built. The DEM will serve to extract the channel drainage network and to delineate the watershed boundaries.

4.2 Overview

A DEM is "a digital representation of the continuous variations of the relief over space" (Burrough, 1990). The widely used storage format of DEM data is as a grid of regularly spaced points of known (x, y, z) co-ordinates.

4.2.1 DEM extraction

DEMs are generated by fitting a mathematical surface to a set of data points of known elevation. The quality of the resulting DEM depends mainly on the accuracy, density, and distribution of the input data points as well as the method of interpolation used. The resolution of the DEM sets the step at which DEM elevation data points are interpolated from the mathematical surface.

The elevation data required for DEM generation are usually provided by photogrammetric methods or field surveys. Contour maps also present a common source of elevation data that can be used for generating DEMs. However, the under sampling of elevation data between contour lines, especially in flat areas, often results in producing poor quality DEMs. For the purposes of this study, contour maps are the only source of data available for generating a DEM.

4.2.2 DEM errors

The most common errors in DEMs are the presence of artificial sinks and peaks. These errors originate in the DEM as a result of errors in the input elevation data or, in most of the cases, as a result of manipulating integer elevation data. Sinks represent locations of internal drainage that will, if not eliminated, disturb the direction of flow of the channel network (ESRI, 1996). Before using the DEM for extracting hydrological features the sinks must be eliminated.

4.3 Generating a DEM for the study area

A 30 meters resolution DEM of the study area has been extracted from the contour maps at scale 1/50,000 produced by the Royal Jordanian Geographic Centre. The contour interval is 10 metres except for the upper left part of the area that extends into the Syrian territories where the contour interval becomes 25 metres. The change in contour interval appears in the DEM as an area of more generalised or smooth relief. The ARC/INFO-TOPOGRID command is used to generate the DEM. The TOPOGRID command is based on the ANUDEM programme developed by Hutchinson (1989). The programme was originally designed to generate depressionless DEMs from a small number of well-selected elevation data points (ESRI, 1996).

4.3.1 The interpolation algorithm (source :Hutchinson, 1989)

Basically, the procedure for gridding elevation data consists of an iterative interpolation technique coupled with a drainage enforcement algorithm. The interpolation technique uses an iterative method for calculating elevations at regularly spaced grid points from a set of input elevation-data points. The procedure begins with a grid at a coarse resolution and

proceeds with successively finer resolution grids until the user-specified resolution is reached. At each grid resolution the drainage enforcement algorithm is applied to remove any spurious sinks found at this resolution.

The algorithm of drainage enforcement proceeds by first signalling as a sink any grid point of elevation that is equal to or lower than the elevations of its immediate neighbouring points in a 3 by 3 window. Each sink is assumed to have at least one *saddle* point in its vicinity. A saddle point is defined as the grid point that has "at least two immediate neighbour points strictly higher than itself interleaved by a neighbour point no higher than itself" (Hutchinson, 1989). The algorithm associates saddle points with sink points by searching in the downslope direction out of each saddle point until reaching a sink point or the grid boundary. This is illustrated in figure (4-1) where saddle points A, B, C, D E are associated with the sink point S1. Chains are then inserted to link between the sinks. These chain links start at a high elevation sink and continue through the associated saddle point until reaching a lower elevation sink or intersecting with another channel link. Figure (4-2) shows two channel links; the first between S1 and S2 vi the saddle point D while the other one starts at S3 and joins the chain linking S1 and S4.

The final step in the process of drainage enforcement consists of opening the flow path between the sinks along their joining chains. Eventually, this implies that either the sink will

be raised to a certain elevation that allows water to flow out of the sink or the saddle point blocking the passage will be cleared. The action taken depends on whether the sink or the saddle point is verified by an elevation data point There are four possible cases, the first case when the sink is associated with a data value and the saddle is not then the saddle will

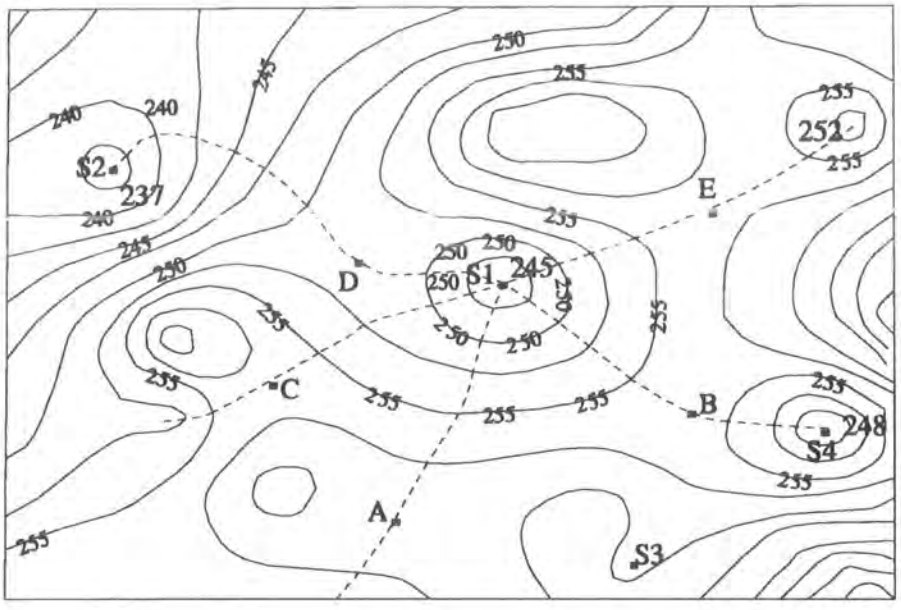

Figure (4 - 1) Associating sinks with saddle points via flow lines (indicated by dash lines)
(Source : Hutchinson (1989))

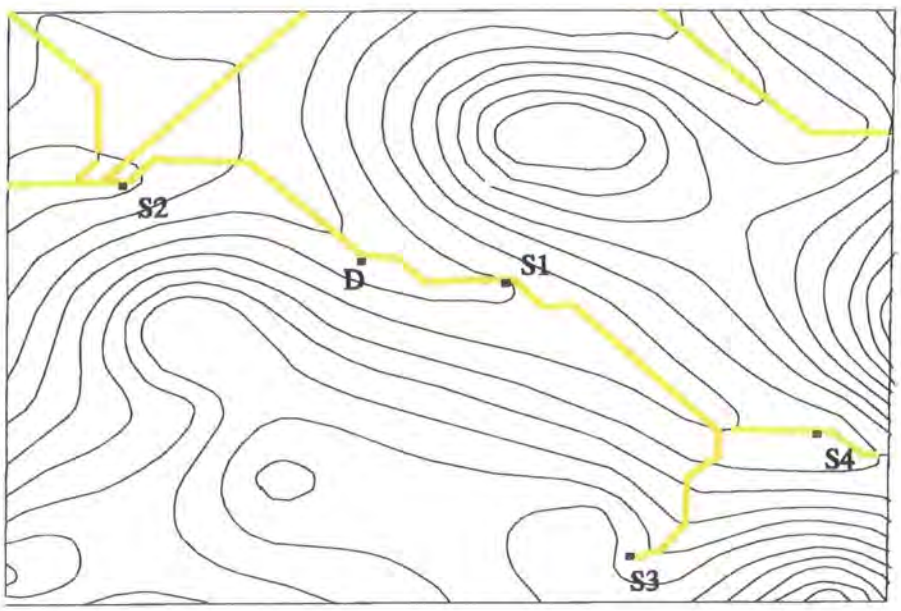

Figure (4 - 2) Results of the drainage enforcement
(Source : Hutchinson (1989))

be cleared. In the opposite case the sink will be raised to a higher elevation than the saddle point. The third case occurs when neither the sink nor the saddle point is associated with an elevation data value, then both of them will be adjusted so that the flow can pass. The fourth case, when both of the sink and the saddle point are associated with elevation values then the user has the choice to decide whether to open the passage or to maintain the sink. Any adjustment made, whether to the sink or the saddle, elevations of all the points along the chain in between will be linearly adjusted. The process of clearing the sinks is controlled by tolerances set by the user. These tolerances define the maximum depth of sinks that can be filled or the maximum height of saddles that can be cleared to open the flow path. sinks of depths beyond the tolerance will remain in the DEM and will be flagged as sinks.

4.3.2 Running the command

Before starting the process of DEM generation the resolution of the output DEM has to be decided. The choice that has been made for Wadi Rajil watershed was to extract the DEM at 30-metre resolution. This resolution is of the order of the graphical error of the 1/50,000-scale maps used in generating the DEM. The 30 metre resolution is also identical to the resolution of the TM satellite images and thus makes a good basis for a raster database that includes both map layers and remotely sensed data. In addition, it has been shown by Quinn *et al* (1993) that at resolutions finer than 50 metres, the widely used concept of single flow path along the steepest flow direction could be applied without significant errors.

4.3.2.1 Manipulating the contour data

In order to cope with the memory requirements of the TOPOGRID command, the contour map data that covers the study area had to be split into 5 smaller blocks. An overlapping distance of 700 metres was maintained between the blocks to ensure smooth transition of elevation data when *mosaicing* the adjacent blocks. TOPOGRID was run for each block independently and all the blocks where then *edgmatched* and combined together. Figure (4-3) shows the resulting DEM.

4.3.2.2 Incorporating the channel network

To enable accurate enforcement of the drainage channel network in the generated DEM, the topographic map layer of the wadis network needs to be provided as input to the TOPOGRID command. Before inclusion of the wadis, all the wadis have to be digitised according to the downstream direction. Since the maps were not digitised according to downstream direction, an automatic procedure was implemented to flip the direction of wadis as required. The procedure consists of the following steps:

1. Convert the wadi arcs into nodes in point coverage (using the ARC-NODEPOINT command).
2. Associate an elevation value with each node according to the elevation of the nearest contour line (using the ARC-NEAR and RELATE commands).
3. Select and flip all the arcs with the from-node elevation lower than the to-node elevation (using ARCEDIT module).

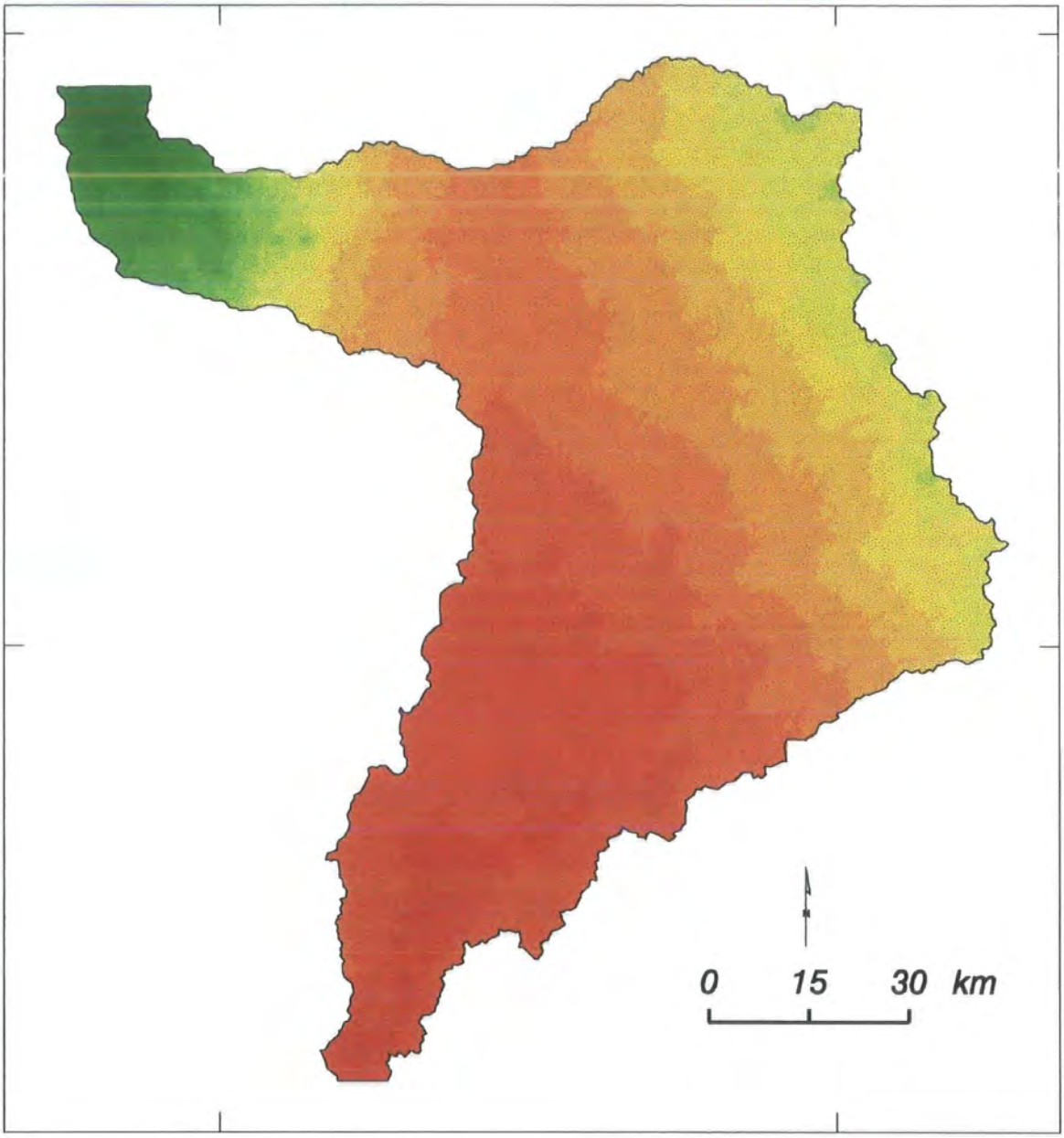

Figure (4 - 3) The digital elevation model of wadi Rajil watershed

4.3.2.3 Clearing the sinks

The automatic clearing of sinks as performed by the TOPOGRID command is controlled by the user-defined tolerances and hence, many sinks may still remain uncleared after running the command.

These sinks must be cleared before using the DEM for extracting hydrological features. At this stage it is important to look at the depth values of the sinks and to check for any sinks resulting from errors in the input data. The procedure of clearing the remaining sinks involves running a sequence of GRID functions that can be run automatically using the ARC/INFO GRID-FILL function.

4.3.3 Assessment of the quality of the DEM

The quality of the DEM depends on the quality of the original data used in its extraction and the errors introduced by the interpolation method. In addition, the resolution at which the DEM was originally extracted controls the resolution of any hydrological features extracted from it.

The accuracy of the DEM can be tested at two levels: relative and absolute. The relative accuracy of the DEM has been checked by interpolating the contour lines from the DEM and comparing the results with the original map contours. As shown in figure (4-4) there is a good match, in general, between the two sets of contours. The differences in the flat areas are mainly due to the low density of the original contour lines.

The absolute accuracy measures the precision of the elevation data extracted from the DEM with respect to an independent reference level. The test for the absolute accuracy consists of comparing the DEM-interpolated elevations for a set of well-distributed points with their corresponding field-measured elevations. A set of 114 points distributed over the

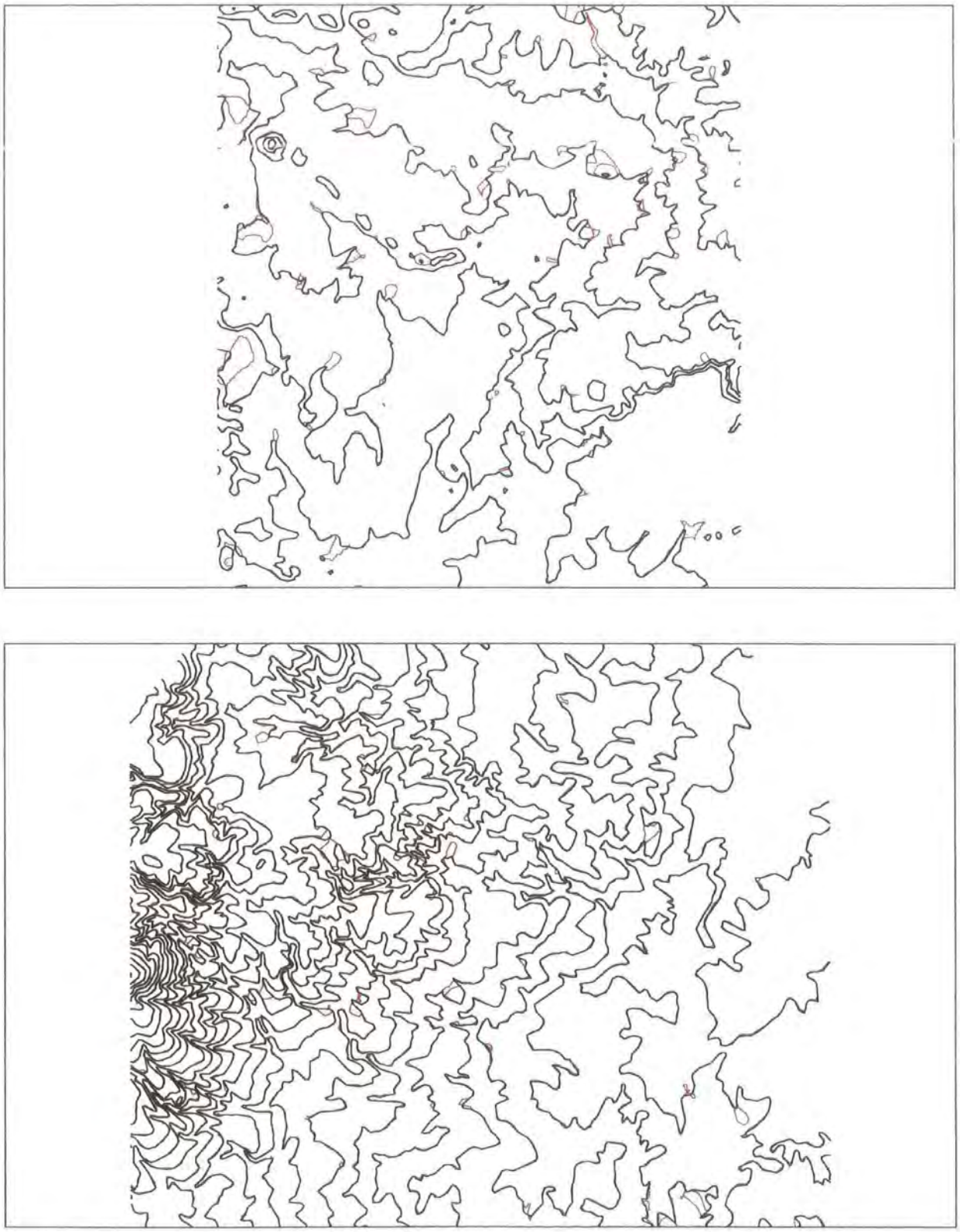

Figure (4 - 4) Comparison between the contour lines generated from the DEM with the map contours in a flat area (up), and a hilly area (bottom)

area, as shown in figure (4-7), were used in the test. The Royal Jordanian Geographic Centre conducted Field measurements of the elevations of these points using GPS surveying in 1995. The same set of points was used for the extraction of DEM from space imagery by Al-Rousan at Glasgow University. The results of the absolute accuracy test has shown a mean error of 21.08 metres and a standard deviation of 3.97 metres. As shown in appendix(2) the test results have indicated a constant systematic error of about 20 metres for most of the points. Actually, this difference between the GPS heights and the map heights is due to the difference between the *geoid* and the *ellipsoid* in the area which implies that all GPS heights have to be reduced by an average value of 20 metres. Therefore, subtracting 20 metres from all the elevation differences results in reducing the mean error to 1.82 metres and the standard deviation of 3.89 metres. This implies that the absolute accuracy of the generated DEM is about 4 metres which is of the same order as the mapping accuracy of the contour lines usually estimated as half the contour interval.

4.4 Extraction of the channel network

Channels on a DEM are defined as "all points with accumulated area above some threshold" (O'Callaghan and Mark (1984) according to Tarboton *et al*, 1993). Accordingly, the procedure for extracting channels from DEMs as described by O'Callaghan and Mark (according to Tarboton *et al*, 1993) consists of the following steps:

1. Create a depressionless DEM.
2. Calculate the flow accumulation grid.

Extract channels by a thresholding process where cells are identified as wadi channel cells if their accumulation exceeds a certain threshold.

Other algorithms for extracting networks from DEMs are discussed in Burrough (1990) and Tarboton *et al* (1990).

4.4.1 Application of the procedure

There are two basic concepts behind the procedure of automatic extraction of the drainage network. First, the flow of water from each cell to the watershed outlet follows always the same path. Secondly, the flow path is one-dimensional and follows the direction of the steepest slope. Although it may not be representative of the real water flow conditions, the single flow direction has the great advantage of simplifying the complex flow dynamics (Maidment, 1993).

In this section the procedure of extracting the channel network for Wadi Rajil watershed is described.

4.4.1.1 Creating the flow direction grid

The flow direction information represents one of the key elements for defining the flow pathways (ESRI, 1996). The most widely used approach to define the flow direction is based on the single flow direction concept where water is assumed to flow out of each cell into one of its eight immediate neighbour cells in a 3 by 3 window. The flow takes place along the steepest slope direction.

The GRID-FLOWDIRECTION command calculates the slopes along all the eight directions out of each cell and determines the steepest slope accordingly. The formula used is as follows,

$$S = \frac{\Delta z}{D}$$

where,
S : slope,
Δz : change in elevation between cells,
D : distance between cells.

The distance between cells is given as follows

$D = 1 *$ cell size for the orthogonal cells (figure 4-6)
$D = \sqrt{2} *$ cell size for the diagonal cells

Once the direction of the steepest slope is found the number indicating the cell in that direction (see figure 4-5) is allocated to the processing cell.

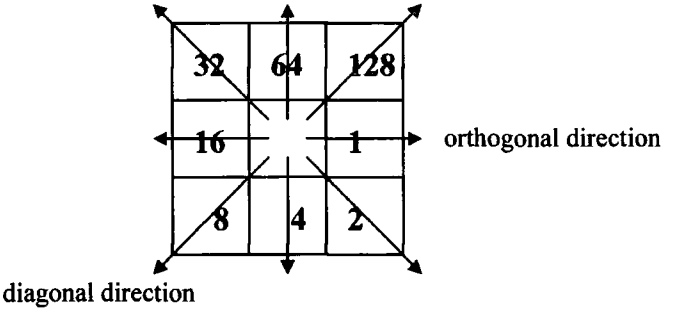

Figure (4-5) A 3 by 3 cell arrangement showing the directions of flow out of the process cell
(Source : ESRI, 1996)

In cases where no steepest slope is found or when a steepest slope is found in more than one direction the processing cell is signalled as a sink that needs to be filled later.

4.4.1.2 The flow accumulation grid

The single flow direction implies that the whole quantity of water that accumulates at a cell location will flow out of the cell into one of its neighbour cells. A study of Quinn *et al* (1993) has shown that the single flow direction concept gives the impression of rapid concentration of overland flow into channels, while the multi direction flow shows a more realistic pattern of the distribution of overland flow. On the other hand, when the water flow reaches a channel it will flow in a concentrated manner and therefore, the single flow

direction represents the channel flow better than the multi-direction flow which tends to redistribute the flow out of the channel.

The computation of the flow accumulation is carried out by the GRID-FLOWACCUMULATION command, which performs the computation for each cell according to the flow direction defined by the FLOWDIRECTION command.

4.4.1.3 Channel extraction

The channel network is usually represented as a tree with its root at the watershed outlet. The network consists of nodes and links. The nodes represent the points where two sections of the network join. The exterior nodes of the network are called sources (Tarboton *et al,* 1993). The links are the channel sections that link between the nodes. The links are classified as exterior links and interior links. Exterior links are the sections connecting a source and a node, while interior links are the sections linking between two nodes.

The process of extracting channels from the flow accumulation grid consists of selecting the cells with accumulation flow exceeding a certain threshold value. An important issue here is to decide at which threshold should the channels be extracted. Tarboton *et al* (1993) suggests extracting the channels at a density equivalent to that of the blue lines on the topographic maps. The drainage density is defined by Horton (according to Tarboton *et al*, 1993) as,

$$D_d = \frac{L}{A}$$

where,

D_d : drainage density (km^{-1}),

L : total distance of channels (km),

A : the contributing area (km^2).

Experiments on extracting the drainage network at different threshold values has resulted in the drainage densities shown in table (4-1). It is seen from the table that the drainage network extracted at threshold value of 250 cells provides a drainage density comparable to that of the topographic blue lines network. Figure (4-6) shows an example of the channel network extracted at different thresholding values. The figure clearly indicates that a threshold of 250 pixels is required to achieve a drainage density equivalent to that of the mapped wadi-network.

Table (4-1) The drainage densities of the channel network at different threshold values

Threshold value	Drainage density (km^{-1})
250 cells	1.43
500 cells	1.09
1000 cells	0.8
5000 cells	0.4
wadis-line and wadi spread areas (map 1/50000)	1.9

4.4.2 Assessment of the extracted drainage network

A comparison between the extracted drainage network and the original wadi blue lines show a perfect match over the whole area (figure 4-8). In addition, the extracted network links the drainage lines through the *qa'* areas where the original topographic wadis appear disconnected. The extracted links are only estimates of the flow pathways and need to be verified using Arial photographs or high-resolution satellite images. However, these links have little significance on the modelling process for two reasons: first, the average length of these links is less than 1 km; secondly, each link is connected to a single downstream link and therefore no split of the downstream flow is expected.

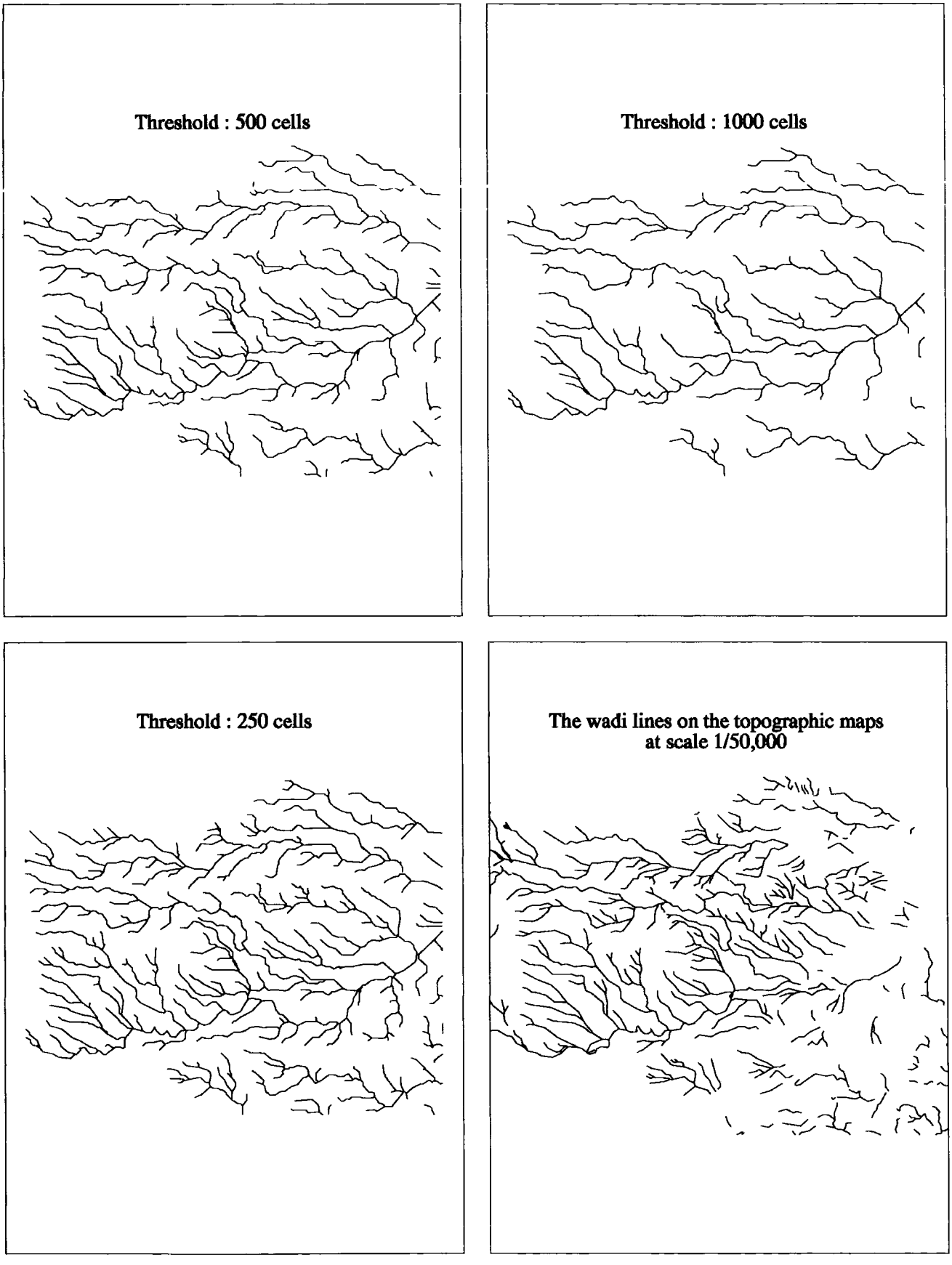

Figure (4 - 6) Examples of extracting the drainage network at different threshold values

(Based on Tarboton et al, 1993)

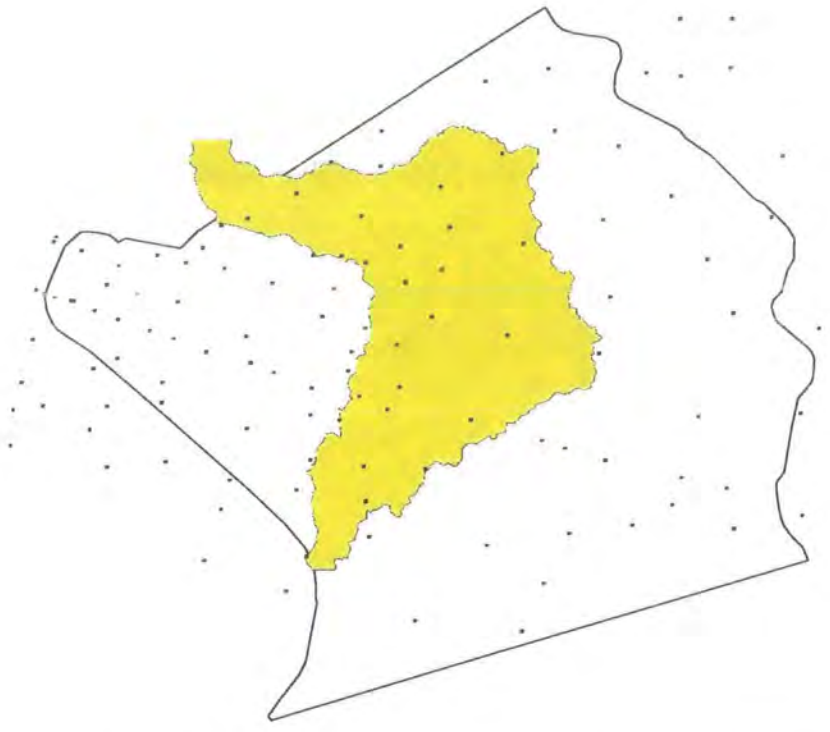

Figure (4 - 7) The distribution of the GPS control points within the study area

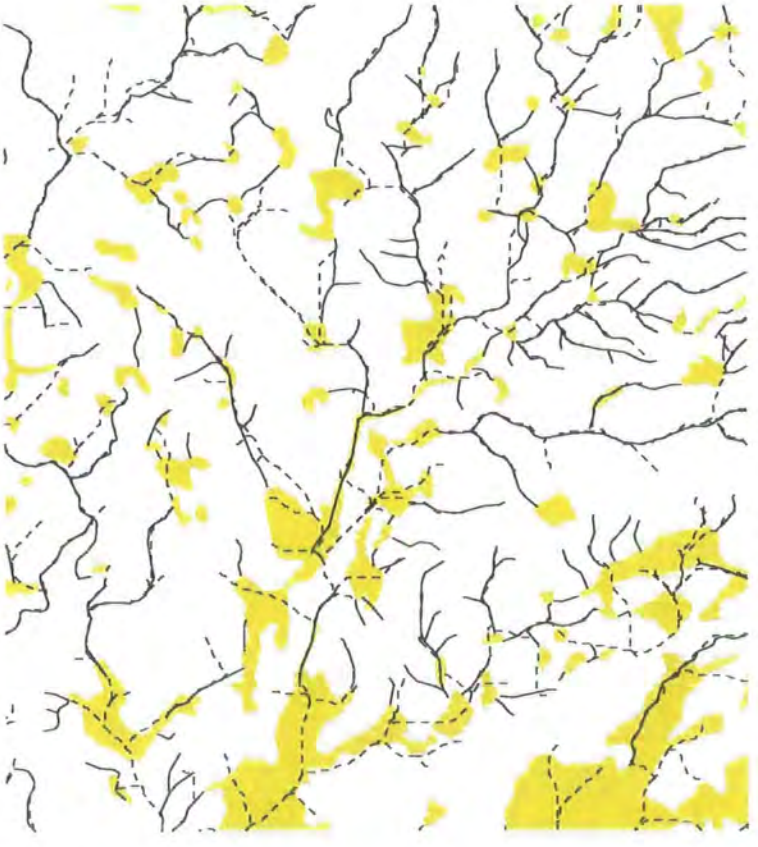

Figure (4 - 8) The discontinuity of the map blue lines througth the qa'a areas. The dashed lines represent the streams extracted from the DEM

The following paragraphs present quantitative assessment of the extracted drainage network by investigating the applicability of some of the Horton ratios and laws that characterise the drainage channel networks.

4.4.2.1 The Horton ratios

The mathematical representation of the Horton ratios is given as follows (Tarboton *et al*, 1993),

$$R_b = N_{w-1} / N_w$$
$$R_l = L_{w-1} / L_w$$
$$R_s = S_{w-1} / S_w$$

where,
N_w : the number of links of order w,
L_w : the mean length of links of order w,
S_w : the mean slope of links of order w.

These ratios are approximately constant for any drainage network. In order to apply these ratios the drainage network is ordered according to Strahler/Horton ordering system (figure 4-9). The mean values of channel lengths, slopes and the frequency of channel links are calculated for each order. Table (4-2) illustrates the results of the application of the above ratios for the extracted drainage network of Wadi Rajil. The table shows that the Horton ratios are relatively constant especially for the lower order links. Arcs representing higher order links are subject to be intersected by small arcs of insignificant lengths created by the procedure of automatic extraction of drainage network. Although these small arcs do not affect the Strahler order of the higher order links their intersections with these links are, however, recognised as nodes. This will result in segmenting the arcs of the higher order links into smaller arcs that will affect the Horton ratios for these links.

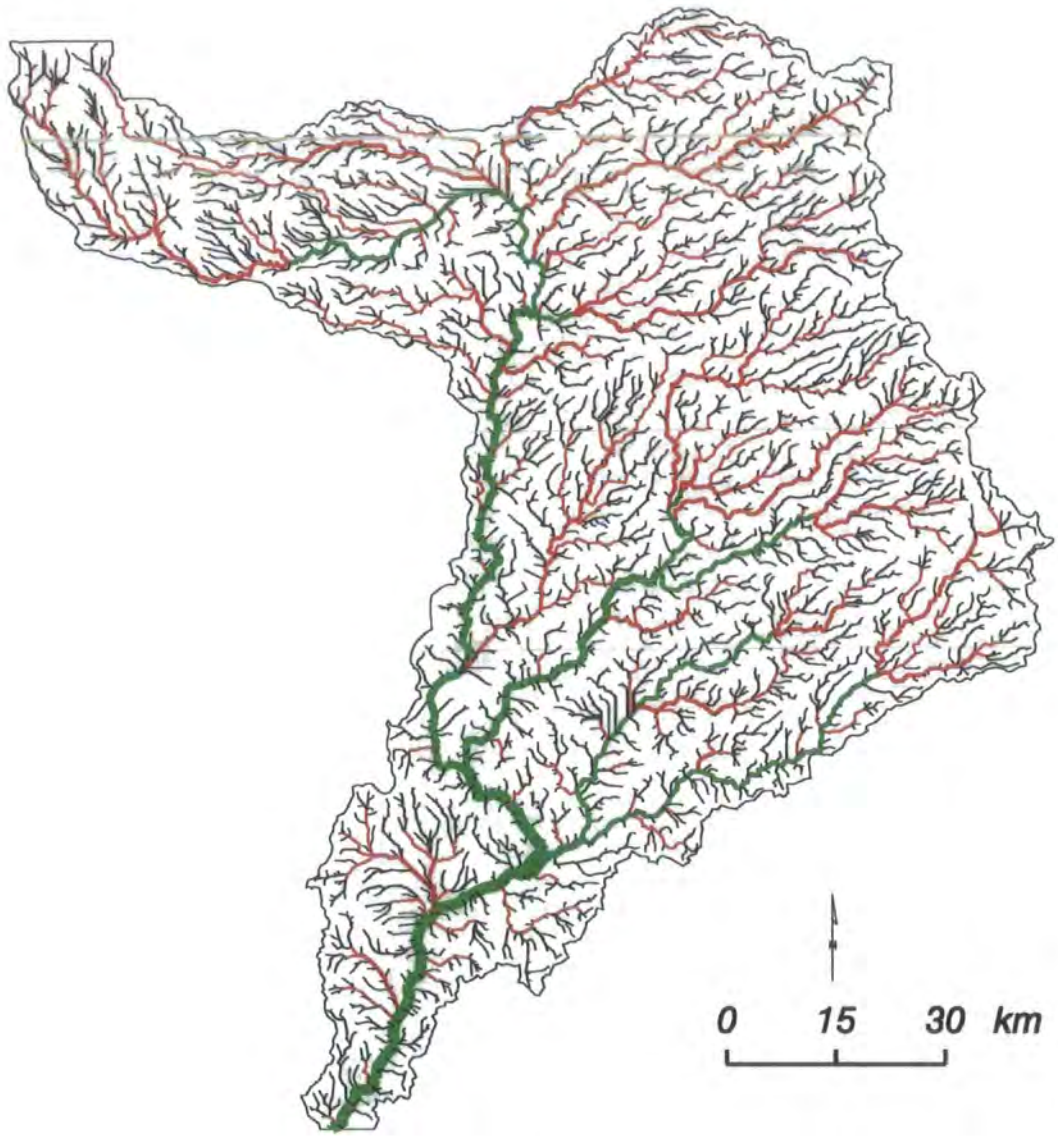

Figure (4 - 9) The Strahler orders of the extracted drainage network

Table (4-2) Application of the Horton ratios for the extracted drainage network

Stream order	Mean length L_w (metre)	Length ratio L_w / L_{w-1}	Mean slope S_w	Slope ratio S_{w-1} / S_w	Frequency N_w	Freq. ratio N_{w-1} / N_w
1	712		.0137		2499	
2	1484	2.084	.0107	1.280	613	4.076
3	4396	2.962	.0089	1.202	128	4.789
4	10649	2.422	.0062	1.435	28	4.571
5	19374	1.819	.0051	1.215	6	4.666
6	25545	1.318	.0019	2.684	3	2.000
7	42231	1.653	.0011	1.727	1	3.000

4.4.2.2 Horton's slope law

Horton's slope law quantifies the relationship between the slopes of links of successive orders. This relationship can be described by the following equation,

$$S_w = (R_s S1) R_s^{-w}$$

Table(4-3) shows the results of computation of the mean slope S_w for all link orders based on the mean slope of links of order 1. The value of R_s (i.e. 1.283) is taken as the average slope ratio of the links of order less than five. The table shows that Hortons slope law applies well for all the orders except the upper two orders. This is mainly due to the biased choice of the value R_s used in the formula.

Table (4-3) Application of the Horton slope law for the extracted drainage network

Stream order	Mean slope S_w	Computed mean slope
1	0.0137	
2	0.0107	0.0107
3	0.0089	0.0083
4	0.0062	0.0065
5	0.0051	0.0050
6	0.0019	0.0039
7	0.0011	0.0030

4.5 Watershed delineation

The watershed is "the upstream area contributing flow to a given location" (ESRI, 1996). It has been recognised that delineating watershed boundaries by manual methods is a laborious and not very accurate procedure. The automatic delineation of watershed boundaries relies mainly on defining all the cells that contribute flow to a given cell. The method can also be applied to delimit the watershed area that contributes flow to a given channel link instead of an outlet point. Using this feature, a hierarchy of sub-watershed levels can be defined in a scaled manner where each sub-watershed is drained by a single link. For each sub-watershed the important hydrological parameters like input node, outlet node, area, length of main channel, slope, upstream contributing area, and downstream link can be defined.

4.6 Summary

The automatic extraction of the drainage network has the critical advantage of providing a continuous network that can be used for modelling the surface runoff in the study area. This chapter has discussed the procedure of extracting the drainage network and the delineation of the sub-watershed structure for Wadi Rajil. The threshold value at which the network was extracted has been set to provide a drainage density that is approximately equivalent to that of the 1/50,000 topographic wadi network.

CHAPTER 5

DESCRIPTION OF WADI RAJIL HYDROLOGICAL DATABASE

5.1 Introduction

In a GIS application, a database is the core element that the different application components access for retrieval of information or adding new data. The need for a database is more obvious for resources management applications like hydrology where a wide range of relevant data have to be handled and analysed. This need justifies the effort spent on designing and building the database usually estimated to consume 60 to 80 % of the whole project duration.

Basically, a database is a computerised record keeping system to hold and manage the data used by a given application (Date, 1995). Furst *et al* (1993), define the database for a groundwater application as "a large amount of different categories of data that form the model of the groundwater system in the computer". This definition also applies to the database of a surface water system.

The first part of this chapter describes the structure of a database for surface water applications in Wadi Rajil watershed area. The second part describes a query application to provide information on the characteristics of the watershed and the channel drainage network.

5.2 The general structure of a GIS database

A GIS database is a collection of interrelated data about the location, shape and characteristics of geographic features (ESRI, 1992). These data are stored as tables in a relational database system. Shapes and locations are represented using a geo-relational data model where spatial data are linked to their attribute tables by internal links created and maintained by the GIS system. Using these links the data in the database can be accessed by specifying the location or any of the descriptive attributes. The data can also be accessed by specifying the spatial relationship that connects the data to other geographical features in the database. Besides the system-defined links between the geographical data and the attributes, relationships can be established between any two tables in the database that share a common item (ESRI, 1992).

5.3 Building a database for Wadi Rajil watershed

Building a database consists of two phases, designing the database and automating the data. In the design phase a conceptual model that aims to define an optimised structure of the database entities and their relationships is prepared. The design phase provides a detailed description of the specifications of the data to be collected and stored in the database. The automation phase is concerned with bringing the data into the database, insuring co-ordinate registration, checking consistency of the data and setting quality control procedures (ESRI, 1992).

5.3.1 Database design

The basic objective of the design phase is to decide upon a suitable structure for the data in the database (Date, 1995). In the case of a GIS database this can be interpreted as deciding upon the data layers to be included in the database and the attributes that should be assigned to the features of each layer.

There is no standard procedure to follow for the design of the database. However, the design should reflect the intended applications and the user needs. Therefore, a detailed description of the objectives of the database and the functions it should serve is an essential pre-design step. Once the functions of the database are defined, a top-down approach is usually used to complete the design process. This approach consists of the following sequence of steps.

1. Define the themes to be included in the database.
2. Organise the themes into data layers.
3. Define the attributes of each layer.

5.3.1.1 The database objectives

When building a database from scratch a considerable knowledge of the future applications of the database is required. This knowledge is usually based on surveys of the user needs or can be based on the objectives of the project or the organisation for which the database is built. The main function of the database is to provide support for the surface water studies in the area. This includes providing detailed description of the watershed characteristics and active hydrological processes in the area. The specific objectives of the database are based on the objectives of this research and can be summarised as follows:

1. To provide information about the hydrological parameters of the watershed. The information can be obtained by browsing the database layers or performing queries on the data.
2. To provide support for the query application described later in this chapter.
3. To provide support for the modelling exercise described in chapter six.

5.3.1.2 The database layers

The geographical data layers are the main objects or entities of a GIS database. The term *layer* usually refers to the digital representation of a theme that extends over the whole geographical area represented in the GIS database (ESRI, 1992).

The database layers can be classified into two groups, the basic layers and the derived layers. The basic layers represent the original sources of information of the database. These layers are produced and maintained by specialised institutions using field-surveying techniques. The derived layers are produced by processing the basic layers or other derived layers. From a functional point of view the derived layers are further classified into three groups:

1. Hydrological parameters layers
2. Watershed characteristics layers.
3. Model layers.

Table (5-1) shows a complete list of the database layers. The structure of the database is shown in figure (5-1).

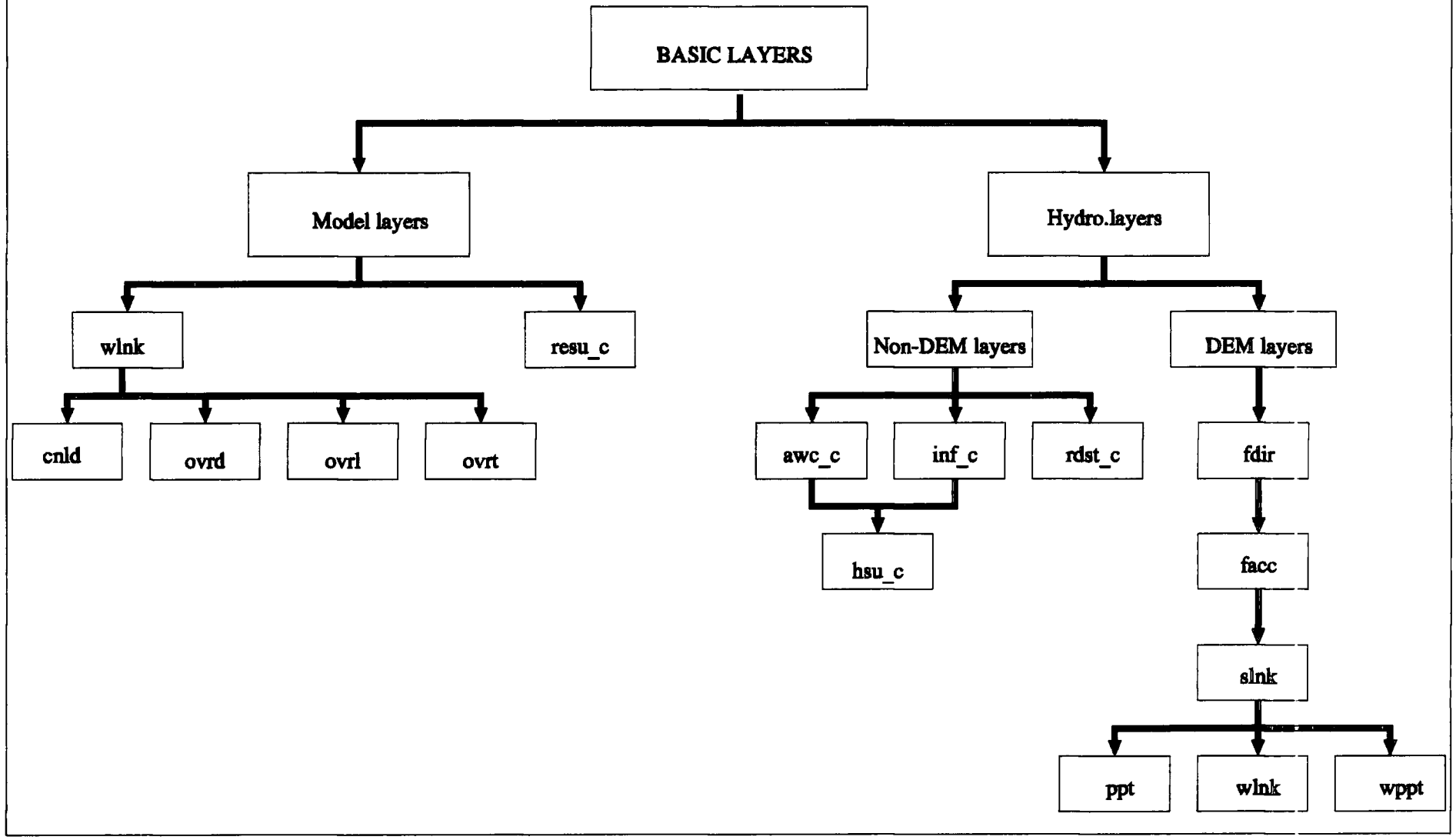

Figure (5 - 1) The layer structure of the Wadi Rajil database

5.3.1.3 Layer attributes

The attributes are the descriptive information associated with the geographical features. The attributes are related to their corresponding features by internal system links. The layers attributes are provided in appendix (3).

Table (5-1) The database layers

Category	Layer name	Data structure	Brief description
Basic layers	cont_c	vector-line	contour lines
	wadi_c	vector-line	wadis network
	wsprd_c	vector-polygon	wadi-spread areas
	qa'_c	vector-polygon	mud-flat areas
	spoth_c	vector-point	spot heights
	soil_c	vector-polygon	soil classification
	geo	grid	basalt formations
	clst_c	vector-point	climate stations
Hydrological parameters	rdst_c	vector-polygon	rainfall distribution
	inf_c	vector-polygon	infiltration
	awc_c	vector-polygon	available water holding capacity
	evap_c	vector-polygon	evaporation
	hsu_c	vector-polygon	hydrologically similar units
Watershed charact.	dem	grid	digital elevation model
	fdir	grid	flow direction
	facc	grid	flow accumulation
	slnk	grid	drainage network links
	slnk_c	vector-line	drainage network links
	wlnk	grid	sub-watersheds for links
	wlnk_c	vector-polygon	sub-watersheds for links
	ppt_c	vector-point	drainage network nodes
	wppt	grid	sub-watersheds for nodes
Model layers	resu_c	vector-polygon	rainfall-excess similar units
	subw_c	vector-polygon	sub-watersheds structure
	ovrd	grid	cell-based overland flow distance
	ovrt	grid	cell_based time-of-flow parameter
	ovrl	grid	cell_based trans. losses parameter
	cnld	grid	sub-watershed channel distance

5.3.2 Data automation

Secondly, the co-ordinate system of the database should be defined. Registration of all the database layers to the same co-ordinate system is an essential requirement to enable accurate overlay processing. The co-ordinate system used in the database is the Jordan Transverse Mercator projection (JTM). The projection parameters are as follows:

-Spheroid : Hyphord 1909

-Central meridian : 37^{o} east

-Scale factor : 0.9998

-False easting : 500,000 metres

-False northing : -3000,000 metres

The following paragraphs describe the database layers and the data conversion techniques used to generate each layer.

5.3.2.1 The basic layers

A. The topographic layers (*cont, wadi, wsprd, qa', spoth*)

These layers are extracted from the topographic maps of Jordan at scale 1/50,000. The maps were produced and digitised by the Royal Jordanian Geographic Centre. However, the layers required checking for *edgematching* and attribute coding before being integrated into the database. Furthermore, the wadis network layer (*wadi*) has to be manipulated to ensure that the wadis line segments are coded in a downstream direction. This is an essential requirement for both the DEM extraction, discussed in chapter four, and the determination of the upstream links that contribute flow to a given point as required for the query application discussed later in this chapter. Figure (5-2) shows the topographic layers.

B. Climate-stations layer (*clst*)

This layer represents the locations of the climate stations in and around the study area. The Department of Meteorology in has provided the co-ordinates of the stations

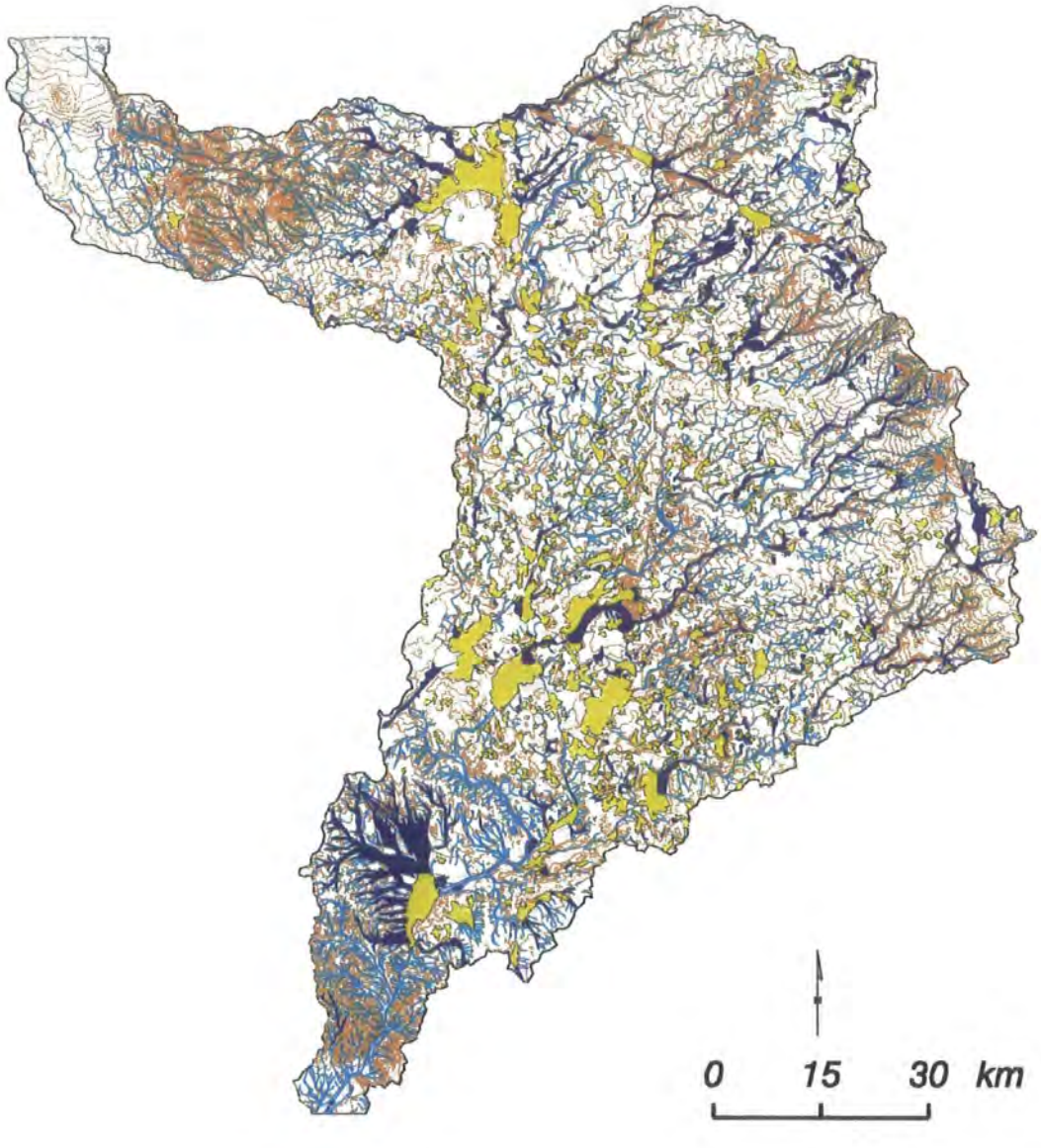

Figure (5 - 2) The topography layer

decimal degrees. A point-layer has been generated from the stations' co-ordinates. The estimated accuracy of the station locations is about 500 metres.

C. The geology layer (*geo*)

Figure (2-6) provides a generalised view of the main basalt formations in the study area. A more detailed surface lithology map was derived from a supervised classification of a Landsat Thematic Mapper image from 1995. The TM image was geometrically corrected to the topographic maps at scale 1/50,000. Training sites were selected from the field and from the available geological maps. Four geological maps at scale 1/50,000 covering parts of the area were used to help select the training sites. Figure (5-3) shows an index map of the geological maps and the TM image. The geological maps were scanned and registered to the JTM co-ordinate system. By overlaying the scanned maps and the TM image the training sites could be accurately delimited. A minimum number of six training sites were selected for each basalt formation. Figure (5-4) shows some of the training sites used in the classification. An evaluation of the spectral separability of the different formations was performed by plotting the means and standard deviations of the signature files. Figure (5-5) illustrates the ellipses of the signature files for the different formations. The figure suggests that the following formations can be separated: *Ushayhib* (UB) from *Asfar* group, *Fahdal* (a sub-class of *Fahda* FA) from *Bishriyyah* group, *Abed* (AOB) from *Safawi* group and *Aritain* (AT) from *Rimah* group. Other formations show similar spectral characteristics and therefore, cannot be uniquely distinguished using the selected signatures (ERDAS, 1995). White (1996) has shown that even under laboratory conditions the spectral characteristics of the basalt formations are very similar. However, the results of a maximum likelihood classification has shown that some of the basalt formations can be correctly classified as shown in the contingency table (Appendix 4). The relative

accuracy of the classification has been investigated for a number of selected areas by an overlay of the geological map and the classified image (figure 5-6). The verification has shown that the classification was more precise for the areas of homogeneous basalt cover as compared to the areas with mixture of different basalt formations. An overall evaluation of the classification results suggests that *Abed, Salman, Fahdal, Aritain,* and *Ushayhib* can be separated with adequate accuracy. A similar classification by Francis (1995) has shown that *Salman, Madhala, Abed, and Fahda* formations can be identified. Figure (5-7) shows the classified lithological layer. The lithology layer can be useful for the study of surface roughness, which controls the overland flow velocity. In addition, knowledge of the permeability of the surface rocks is useful to estimate a representative curve number for the area.

D. Soil layer (*soil*)

This layer is extracted from the soil map of Jordan at scale 1/250,000 produced by Hunting Technical Services for the Ministry of Agriculture and digitised by the Royal Jordanian

Geographic Centre. The soil map of Jordan consists of seven map sheets at scale 1/250,000 covering Jordan. The maps were produced from analysis of Landsat images and aerial photographs and complemented by field surveying. At this scale the soil classification is carried out at the soil-unit level. Each soil unit is associated with a legend that briefly describes the soil sub-groups that occur within the soil-unit and indicates the number of a representative profile for the subgroup (Hunting, 1993). Appendix (5) shows a sample soil-unit legend and a representative profile for one of its constituent subgroups. Figure (5-8) shows the soil layer.

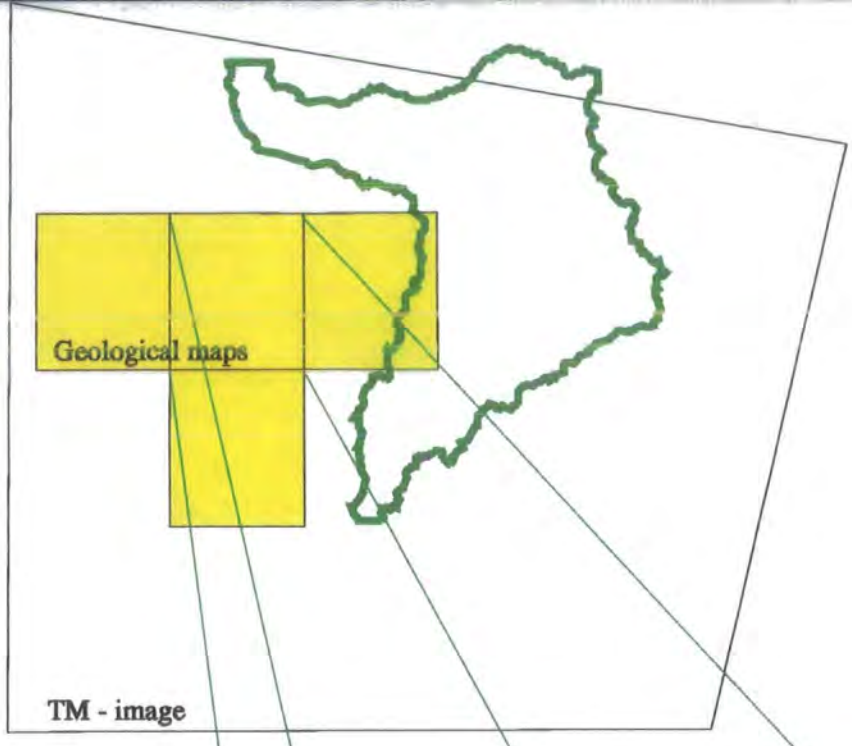

Figure (5 - 3) Index of the TM image and the geological maps used for basalt classification

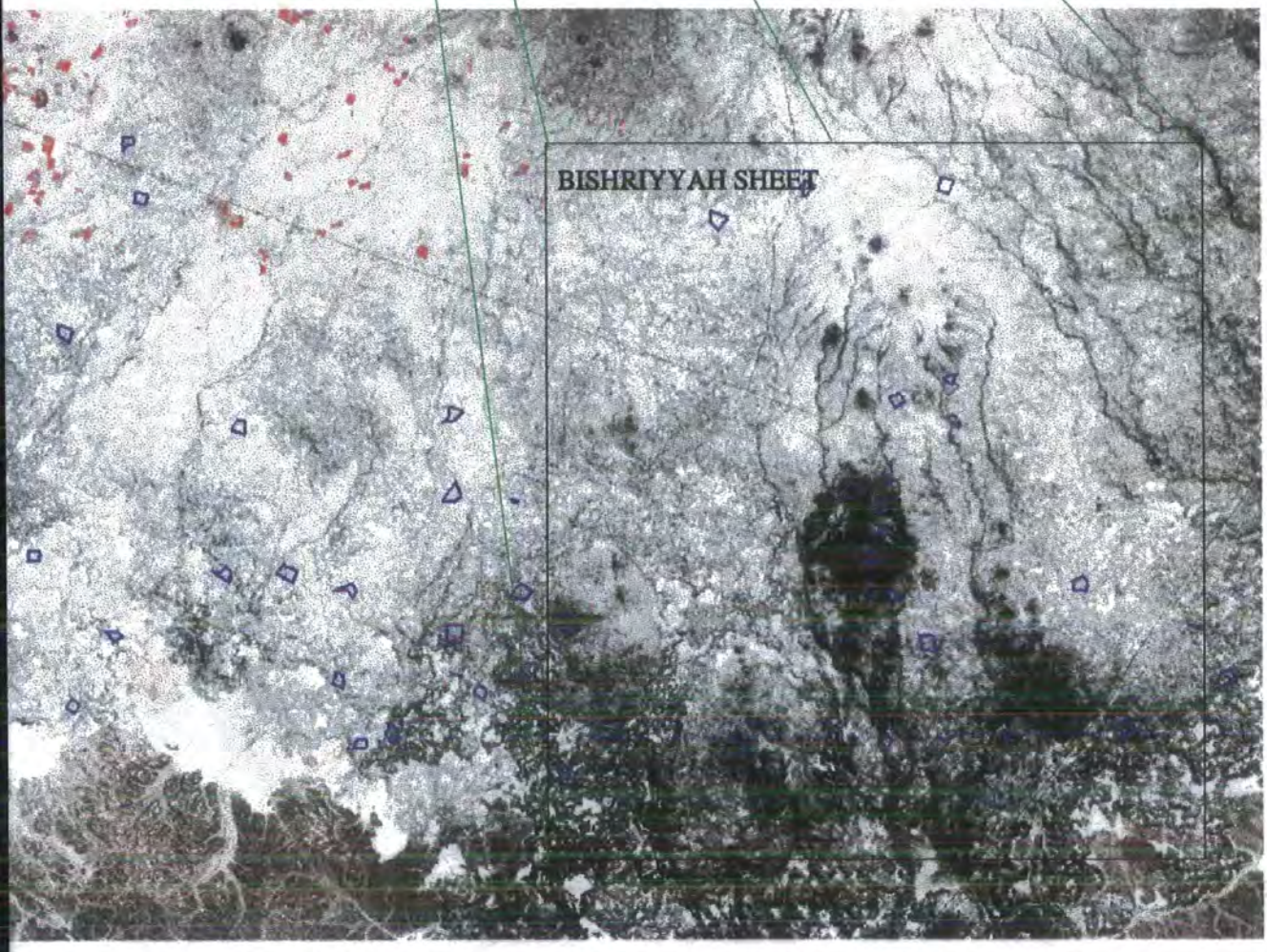

Figure (5 - 4) Locations of the training sites used in the supervised classification

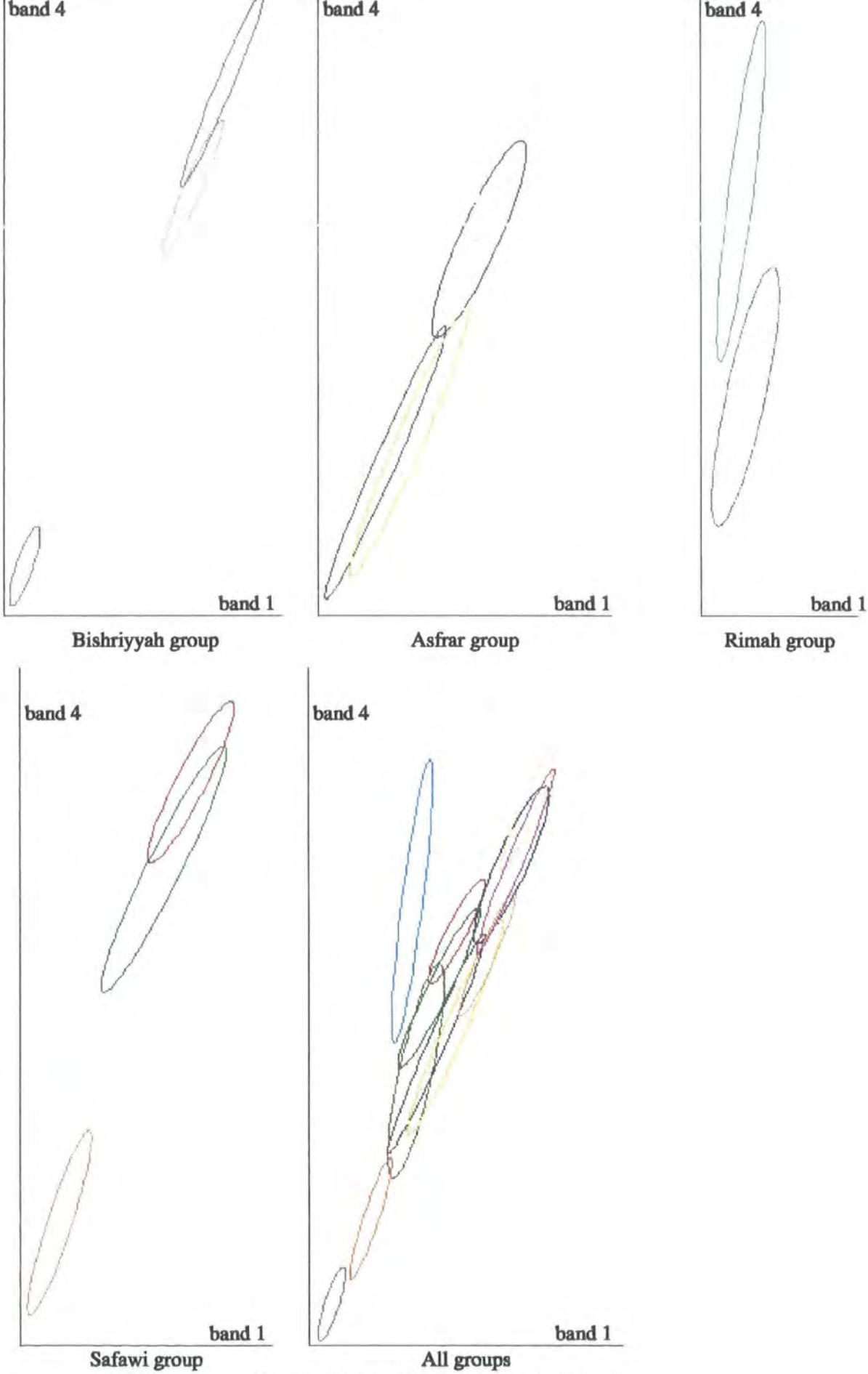

Figure (5 - 5) Ellipses of the signature files

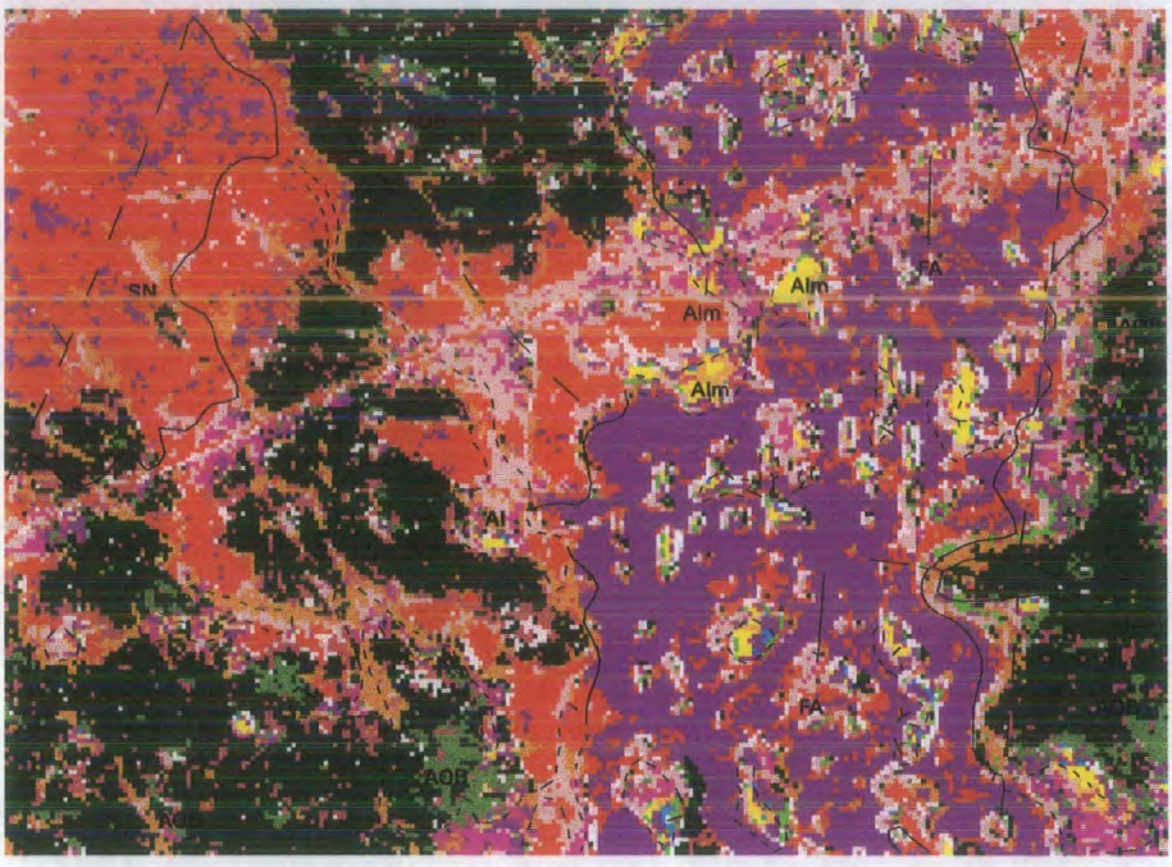

AREA 1

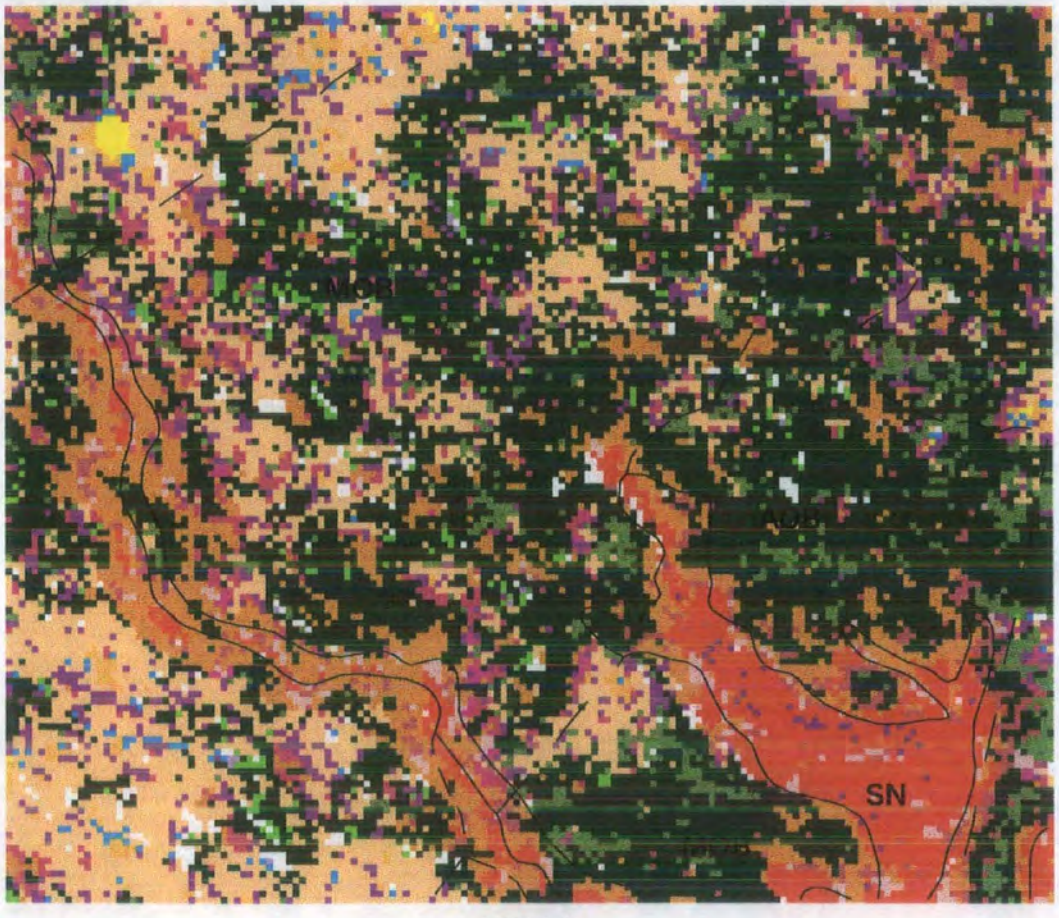

AREA 2

Figure (5 - 6a) Comparison between the geological map and the classified image

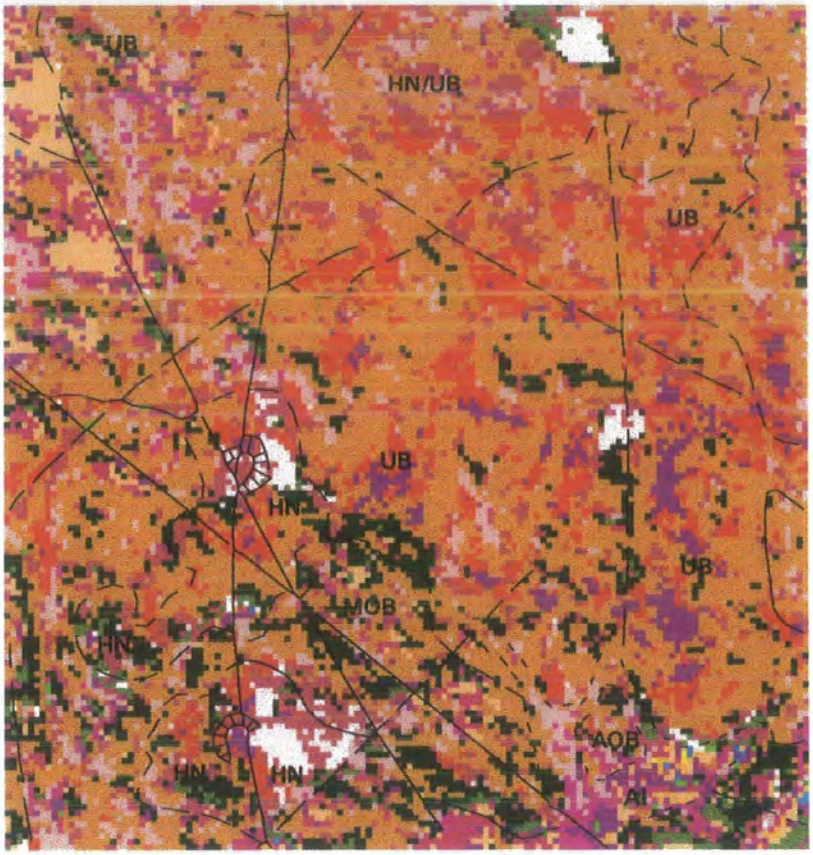

AREA 3

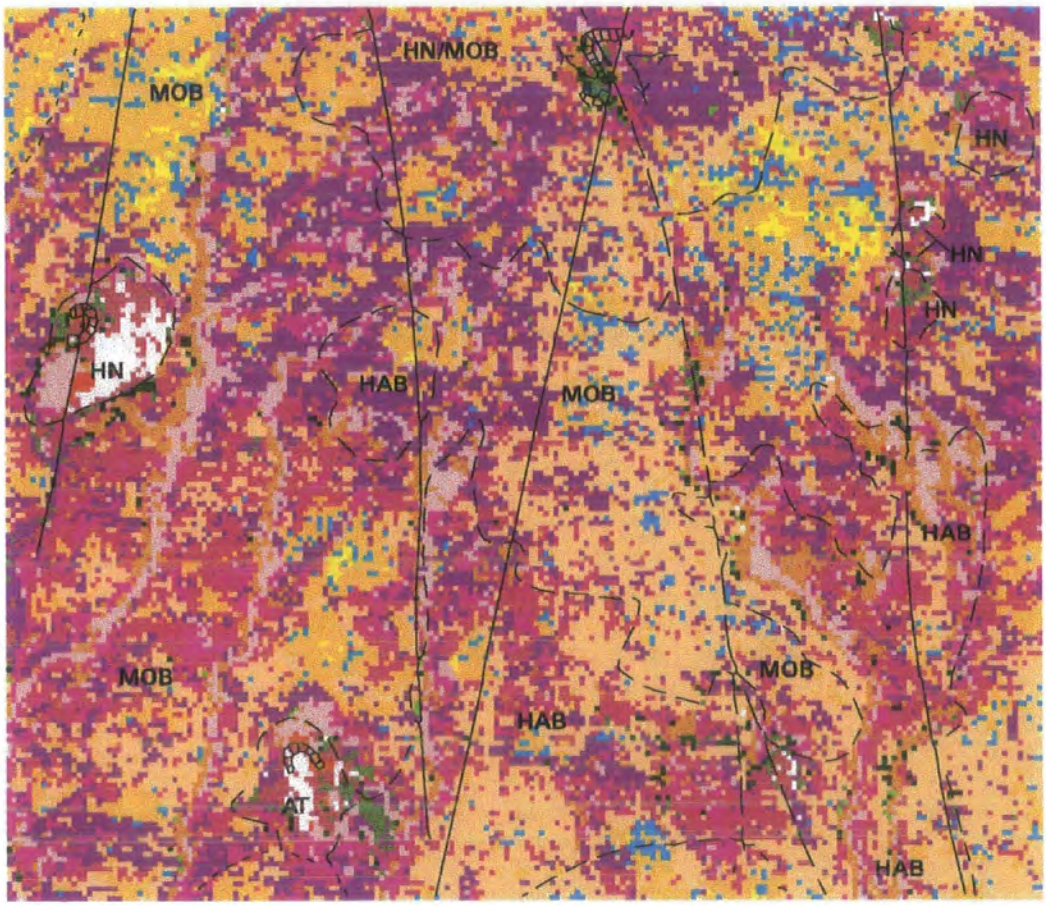

AREA 4

Figure (5 - 6b) Comparison between the geological map and the classified image

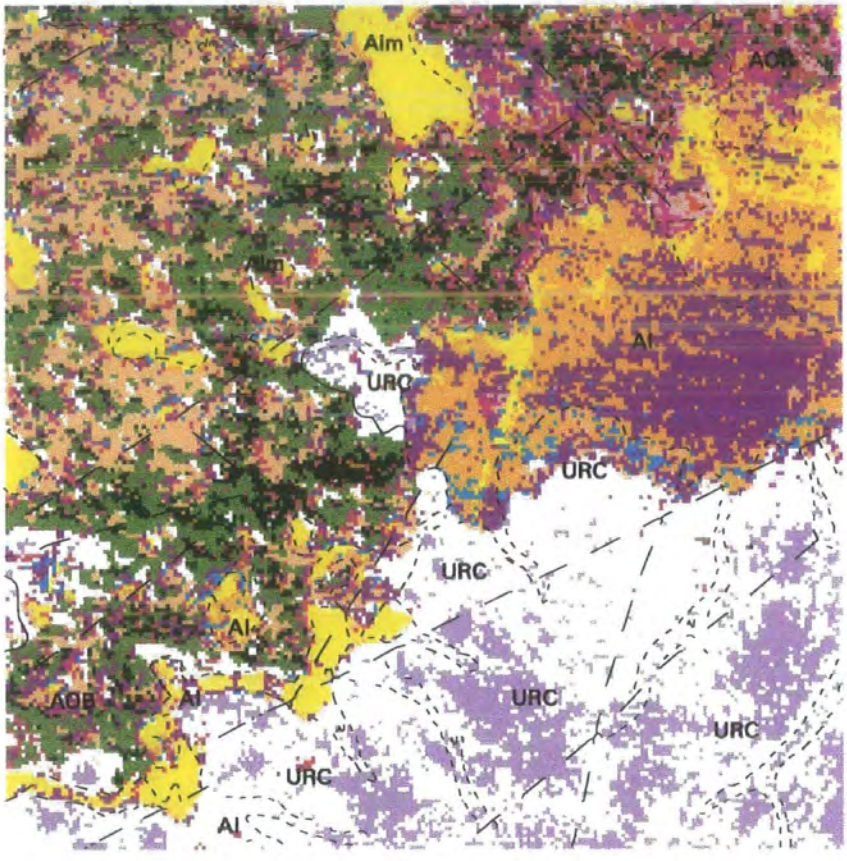

AREA 5

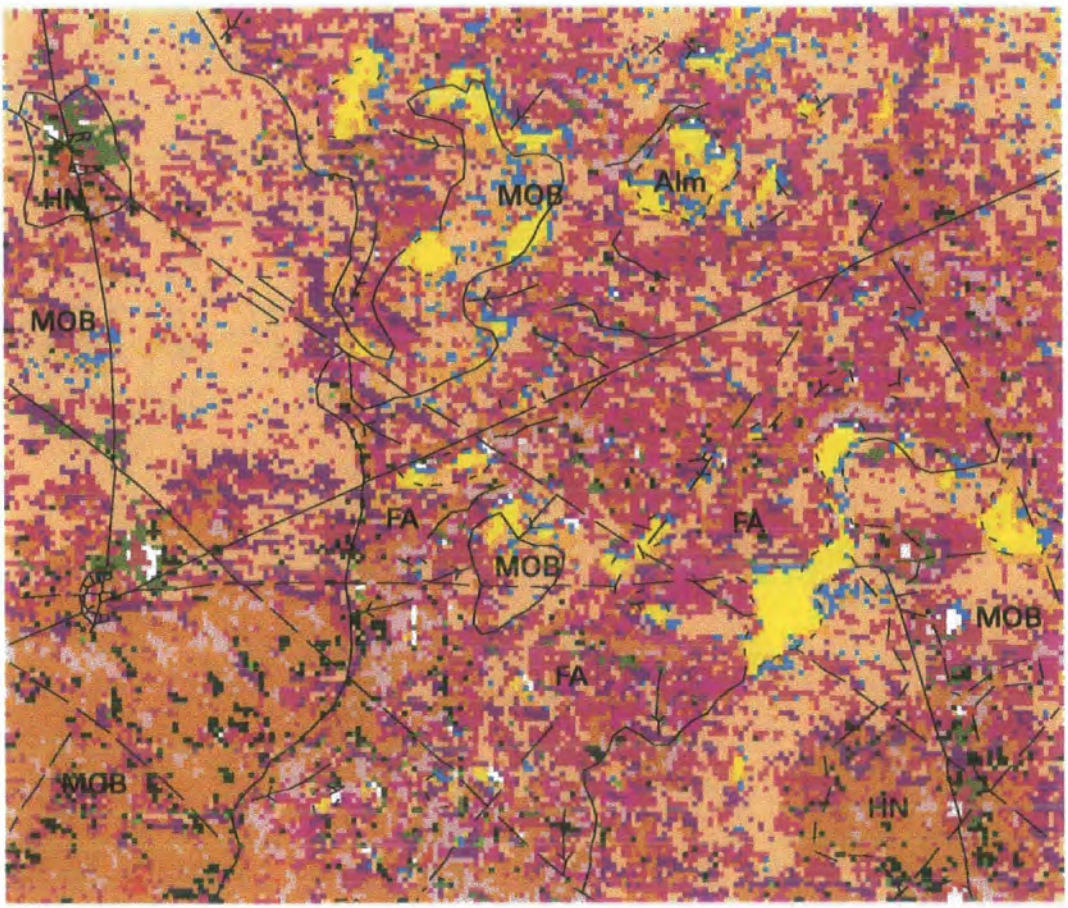

AREA 6

Figure (5 - 6c) Comparison between the geological map and the classified image

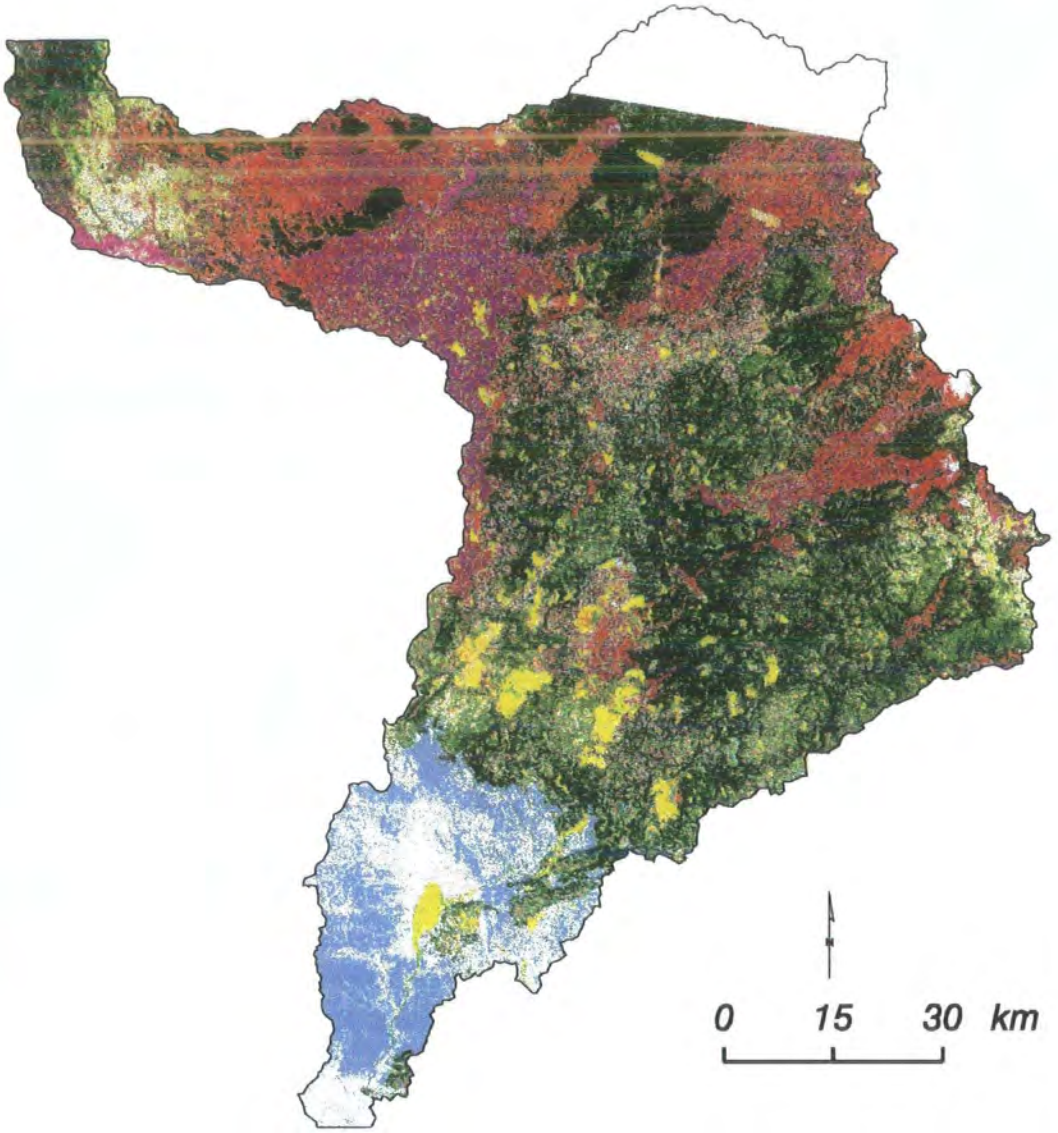

fa1 at ub sn urc alm
fa2 hn um aob aq farm
wmf m mob ai pl

Figure (5 - 7) Classification of basalt formations from Landsat Thematic Mapper

5.3.2.2 Hydrological-parameters layers

I. Rainfall-distribution layer (*rdst*)

This layer shows the Thiessen polygon distribution of the rainfall in the study area. The polygons are generated for the climate stations in and around the study area (figure 3-2). The layer can be used to simulate the aerial distribution of the rainfall when more accurate data about the rainfall distribution are not available.

II. Infiltration layer (*inf*)

This layer represents the infiltration zones according to the classification of Warburton (1997). As described in section (3.3) the area is classified into three zones; the wadi bed areas, characterised by very high infiltration rates; the side slope areas, with relatively high initial infiltration rate and low steady rate and *qa'* areas, with very low infiltration rate. The layer is composed from the union of two topographic layers, *qa'* and *wsprd.* The two layers represent the *qa'* and wadi bed areas while the background polygon represents the side slope areas. Figure (5-9) shows the infiltration layer.

III. The available-water-capacity layer (*awc*)

This layer represents the available water holding capacity of the soil column given in mm/m. In the absence of direct measurements of the water holding capacity of the soil at both the level 1 and level 2 surveying, Hunting (1993) used the *particle size class* (*psc*) as an indicator to the soil *awc*. The following table shows the *awc* values that correspond to each *psc.*

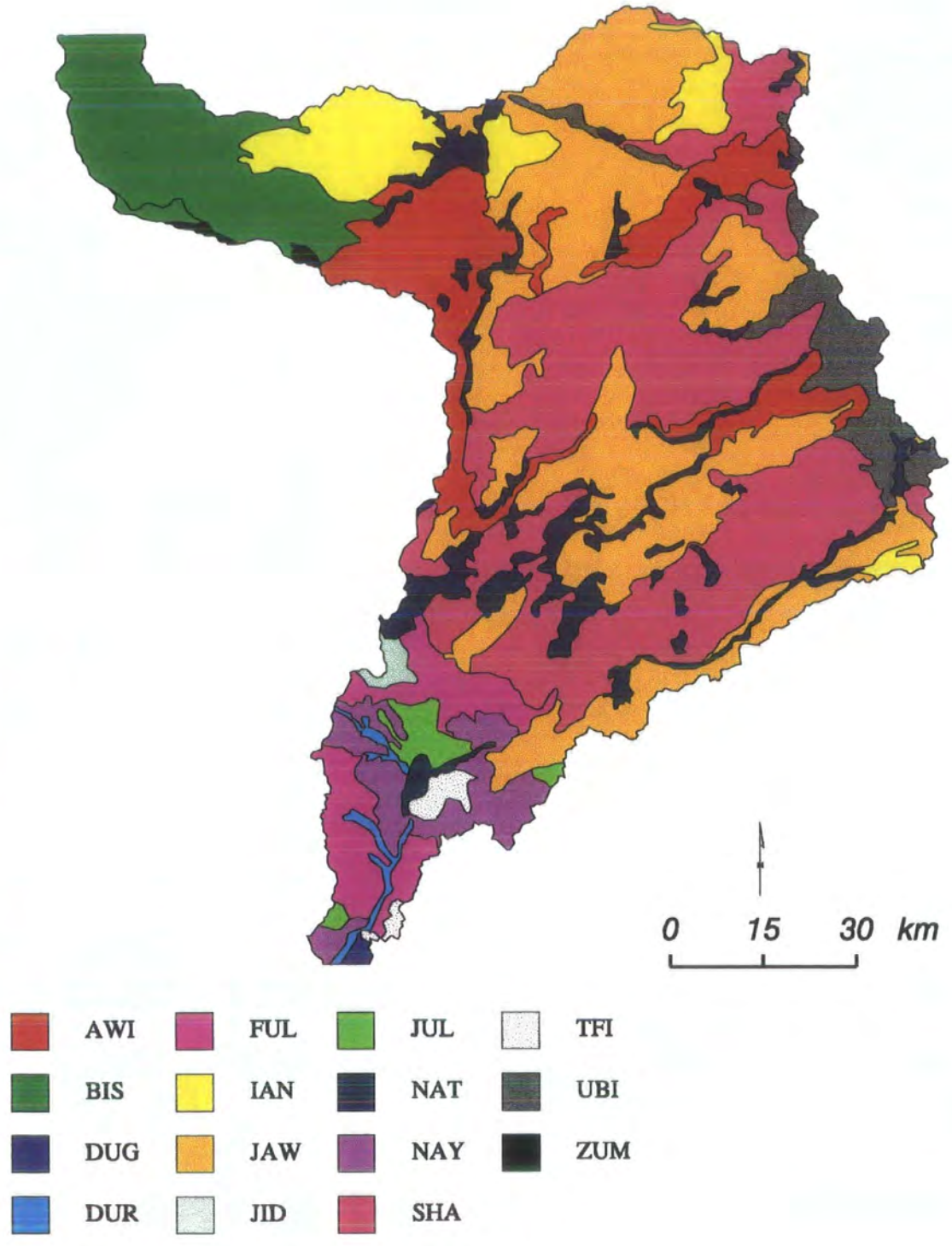

Figure (5 - 8) Soil classification (layer soil)

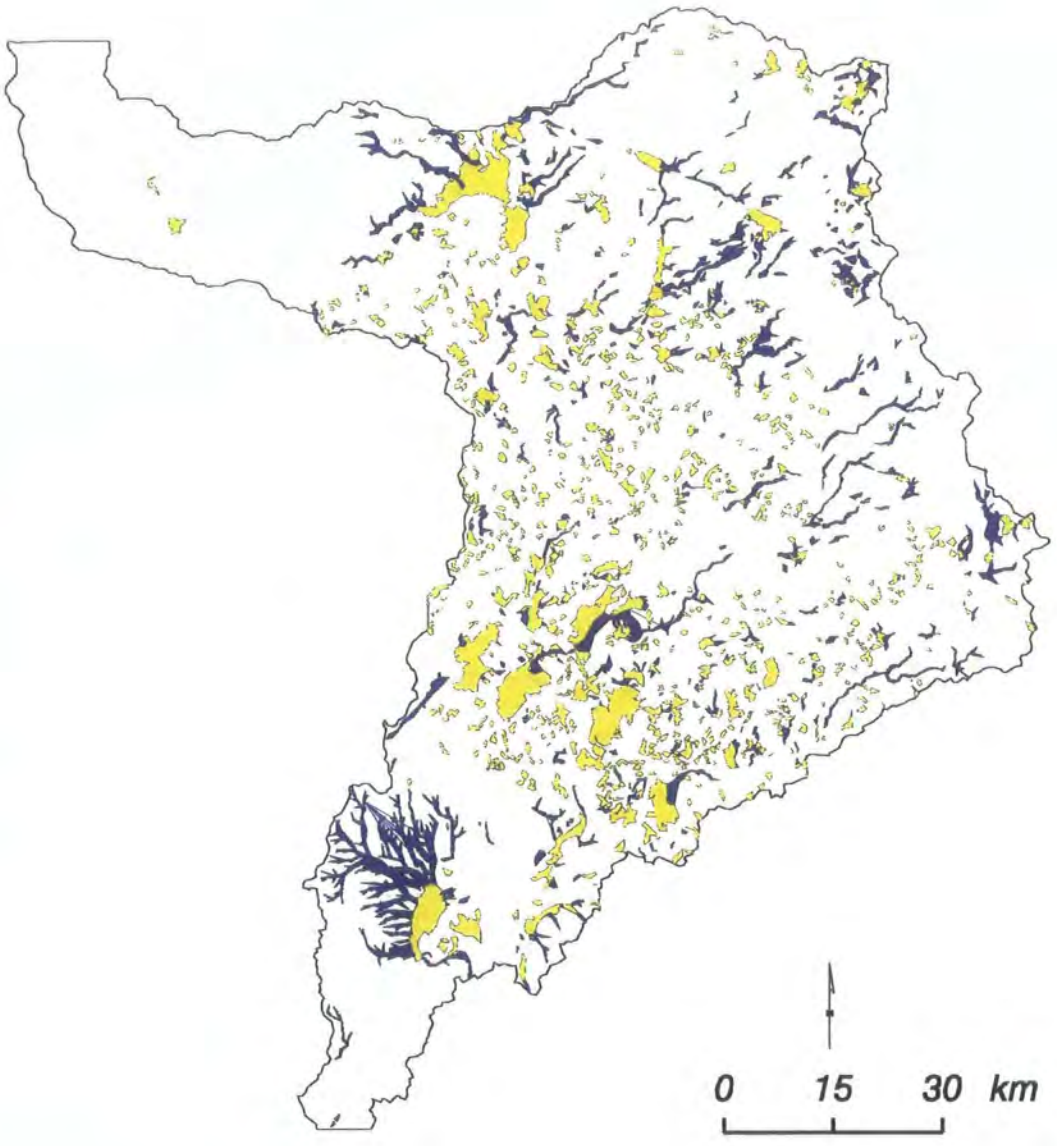

Side-slope areas

Mudflat areas (Qa')

Wadi-bed areas(Qa')

Figure (5 - 9) Classification according to the infiltration capacity of the soil (layer inf)

A weighted average *awc* value is estimated for each soil unit from the *awc* values of its constituent sub-groups weighted by their proportions in the soil unit. For each soil sub-group in the unit an average *awc* value is calculated for the soil column based on the description of the soil profile given in the representative profile associated with the sub-group. Figure (5-10) shows the *awc* layer.

Table (5-2) The awc values corresponding to each particle size class
(source: Hunting, 1993)

PSC	AWC (mm/m)
Very fine (V)	160
Fine-clayey (F)	150
Fine (Hz)	155
Fine-loamy (H)	155
Loamy (Mh)	160
Coarse silty (Mz)	160
Sandy (L)	70
Cleyey skeletal (Qu)	80
Loamy skeletal (Qmh)	75
Sandy skeletal (Ql)	32

IV.The layer of hydrologically-similar-units (*hsu*)

This layer represents a classification of the study area into zones of similar hydrological properties. The classification varies with the criteria used in the classification. The layer presented here is a classification according to the infiltration zone and the available water holding capacity of the soil (figure 5-11). The layer is generated from the *union* of the two layers: *awc* and *inf.*

5.3.2.3 Watershed characteristics layers

The layers of this group are derived from the digital elevation model of the area as discussed in chapter four.

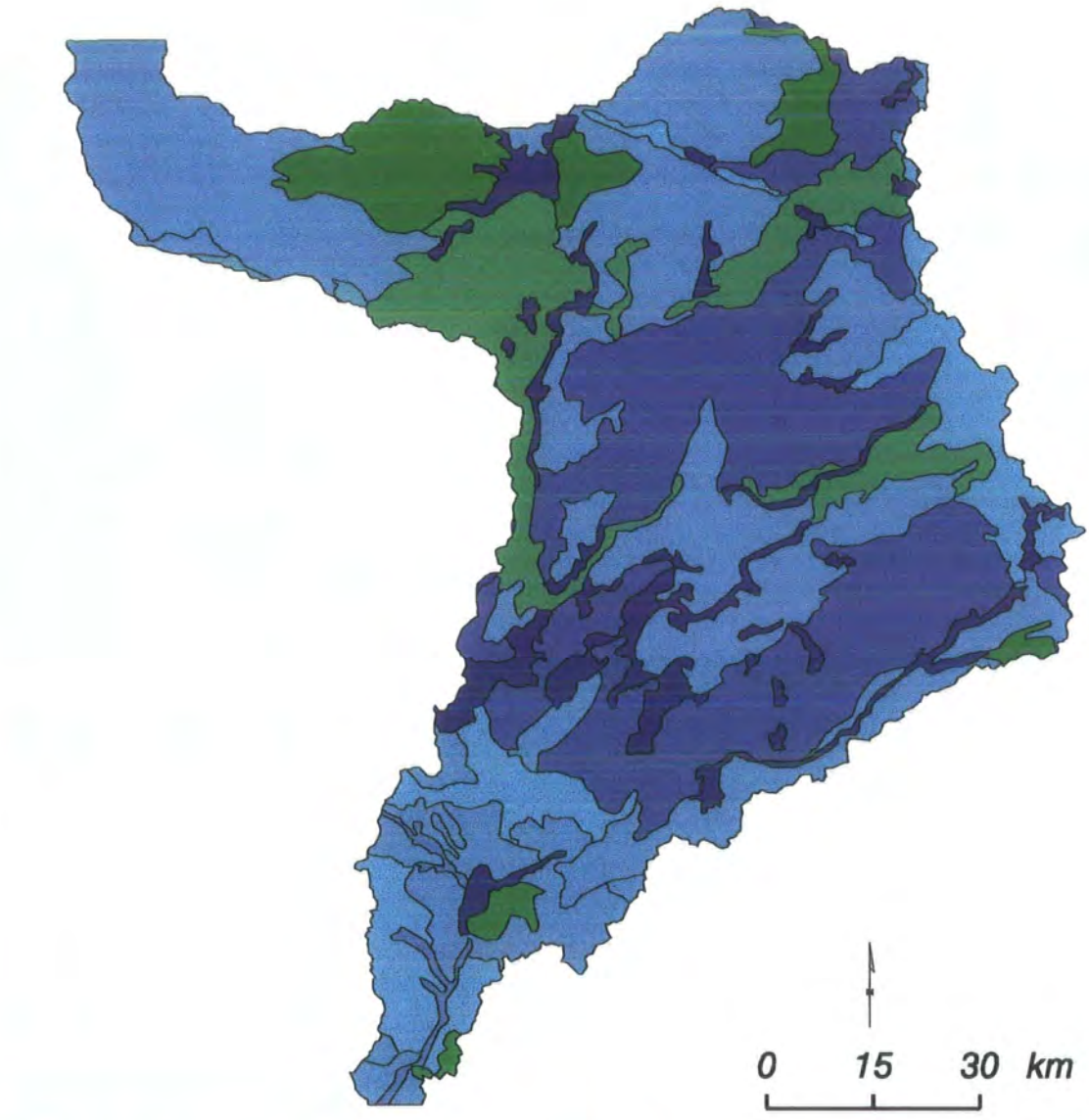

Figure (5 - 10) Distribution of the available water holding capacity of the soil (layer awc)

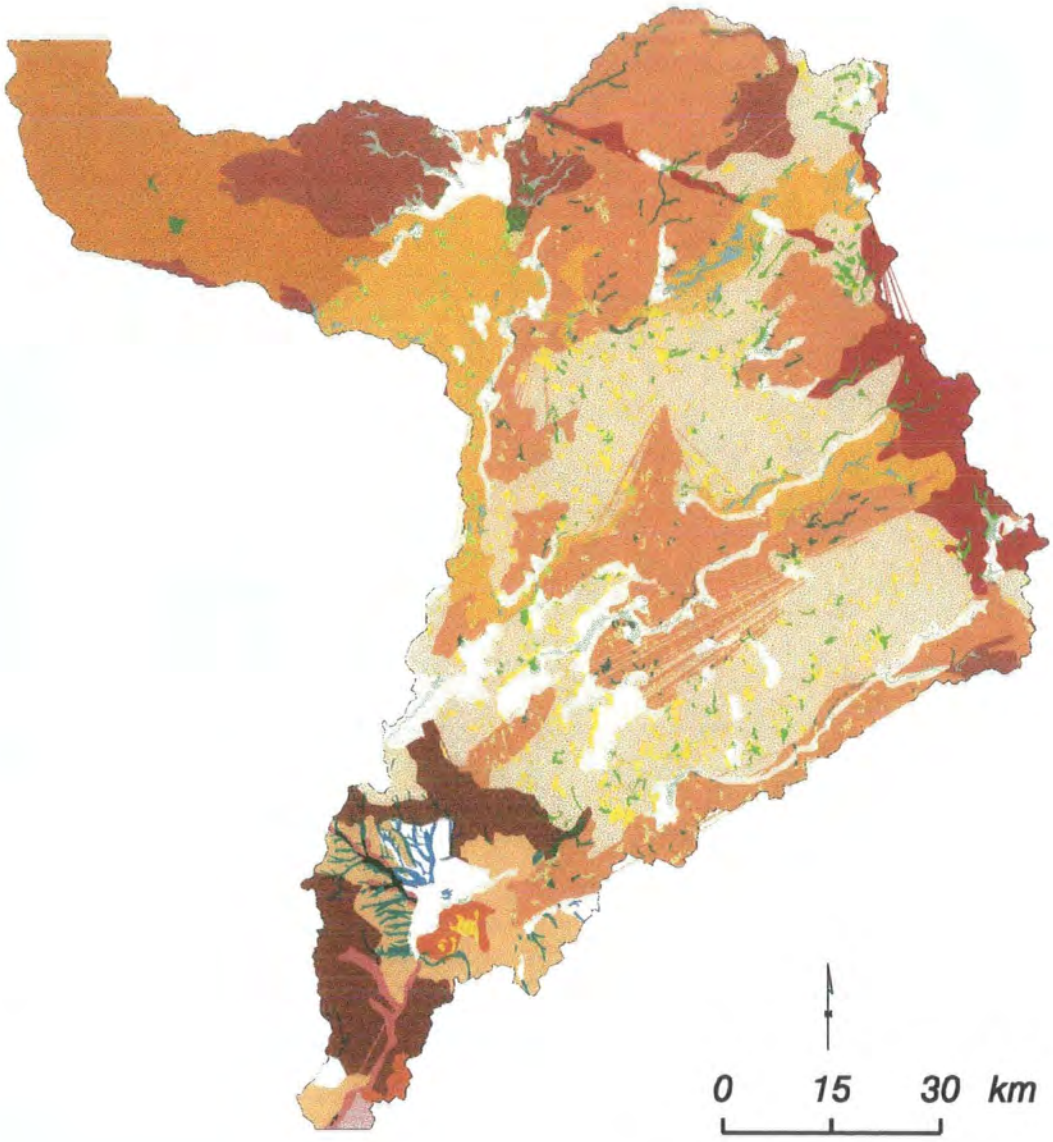

Figure (5 - 11) The hydrologically similar units (layer hsu)

5.3.2.4 Model layers

These layers are used for the spatial hydrological model of Wadi Rajil and will be described in chapters six and seven.

5.4 Description of a query application on the database

The database can be accessed for retrieval of information or for adding new data. The retrieved information can be the results of queries performed on the database or data layers extracted for display or for further GIS analysis. This type of access takes place in one direction from the database to the client application. On the other hand, applications like the hydrological model retrieve data from the database and generate new data layers that are added to the database. Therefore this application has bi-direction access to the database (figure 5-12).

DB : Database.

D&A : Display and analysis application.

Q : Query application.

M : The hydrological model application.

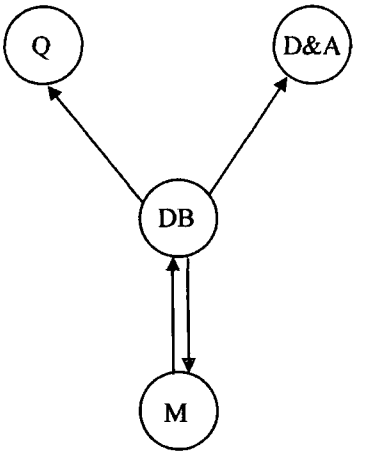

Figure (5-12) The access modes to the database

Access to the database for display, analysis, and query purposes can be performed using ARCVIEW, the ARC/INFO graphical interface. ARCVIEW provides fully functional GIS capabilities that enable non-expert GIS users to perform analysis or build complex queries

on the database. The software also provides a powerful set of tools for presenting the output results as tables, graphs, or as high quality maps. However, frequently used applications that involve complex analysis procedures or queries may be programmed to run as menu-driven applications. An example of such programmed applications is discussed in this section.

5.4.1 Application objectives

A knowledge of the watershed characteristics is essential for estimating hydrographs shapes and peak flows (Wanielista, 1990). Among these characteristics are the following:

1. Watershed area which directly affects the volume and peak of runoff,
2. Channel slope which has influence on the velocity of flow and the time of concentration,
3. Watershed length which affects the time of concentration,
4. Channel density, which has a significant effect on the amount of flow that reaches the outlet due to the loss of water through the wadi beds during transmission.

Watershed parameters like area, slope and length are usually determined from maps by manual methods. Besides being laborious, manual methods are error prone especially in flat areas where the watershed boundaries are not easily determined (Burrough, 1990). Other characteristics, like the time of concentration, are derived from empirical formulas that relate the time of concentration to the overland flow distance and slope. These layers are used to develop a hydrological model for the surface water studies of Wadi Rajil. In many cases these formulas are only valid for specific areas and under certain conditions like watershed area or channel length.

In a GIS environment the morphology of the land surface can be precisely represented in digital form. As discussed in chapter four, this has enabled the use of computer techniques

to analyse and determine the characteristics of the watershed. The accuracy of the results is only limited by the resolution at which surface details are depicted and the accuracy of the original data sources.

The application described here aims to provide the following information about the watershed and the drainage channel characteristics.

- For any channel link:

- Define its length, slope, the drop in height between its two nodes, and the Strahler order.

- Define the local watershed area that contributes flow directly into the link.

- Define the upstream watershed area that contributes flow into the upstream node.

- For any node:

- Define its upstream watershed area.

- Define the upstream links and the downstream link that connect at the node.

5.4.2 Input-output features

The main features of the application are the following:

1. Provide a menu with the following options:

1.1 Window manipulation functions: area definition, zoom-in, zoom-out, and pan.

1.2 Choice option: the user has the choice between delineation of sub-watersheds for links or for nodes.

1.3 Display options: the user can select to display or hide first order links and nodes.

Figure (5-13) shows the application menu

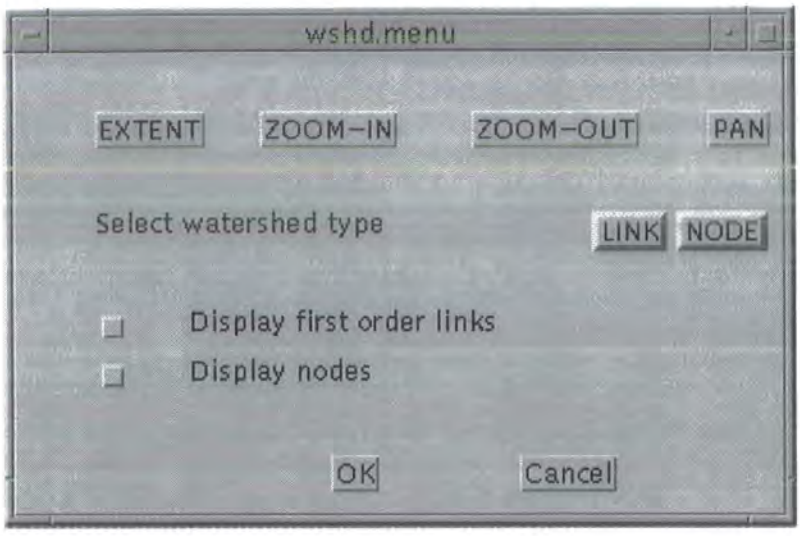

Figure (5-13) The query application menu

2. Provide a full shaded view of the watershed area and the drainage channel network. The network is ordered according to Strahler order.
3. Provide a window on a specific area of interest with zoom-in, zoom-out, and pan capabilities. Figure (5-14) shows the initial window of the application.

5.4.3 The application algorithm

There are four layers involved in the application: the stream links layer (*slnk*), pour points layer (*ppt*), the link-subwatershed layer (*wlnk*), and the node-subwatershed layer (*wppt*). The layers are linked by the following relationships (figure 5-15):

a) One-to-one relationship linking between *slnk* and *wlnk*: each sub-watershed has one and only one link draining it.

b) One-to-many relationship between *slnk* and *ppt*: each link has one upstream node but watershed assigned to it.

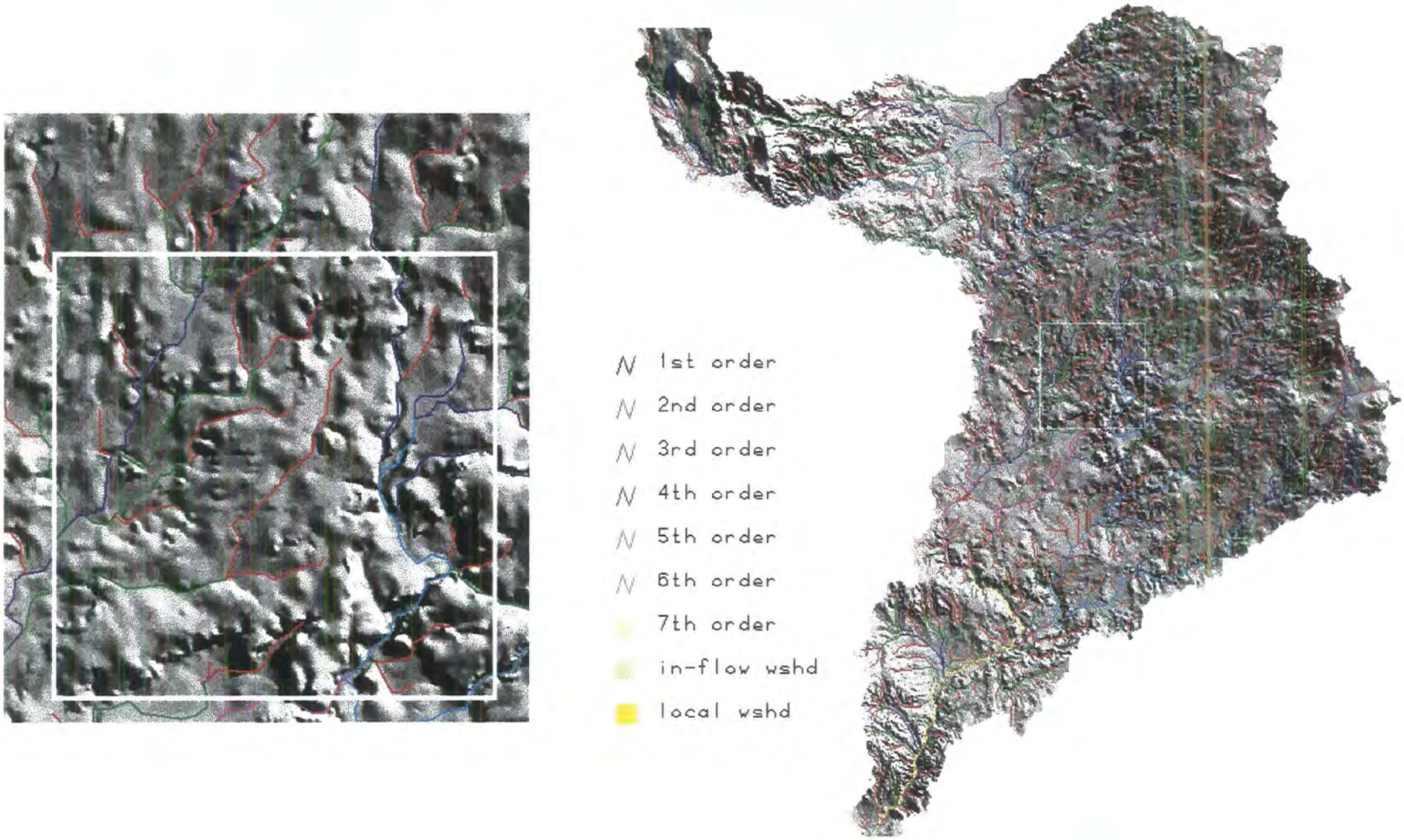

Figure (5 - 14) The initial display window of the watershed query application

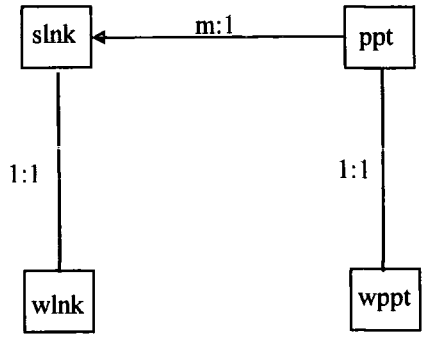

Figure (5-15) The relationships between the query application

c) One to one relationship between *ppt* and *wppt*: each node has one and only one upstream watershed assigned to it.

The application relies on using the ARC/INFO NETWORK module for defining the upstream links and nodes for any selected link. The procedure consists of the following steps:

1. Select a link.
2. Define the upstream links that contribute flow to this link.

each node may have one or more links connected to it.

3. One-to-one relationship between *ppt* and *wppt*: each node has one and only one upstream Select the link sub-watershed that contributes flow directly into the link.
4. Select the upstream nodes of all the upstream links.
5. Select the node sub-watersheds that correspond to the selected set of nodes.
6. Plot the link watershed and the upstream node sub-watersheds.

A similar procedure is applied for the node-sub-watershed option of the application.

5.4.4 Displaying the results

The results are provided as a map showing the local link sub-watershed and the total upstream area contributing flow to the upstream node (figure 5-17). The application also provides a table list of the characteristics of the queried link (figure 5-16)

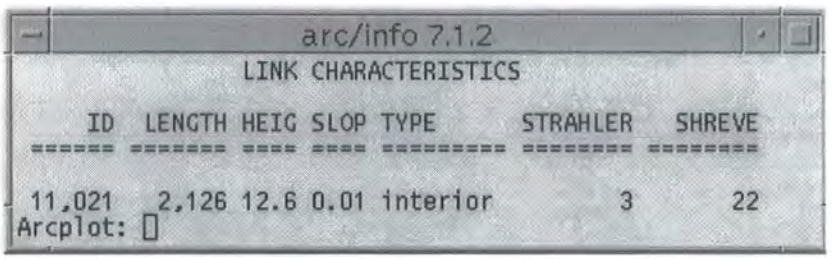

Figure (5-16) Table listing of the link characteristics produced by the query application

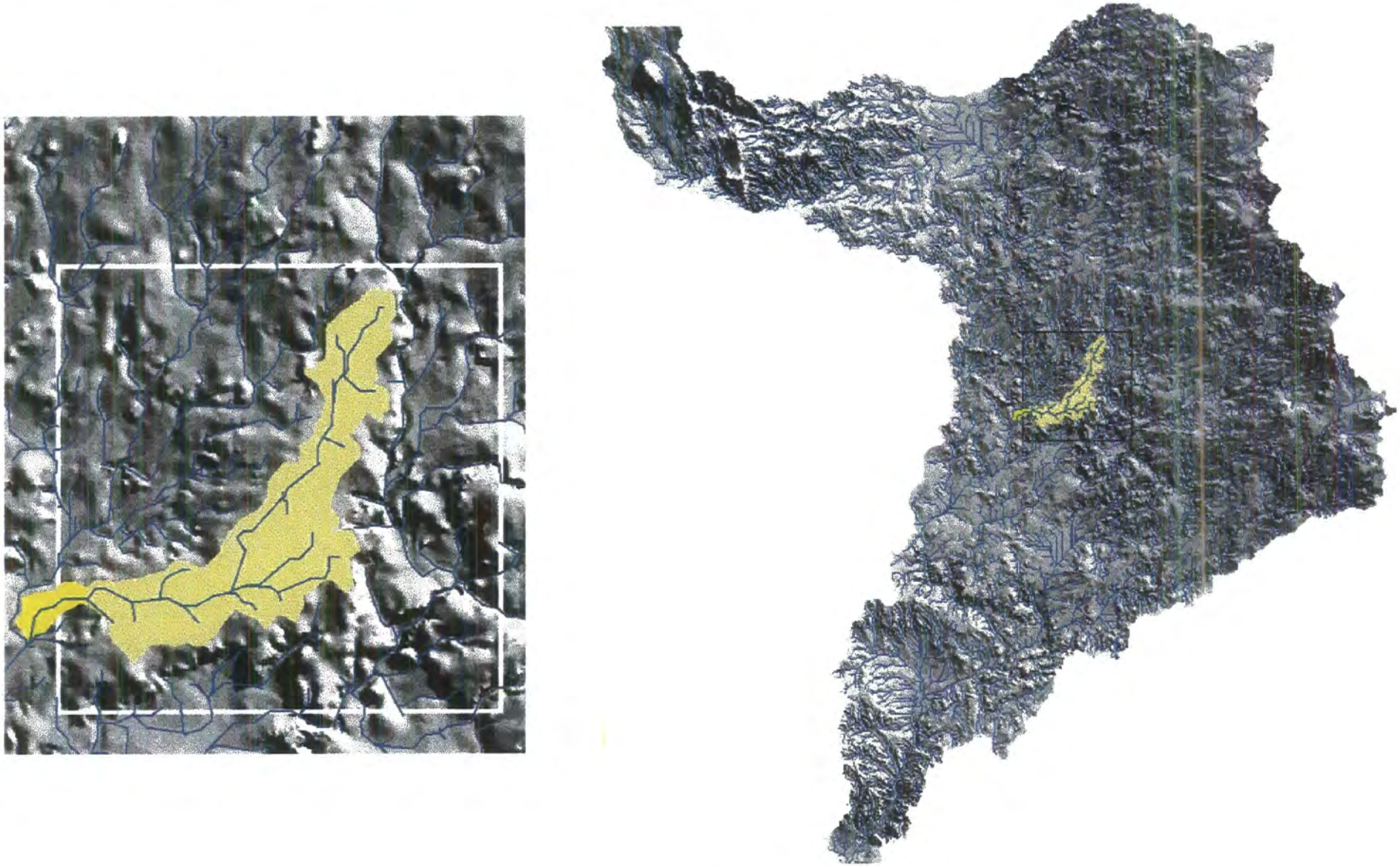

Figure (5 - 17) The local and upstream sub-watersheds contributing flow to the selected link

5.5 Summary

Building a database is the most critical and time-consuming step in any GIS project. The primary goal of the database described in this chapter is to provide support to the applications of GIS for surface water studies of wad Rajil. A description of the spatial and thematic structures of the database has been provided. The database layers have been classified as basic layers and derived layers. The basic layers describe the natural environment and represent the original sources of information for the other database layers. The accuracy of these layers depends on the mapping scale at which they were depicted and the last update of the information. While the 1/50,000 scale appears adequate for semi-distributed modelling at the sub-watershed level, a detailed distributed representation and modelling of the hydrological processes requires maps of larger scale. The derived layers are criteria dependent and their validity depends on the accuracy of the information sources and the criteria used to derive them.

The database provides the basic structure for storing catchment data in an organised way that can be used to define spatial models in the future.

CHAPTER 6

DESCRIPTION OF A GIS-BASED HYDROLOGICAL MODEL FOR WADI RAJIL WATERSHED

6.1 Introduction

A hydrological model may be defined as a simplified representation of the complex hydrological system (Manley, 1977). The hydrological system refers to the land phase cycle that includes the hydrological processes from precipitation to stream flow at the catchment outlet. These processes involve many climatological and physical parameters in their definition.

The need for modelling has resulted from the growing demand for hydrological data, especially stream flow records for decision making on the design of hydraulic structures. In many cases these records are not available or do not cover an adequate time period (Viessmann *et al,* 1989).

The first generation of rainfall-runoff models coped with the complexity of the hydrological processes by directly correlating the precipitation data at the input of the land phase cycle with the corresponding runoff data at the catchment output without the need to simulate the intermediate complex hydrological processes (Porter and McMahon, 1971).

With the advent of high-speed computers it has become possible to simulate the more complex hydrological processes. This has resulted in the development of a new

generation of physically based hydrological models the first of which was the Stanford Watershed Model in 1962 (Shaw, 1988).

The major problem in simulating the hydrological processes based on their physical governing laws is the variability in time and space of the parameters that control these processes (Porter and McMahon, 1971). This problem has been dealt with by assuming homogeneous properties for the whole catchment being modelled (Drayton *et al,* 1993) or for subdivisions of the catchment, as in the Stanford Watershed Model (Moore *et al,* 1993), where the catchment is subdivided into smaller areas of similar hydrological properties. Models of this kind are referred to as lumped parameter models.

Over the last twenty years the need for hydrological models has shifted from generating stream flow data to the need to estimate the distributed surface and subsurface flows (Moore *et al,* 1993) and to predict the effect of local land use practices on water resources (Abbott *et al,* 1986a).

These needs require a more detailed description of the catchment hydrological characteristics that is not accounted for in the lumped parameter models. This has led to the development of distributed hydrological models that account for the spatial variability of model parameters by applying parameterised mathematical equations. Numerical methods, like the finite difference method, are used to approximate the parameter values at different time and space intervals.

With the emergence of remote sensing techniques as possible sources for estimating the distributed values of model parameters and the increasing awareness of the effect of topography, represented by digital elevation models (DEM), on the catchment hydrology (Moore *et al,* 1993) GIS techniques have gained a prominent role as a hydrological modelling tool (Furst *et al,* 1993). This is due to the inherent capabilities

of GIS to manage and analyse spatially distributed data that makes it the perfect tool to integrate data from remote sensing, DEM, and spatially distributed hydrological data.

6.2 Classification of hydrological models

Hydrological models are classified according to a wide range of criteria (Bedient and Huber, 1988). Models could be classified, in terms of their approach to the simulation of the catchment processes, into two categories: deterministic models, which use mathematical equations to represent the catchment processes, and stochastic models which use a probabilistic approach for simulating these processes (Shaw, 1988).

Another global categorisation of models is given by Viessman *et al* (1989) where models are classified into mathematical or physical models according to the simulation technique used in the model. But, in general terms, the most widely used criteria for classifying hydrological models include the following (Viessmann *et al,* 1989; Bedient and Huber, 1988).

1-Models are classified according to the periods of simulation into continuous simulation models and event-based simulation models. Continuous models provide continuous tracking of the moisture storage conditions of the catchment while event-based models simulate the discrete rainfall events.

2- In terms of the spatial representation of the catchment characteristics models are classified as lumped parameter models or distributed models. Lumped parameter models use average values for their parameters while distributed models rely on a more realistic representation of these parameters (Porter and McMahon, 1971).

6.3 The general structure of hydrological models

The hydrological system that forms the land phase cycle (from precipitation to stream discharge) can be abstracted as a series of inter-linked processes and storages that simulate the dynamic situation of moisture within the catchment (Shaw, 1988). Hydrological processes control the movement of moisture into or out of each of these storages. The characteristics of the storages and the processes that act on them are dependent on catchment characteristics.

The first general function of the model is the calculation of the moisture transfer between the different storages. This task is usually carried out through the use of a water budget equation that balances the amount of moisture passing into and out of each storage compartment. This water budget equation is based on the fundamental concept of the continuity equation expressed as

$$I - Q = \frac{ds}{dt}$$

where,
I : The total moisture input into the storage.
Q : the total moisture output out of the storage.
$\frac{dS}{dt}$: The rate of change in storage.

The second main function of a hydrological model is to simulate the process of transfer (or routing) of any excess amounts of water to the outlet of the catchment area. One approach to the problem of routing, known as the hydrological approach, is through the use of a storage-discharge relationship. This relationship could be linear (of the form $S = kQ$) or non-linear (of the form $S = kQ^m$) where k, m are parameters. This approach is widely used for flood routing in the majority of

hydrological models. The second approach uses more complicated and more precise hydraulic techniques based on the simultaneous solution of both the continuity and momentum equations (described in appendix 6) at a regularly spaced (both in time and space) intervals. Hydraulic routing methods have gained importance with the widespread use of computerised forms of the finite difference method, which provides a numerical substitute to the complex differential form of the momentum equation. Appendix () provides more details of the continuity and momentum equations.

The remaining part of this section discusses the general components of a mathematical model and explains the interactions that take place between the different storage areas. Descriptions provided here are derived from the conceptual structures of some hydrological models as described in the literature used in this study.

6.3.1 Model input data

The input data to the hydrological model are in general time series data of precipitation amounts and climatological parameters that enable the calculation of potential evaporation.

6.3.2 Moisture transfer computation

This component of the model deals with the storage compartments and functions discussed below

6.3.2.1 Interception storage

the hydrological models, in general, assume that all the falling precipitation is intercepted by vegetation. The capacity of the interception storage is variable and depends on the type and density of the vegetation cover. This interception storage is

filled from the falling precipitation and depleted, at the potential rate, by evaporation. The loss of precipitation to the interception storage is considered as an initial loss since no precipitation reaches the ground surface before this storage is filled (Porter and McMahon, 1971).

6.3.2.2 Infiltration

After satisfying the interception storage capacity, the excess precipitation will either infiltrate into the soil surface or run over the catchment surface. The infiltration function controls the amount of water that penetrates through the surface soil. The rate of infiltration is a function of the hydraulic properties and moisture content of the soil. Such properties are, in general, of high spatial variability. Such variability is usually simulated by mathematical models.

6.3.2.3 Soil moisture storages

Two moisture storages; the upper soil storage zone and the lower soil storage zone usually model the soil moisture content. The need for two storages to represent the soil moisture conditions is due to the variability of soil hydraulic properties in the profile of the soil. The upper moisture storage represents the root zone of soil. This storage releases its water to the atmosphere, by evapotranspiration that takes place at the potential rate, or to the lower zone storage, by percolation of the water through the unsaturated zone. Some models also account for the subsurface horizontal movement of water as interflow. The lower zone storage represents the unsaturated soil layer that extends from the upper zone until the water table. The movement of water from the upper zone to the lower zone is subject to the conditions of water movement through an unsaturated medium. Evapotranspiration from the lower zone is assumed to take

place at a lower rate than the potential rate and this rate is usually a function of the actual moisture content of the soil.

6.3.2.4 Groundwater storage

When the soil moisture storages reach the field capacity any excess amounts of infiltration drains down to the groundwater storage under the action of gravity. Depending on the level of the water table, a certain amount of groundwater finds its way out to the drainage network as baseflow.

6.3.2.5 Surface depression storage

This storage represents an abstraction of the overland flow water that is kept in the surface depressions.

6.3.2.6 Overland flow

Overland flow occurs when the infiltration capacity of the soil is exceeded by the precipitation rate or when the soil moisture storage is saturated. The translation movement of the overland flow towards the drainage channel network is usually represented by the unit hydrograph theory or by the application of the kinematic wave equation and Manning's formula.

6.3.2.7 Channel flow

The down stream routing of the accumulated flow is usually carried out by applying hydrologic or hydraulic routing techniques. The objective of the routing component is to simulate the effects of translation, due to travel time, and attenuation, due to channel storage characteristics, on the routed flood wave.

6.3.3 Model output

The final output of the hydrological model is usually a hydrograph simulating the discharge over time at the outlet of the modelled watershed. Other results of the modelling process include estimations of the amounts of evaporation or recharge to the groundwater storages.

6.3.4 Model calibration

Before putting the model in use the parameters involved in the mathematical formulation of the hydrological processes included in the model need to be known. These parameters reflect certain characteristics of the phenomena modelled and are assumed to have fixed values within the time and space frames of the model. Parameter optimisation is carried out by running the model using observed or previously known input-output data sets and correlating the model computed output to the measured output.

6.4 Review of hydrological models

This section provides brief descriptions of some of the widely known hydrological models. The basic structure and the main features are provided without going in details into the mathematical representation of the hydrological processes.

6.4.1 Stanford Watershed Model (source: Viessman *et al*, 1989)

Designed by Crawford and Linsley in 1962, this model was the first to include simulation of the land phase processes based on their physical laws. The main objective of the model is to provide continuous simulation of the watershed outflow

hydrograph. The model uses a lumped parameter approach. However, it includes a crude simulation of the spatial variability of the hydrological processes through the subdivision of the watershed into smaller size sub-watersheds or hydrologically similar areas each of which has its own locally averaged parameters (Moore *et al*, 1993).

6.4.2 HEC-1 model (source: Bedient and Huber, 1988)

HEC-1 was developed by the US Army Corps of Engineers, Hydrologic Engineering Centre, to simulate the catchment response during flood events. The model subdivides the watershed into smaller homogeneous sub-watersheds of areas between 1-10 square miles. Lumped parameters averaged in time and space are derived for each subdivision and used in the simulation of the runoff process.

The model provides several options to simulate the losses of rainfall to interception and infiltration. Several methods for surface runoff computation are also provided including the kinematic wave method. Surface and base flow runoff are routed using the kinematic wave or the Muskingum flood routing methods

6.4.3 The SHE model (source: Abbott *et al,* 1986a, Abbott *et al*, 1986b; Bathrust, 1986)

The Système Hydrologique Européen (SHE) is a physically based distributed model that has been developed by hydrologists from the UK, Denmark and France. The development of the model has resulted from the need for models capable of predicting the hydrological effects of human activities like landuse practices and non point source pollution

The primary land phase hydrological processes including snow melt, interception, evapotranspiration, overland flow, channel flow, and subsurface saturated and unsaturated flows are modelled in the SHE. A grid of points in the horizontal direction and a column of nodes in the vertical direction represent the spatial variability of the hydrological processes. At each node (either in the horizontal or vertical direction) the values of the hydrological parameters are estimated using the finite difference method.

6.4.4 TOPMODEL (source: Beven *et al*, 1995)

The TOPMODEL is a physically based model developed by Kirkby and Beven in 1974 (Moore *et al,* 1993). The model simulates the soil moisture storage in the catchment as a series of moisture storages including the interception storage , the infiltration storage, and the saturation zone storage (Chairat and Delleur, 1993). The model is an event-based model that simulates the runoff occurring as an infiltration excess quick flow or as a subsurface flow.

The subsurface flow results from saturated areas with negative or zero moisture deficit The approach used in TOPMODEL to identify these zones is based on the use of the topographic index ($\ln\frac{A}{\tan B}$). This index, known as the wetness index, is related to the soil moisture conditions by the following equation (Moore *et al,* 1993)

$$S_i = S - m * \ln\left[\frac{A}{T_i \tan B}\right]_i + m\xi$$

where,

S_i : the local moisture deficit at point i ,

S : mean value of S_i for the entire catchment,

m : a recession parameter,

A : the total upslope area contributing runoff to a grid element per unit of contour length orthogonal to the direction of flow (Quinn *et al,* 1993),

B : the slope angle,

T : the soil transmissivity,

ξ : mean value of $(\ln \frac{A}{\tan B})$ for the entire catchment.

The runoff generated within the catchment is routed to the outlet using a linear routing method assuming constant velocities for both overland flow and channel flow.

6.5 Description of Wadi Rajil hydrological model

This section describes the structure of a proposed hydrological model for the study of surface water at the Wadi Rajil watershed area. The model aims at generating the hydrographs at the watershed outlet from the input rainfall data all in accounting for the watershed characteristics and the active hydrological processes within it. The hydrological processes involved in the model are simulated at a time step interval set by the time step of the input rainfall data. Thus the model can be used for both event-based and continuous simulations.

At this stage of development the model is meant to be simple in its structure and its mathematical representation of the hydrological processes involved. This simplification is mainly due to two factors. First, there is no available mathematical description of the hydrological processes involved. In addition, field measurements of most of these processes are either not available or of very low density to be representative of the spatial and temporal variability of the processes. Secondly, the primary objective of this study is to establish a GIS based hydrologically oriented database and to demonstrate the application of GIS techniques for hydrological modelling rather than building a fully operational hydrological model.

6.5.1 Model assumptions

The functionality of the model is based on the following assumptions:

1. Since no quantification of the infiltration rate in the study area is available, the estimation of the infiltration capacity of the soil will be based on the observations of Noble (1994) discussed in section (3.4.2). Thus the amount of water that infiltrates into the soil shall be calculated based on the available water holding capacity of the upper soil.
2. There is no contribution to the runoff from the base flow component.
3. Percolation of the soil moisture to the ground water storage is not considered in the model.
4. The flow routing process relies on the linear routing principle (discussed later in section 6.5.4). In addition, the routing process does not include any sort of storage-discharge relationships. However, the transmission losses through the channel bed are considered as abstractions of the routed flows. This implies that the flow towards the outlet occurs as a movement of translation where the amount of rainfall excess generated at each cell appears at the watershed outlet reduced by the amount of transmission losses and shifted in time by a period equivalent to the cell-based time of flow.

6.5.2 Structure of the model

The model is structured as a GIS application. All the data involved in the model computations are represented as GIS layers according to the vector or raster data models. In addition, most of the model computations are carried out on a cell-by-cell basis using GIS raster processing tools. Conceptually, the model consists of two main components: the runoff generation component, and the flow routing component

(figure 6-1). Each component consists of a group of functions that represent the hydrological processes of influence on the circulation and distribution of the surface water within the watershed area. The distribution of moisture in the watershed area is abstracted into two moisture storages only: the upper soil moisture storage of finite capacity, and the transmission loss storage considered of infinite capacity. The following sections provide description of the model components.

6.5.3 The runoff generation component

This part of the model provides an estimate of the rainfall excess amounts produced at each cell for each time step of computation. The general form of the water budget equation that describes the generation of rainfall excess produced at each cell at the end of each time step can be expressed as follows

$$R = I - O$$

where,
R : rainfall excess produced at each cell at the end of the time step (mm),
I : total moisture input at the beginning of the time step (mm),
O : total water losses during the time step interval (mm).

P precipitation function
F infiltration function
E evaporation function
R rainfall-excess function
O overland flow function
C channel routing function
T transmission loss function

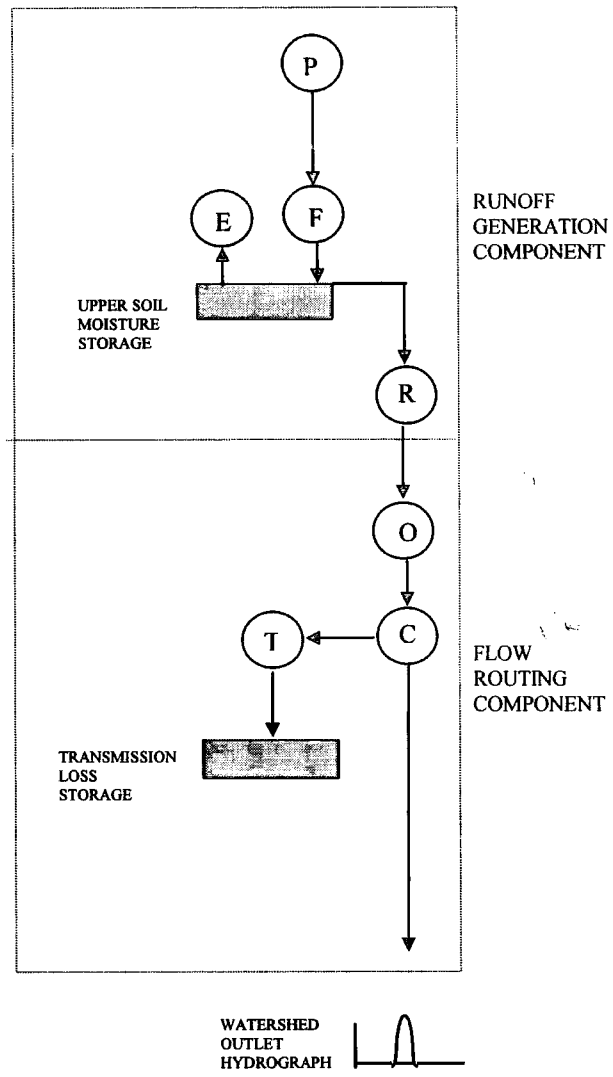

Figure (6-1) A diagram of the general structure of Wadi Rajil model

6.5.3.1 The rainfall function

Rainfall data are the only moisture input to the model. These data are usually provided as time series data that represent the total rainfall accumulated at the rainfall gauge station during a given period of time. Unless otherwise specified, the time step at which the rainfall data are provided sets the time step of the model computations.

For modelling purposes, the point representation of the rainfall data has to be converted into an area representation. Interpolation techniques like Kriging and Thiessen polygons can be used to generate the area distribution representation of

rainfall. The accuracy of the representation depends on the accuracy and density of the input data points. Examples of using these interpolation techniques were discussed in section (3.2.1.1).

6.5.3.2 Infiltration

The infiltration function controls the amounts of moisture that enters the soil. The model assumes that the maximum amount of infiltration is equivalent to the available water holding capacity of the soil. The influence of the hydraulic properties of the soil on the infiltration is not considered. This great simplification of the infiltration process is based on the discussion of the infiltration characteristics presented in section (3.3).

The spatial variability of infiltration is simulated using the linear cumulative distribution method (figure 6-2).

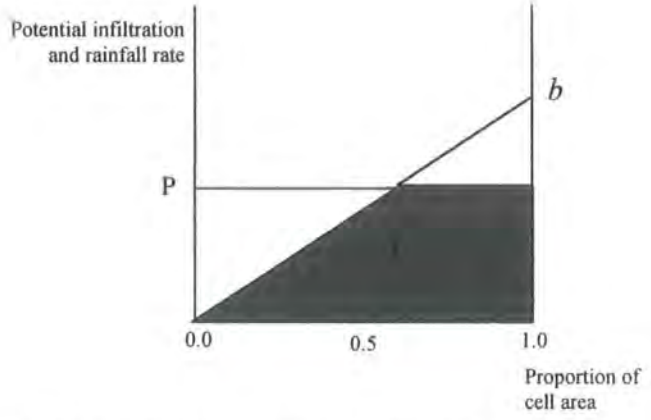

Figure (6-2) Linear representation of the spatial distribution of infiltration

Computations of infiltration are performed at the cell level for each time step. For each time step the actual amount of water that infiltrates through the cell area can be expressed by the following equation

$$F = (P - \frac{P^2}{2b}) \qquad \text{for } P < b$$

$$F = AWC \qquad \text{for } P > b$$

where,

F : the infiltration amount averaged over the cell area (mm),
P : the rainfall amount averaged over the cell area (mm),
AWC : the available water holding capacity of the soil (mm),
b : the point that fixes the line representing the infiltration spatial distribution.

Under the assumption made above the value of b is given by the following equation,

$$b = 2 * AWC$$

The computed amount of infiltration is adjusted for the initial moisture conditions of the soil. The adjustment made can be expressed by the following equations:

$$F = F \qquad F < AWC - SMb$$
$$F = AWC - SMb \qquad F > AWC - SMb$$

where SMb represents the soil moisture content (mm) at the beginning of the time step.

6.5.3.3 Evaporation

Hydrological models like Stanford watershed model (Viessman *et al,* 1989) consider transpiration rather than evaporation to be the critical process that acts on the depletion of the upper soil storage. Transpiration of the upper soil moisture storage is assumed to take place at the potential rate. However, for shallow bare soils like that of Wadi Rajil watershed, where more than 30% of the soil is less than 50 cm deep (Hunting, 1993), evaporation rather than transpiration dominates. Since there are no available measurements of the evaporation from bare soil in the area, it is assumed that evaporation from the upper soil moisture storage takes place at the potential rate. The evaporation function performs the computation of evaporation at two levels. First, evaporation occurs at the potential rate from any rainfall amounts remaining after satisfying the infiltration function requirements. Any additional amounts required to satisfy the evaporation potential rate will be withdrawn, at the potential rate, from the

upper soil moisture storage. Therefore the total evaporation for any time interval can be described by the following equation,

$$E = E1 + E2$$

where,
$E1$: evaporation from open surface water,
$E2$: evaporation from the upper-soil moisture storage.

6.5.3.4 The upper-soil moisture storage

The model simulates the soil water conditions by tracking the moisture content of a single storage compartment representing the available water holding capacity of the upper soil zone. This abstraction, as described by Porter and McMahon, (1971) is a simplification of the real soil moisture situation where the moisture content varies significantly across the vertical profile of the soil.

Except for wadi bed cells the soil moisture storage will be considered of finite capacity that could be expressed as,

$$AWC = d * SSC$$

where,
AWC : the available soil storage capacity (mm),
d : depth of the soil moisture storage zone (mm),
SSC : the average water holding capacity of the soil profile (mm/m).

The depth of the soil profile can be set to any value. For the majority of the applications discussed in chapter 7 a depth of 100 mm, based on the discussion in section (3.3), is assumed.

As stated in the model assumptions the soil moisture content is controlled by the infiltration and evaporation processes only. Other hydrological processes that might be of important influence on the soil moisture level such as percolation of water through

the unsaturated soil layer and the near surface horizontal movement of water are not modelled.

The soil moisture level at the end of each time step can be expressed as,

$$SMe = F + SMb - E2$$

where,
SMe : soil moisture level at the end of the time step (mm),
F : infiltration during the time step (mm),
E2 : evaporation from the upper-soil moisture storage (mm),
SMb : the soil moisture level at the beginning of the time step (mm).

The computed *SMe* value at the end of a given time step will serve as an initial *SMb* value for the next time step.

6.5.3.5 Rainfall excess

The rainfall excess generated by each cell at the end of each time step is given by the following water-budget equation :

$$R = P - F - E1$$

where,
R : rainfall excess (mm),
P : rainfall (mm),
F : infiltration (mm),
E1 : evaporation from the infiltration excess rainfall (mm).

The rainfall excess generated at each cell will be routed to the watershed outlet by the functions of the flow routing component.

6.5.4 The flow routing component

The main goal of the routing process is to generate a hydrograph at the watershed outlet. In a GIS environment this goal can be achieved by tracking the flow of rainfall-excess from cell to cell to the watershed outlet (Olivera and Maidment, 1996). The detailed description of the tracking process involves complex flow dynamics

equations. The simplified approach applied by the model is based on the following assumptions.

1. The routing function does not make any assumptions about the within cell movement of water. Instead, the rainfall-excess generated at each cell at the end of each time step is considered as an impulse of water concentrated at the centre of the cell. In addition, the water is assumed to flow out of the cell in one direction along the steepest slope.
2. The linear routing concept is valid. This concept implies that the routed cell flow does not interact or affect the routed flows of other cells even if they share a common flow path (Olivera and Maidment, 1996). This could be better explained using the flow path diagram of figure (6-3). According to the linearity principle the response at point D resulting from input values (i_A, i_B, i_C) at points A, B, C consecutively is expressed as :

$$Q_D = Q_{AD} + Q_{BD} + Q_{CD}$$

where, (Q_{AD}, Q_{BD}, Q_{CD}) are the responses at point D from each cell input independently.

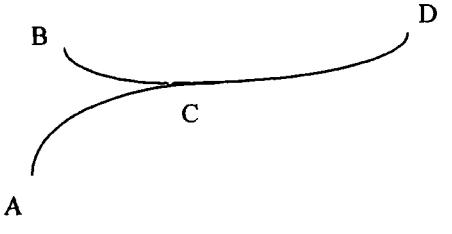

Figure (6-3) The linear routing principle
(Source Olivera, 1996)

The model's approach to the routing process consists in carrying out separate tracking of the time of travel and the discharge expected from each cell at the watershed outlet. Therefore, the length of the flow path from each cell to the watershed outlet and the flow velocity along that path are the key elements to be determined for each cell in the watershed area. Using the available raster processing functions the determination of the flow path lengths is a straightforward application. On the other hand, the definition of a flow velocity field is far less obvious and requires knowledge of the relevant watershed characteristics.

The routing component includes three functions: the overland flow routing function, the channel routing function and transmission loss function. The distinction between the overland flow and the channel flow is made to enable applying different flow velocities and transmission loss conditions for each. In addition, different flow velocities can be applied to the channel flow according to the Strahler order or the geometric specifications of the channel.

Computations of the flow routing functions are carried out on a cell-by-cell basis using raster-processing techniques (see chapter 7).

6.5.4.1 The overland flow function

The complexity of the hydrological processes involved in both the generation of the rainfall excess amounts and the routing process has been traditionally dealt with by subdividing the catchment area into sub-watersheds, which are assumed to have homogeneous hydrological properties. The sub-watersheds are chosen so that a single stream drains each watershed. This arrangement is usually used to serve two purposes: first, lumping of parameters at the more homogeneous sub-watershed level; secondly,

for the purposes of applying a unit hydrograph approach originally designed for small size watersheds (Wanielista, 1990).

For the purposes of running the current model, neither the parameter lumping nor the unit hydrograph approach are required. However, the subdivision of the watershed into smaller sub-watersheds is performed here to define the boundary between the overland flow routing and the channel flow routing. In this regard, the routing within the sub-watershed is considered as overland flow routing, while channel routing takes place along the channels that link the sub-watershed to the outlet.

The overland flow function performs the calculation of both the discharge contributed by each cell, and the time of travel required for that discharge to reach the outlet. These computations are carried out for each sub-watershed in the area. Accumulating all the discharge amounts that reach the outlet within a given period of time will generate a hydrograph at the sub-watershed outlet.

6.5.4.2 The channel flow function

The hydrographs generated by the overland flow function are routed to the watershed outlet using the channel routing function. The function applies the same approach as the overland flow function and produces a hydrograph at the watershed outlet.

6.5.4.3 The channel transmission losses function

This function estimates the channel transmission losses based on the following equation of Walters (1990) (see section 3.5)

$$V_1 = 0.05 * V_0$$

where,

V_1 : the volume of transmission losses at 1 mile from an up stream station,

V_0 : the flow volume at the upstream station.

Walters (1990) suggests that " estimates of transmission loss can be determined for any mile by calculating the flow volume at the beginning of the mile as flow volume minus the transmission loss in the previous mile". This can be interpreted mathematically as follows,

$$q_1 = 0.95 * q_0$$
$$q_2 = 0.95 * q_1 = (0.95)^2 * q_0$$
$$\cdot\ q_n = (0.95)^n * q_0$$

where,
q_0 : the flow volume at the initial upstream station,
q_n : the flow volume at a distance n miles downstream from the initial station.

The transmission loss function uses this equation to estimate the losses to be abstracted from the routed cell flows. Keeping along with the linear routing principle, transmission losses can be calculated for each cell flow independent from the other cells.

Since transmission losses only occur during the passing of the flow over the channel network, only the distance along the channel will be relevant to the computation of transmission losses. The computation method used consists in defining the distance along the channel network from each cell to a given outlet and then extrapolating the volume of flow at the outlet according to the above equations. Since the estimates of the downstream flow volume are calculated at 1-mile steps, the flow volume at any distance other than mile multiple needs to be interpolated from the two immediate neighbour values (figure 6-4). The following equations describe the interpolation process applied by the transmission function.

$$d1 = Int(d)$$
$$d2 = d1 + 1$$
$$q1 = (0.95)^{d1} * q_0$$
$$q2 = (.95)^{d2} * q_0$$
$$q = q1 - (q1 - q2) * (d - d1)$$

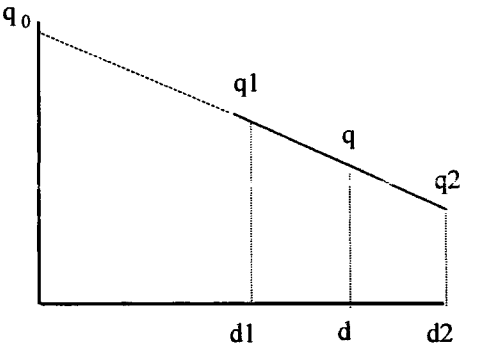

Figure (6-4) Interpolation of the transmission losses

where,

d, q : distance and discharge at the outlet,

$d1, q1$: distance and discharge at a point 1 mile upstream from the outlet,

$d2, q2$: distance and discharge at a point 1 mile downstream from the outlet,

q_0 : initial rainfall-excess at the cell.

6.6 Summary

The structure of a GIS-based hydrological model for the study of surface water at Wadi Rajil watershed has been described. The aim of the model is to generate hydrographs at the watershed outlet from the input rainfall data. The model is based on a simple water budget equation where the balance between input and output water amounts is carried out at the cell level.

The routing process consists of calculating the time of travel and the discharge contributed by each cell for each time step of computation. Accumulating the discharges contributed by all the cells during the hydrograph time step produces the output hydrograph.

CHAPTER 7

RUNNING THE MODEL AND DISCUSSION OF RESULTS

7.1 Introduction

In chapter 6 the conceptual design and the formulation of the hydrological processes of the surface hydrology model of Wadi Rajil watershed have been presented. In this chapter the focus will be put on the practical aspects related to the functionality of the model. The chapter consists of two parts. The first part describes the programs and GIS procedures that simulate the model functions The second part discusses several case studies to investigate the sensitivity of the watershed response to variations in the main hydrological parameters.

7.2 Description of the model programs

When programming the model functions, the key elements to consider are flexibility for future updates, and efficiency of the algorithm. Flexibility is an essential requirement in view of the continuous need to adjust the existing model parameters or to introduce new ones. Software/hardware requirements as well as the time of execution are also important features to be considered if the model is to be put to practical use.

As far as this study is concerned, the objective is to demonstrate the use of GIS for carrying out hydrological modelling tasks making full use of the available GIS software.

However, it is generally possible to tailor ARC/INFO applications to be used with a PC-based ARCVIEW interface.

Efficiency in time of execution can be achieved by a proper selection of the appropriate set of GIS tools that will simulate the required functions. This task is not so easy with the huge number of tools and functions available. On the other hand, the available tools are general-purpose GIS tools that need to be manipulated to match the required hydrological application. For example the FLOWACCUMULATION function calculates the number of cells that contribute flow to a given cell without considering the time required for this accumulation to take place. Knowledge of the time of accumulation can be used for a dynamic simulation of the overland flow process, which provides accurate assessment of the actual evaporation and velocity of overland flow.

The programming approach to simulate the model function consists of two programs: the runoff generation program, and the flow routing program.

7.2.1 The runoff generation program

The program calculates the rainfall-excess amounts generated within the watershed from the input rainfall data provided as time-series point data. A raster grid layer defining the rainfall distribution over the area can be introduced at this stage. If not provided, the rainfall will be assumed uniformly distributed over the area.

7.2.1.1 The algorithm

The program simulates the runoff generation functions described in section(6.5.3) as a sequence of water losses applied to the input rainfall amounts. The computations are carried out on a time step basis. Initially, the program sets the time step to be equal to the time step of the input rainfall data. This however, can be changed to any user-defined time

step if a different simulation resolution is required. Figure (7-1) illustrates the flow diagram of the program components.

Since the model is structured as a distributed model, the computations should be carried out at the cell level for each time step. Given the number of time steps and grid cells involved (more than 3 million cells at 30 metre resolution) a significantly large number of computations are required. A more efficient approach can be applied by grouping into one zone all the cells that would, under the current model assumptions, yield the same amount of rainfall excess. These zones, referred to as similar rainfall-excess units (SREU), can be defined by intersecting the hydrologically similar units (*hsu*) layer described in chapter 5 with the rainfall-distribution layer. The maximum number of different SREUs that result from the intersection of the two layers is equal to the product of the number of classes in the two layers. Thus, instead of carrying out the computations for each cell in the watershed area it will be only required to perform the calculations for the number of SREUs, which will be, under all practical conditions, significantly lower than the number of cells.

7.2.1.2 The program output results

At the end of each time step the program generates the following output results for each SREU,

- The input rainfall amount (P),
- The net infiltration amount (F),
- The actual evaporation from the open surface water (E1),
- The actual evaporation from the upper-soil moisture storage(E2),
- The soil moisture content (SMe),

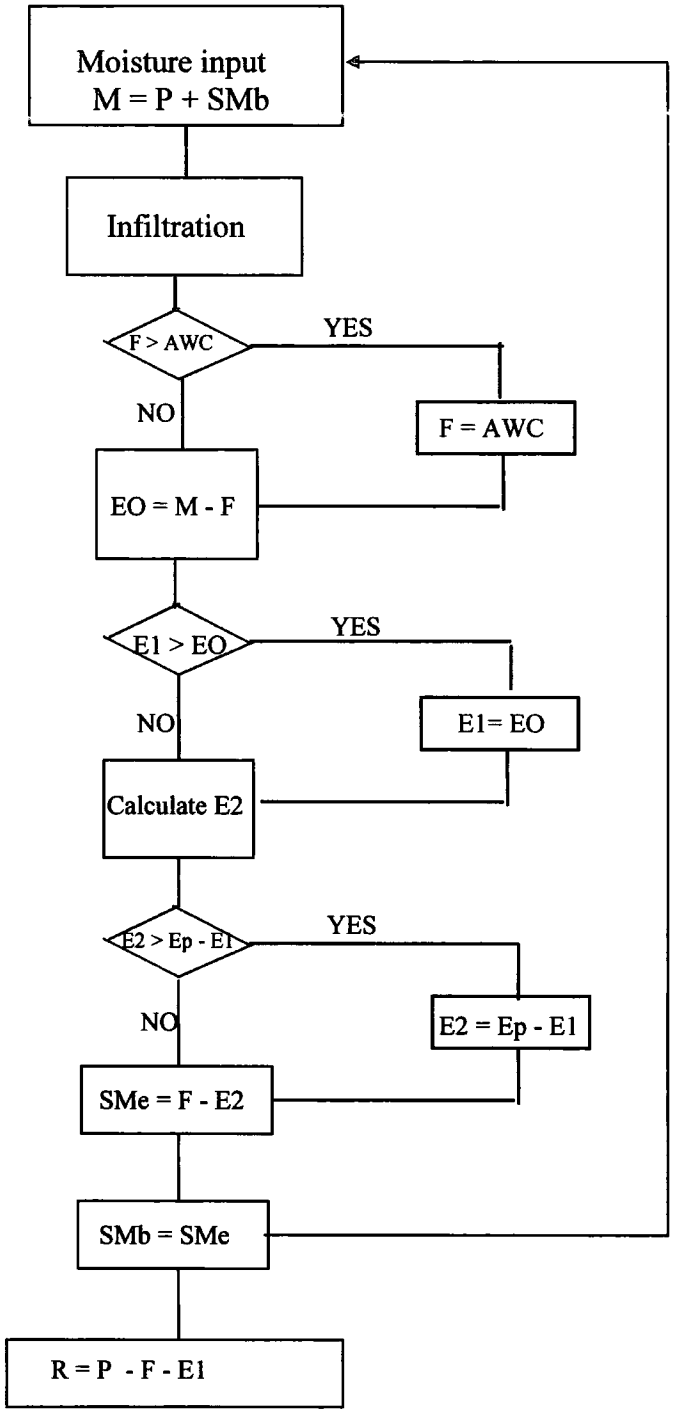

Figure (7 - 1) Flow diagram of the runoff generation program

- The rainfall-excess amount (R).

These results represent time series attributes of the SREUs and therefore, it is required to include these data as attributes in the SREU feature attribute table. This implies that six attributes need to be added to the table for each time step. Since the relate environment currently supported by ARC/INFO only allows for adding or relating attributes as columns, adding the time series attributes will result in a very flat table structure with very long record lengths that can go beyond the length limits supported by ARC/INFO. An alternative approach proposed by Maidment (1996) suggests using the object-oriented language AVENUE to relate the time series data to the feature attribute tables as records rather than columns. However, this arrangement does not help in presenting the time series data as grid layers which is the method applied here to pass the output results of the runoff generation program to the runoff routing program. To overcome this database management problem, the approach applied here is to create a separate table to hold the time-series output results for each output type. The table of concern for the routing process is the rainfall-excess data table. In this table each column represents the rainfall excess amounts produced within the watershed during a given time step, whereas each row represents the time-series sequence of rainfall-excess amounts for one SREU.

7.2.2 The flow routing program

The basic concept of the routing process consists in calculating the discharge contributed by each cell to the watershed outlet and the time required for that discharge to reach the outlet. The calculations are performed on a cell-by-cell basis for each time step.

7.2.2.1 The routing parameters

The routing process, as simulated by the model, is controlled by two distributed cell-parameters: the time of flow factor, and the transmission loss factor. The values of these parameters depend on long-term constant watershed properties like channel slope and flow path length. Both of the two parameters are distributed in nature since their values change from cell to cell.

7.2.2.1.1 The time of flow factor

The term time of flow, as used here, refers to the time required for the rainfall excess generated at each cell location to reach the outlet. A grid layer representing the time of flow for each cell in the watershed area can be created using the GRID-FLOWLENGTH function. Generally, the function convolutes the cell values of an input cost grid along the direction of flow from the cell location to the outlet. The cell values of the cost grid must be provided as costs per unit distance. The convolution process can be expressed mathematically as follows,

$$v_{ij} = \sum_{p} c_p * d_p$$

where,
v_{ij} : the output result of the convolution for cell (i, j),
d : the slope distance between the centres of two adjacent cells along the minimum-cost path,
c : the unit-distance cost value,
p : the minimum-cost path.

By manipulating the cell-based cost values the function can be used to perform any sort of convolution required. Olivera and Maidment (1996) have reported such an application for a cell-based routing application using the diffusion wave model. In this context, the

FLOWLENGTH function can be used to calculate the time of flow for each cell by providing the time of flow over one metre distance as the cell value of the cost grid. This cell value can be expressed as follows,

$$t = \frac{1}{v}$$

where,
t : the unit-distance time of flow (t),
v : the flow velocity (ms^{-1}).

Since the time of flow is defined in terms of the flow velocity, there are two approaches to consider.

1. The flow velocity is constant. Since there is no data available on the flow velocity in the area, it is assumed here that both the overland flow velocity and the channel flow velocity are constant and equal to 1 m s^{-1}. Abdallah (1995) adopted this value as an acceptable average flow velocity value. Therefore, the unit-distance time of flow will be constant for all the cells and equal to 1 second.
2. The flow velocity is variable. The assumption made here is that the overland flow velocity is variable while the channel flow velocity remains constant and equal to 1 m s^{-1} The variability of the overland flow velocity is modelled according to the following formula of Manning,

$$v = \frac{1}{n} * s^{0.5} * y^{0.67}$$

where,
n : Manning's roughness coefficient for overland flow,
y : overland flow depth (m),
s : ground slope.

Therefore, the unit-distance time of flow for the overland flow routing can be expressed as follows,

$$t = n * s^{-0.5} * y^{-.67}$$

The convolution of this value over the flow path from the cell to the watershed outlet, as computed by the FLOWLENGTH function, can be expressed as,

$$t_{ij} = \sum_{p} n_p * s_p^{-0.5} * y_{ij}^{-0.67}$$

where,
i, j : the cell co-ordinates,
p : path of travel.

As described in section (6.5.1) the model assumes that rainfall excess generated at each cell is routed independently from interactions with flows from other cells. Moreover, the routed cell flow is assumed not to be subject to transmission losses until it reaches a channel cell. Under these assumptions the depth of overland flow remains constant and hence, the previous equation can be rewritten as,

$$t_{ij} = y_{ij}^{-0.67} * \sum_{p} n_p * s_p^{-0.5} = y_{ij} * k_{ij}$$

where k_{ij} is the time of flow factor considered as a cell parameter independent of the overland flow depth.

Thus, a distributed layer of the time of flow factor k_{ij} can be generated by the FLOWLENGTH function by using the following value as unit-distance cost,

$$c = n * s^{-0.5}$$

This layer can be used to calculate the time of flow for any overland flow depth by simply generating a grid of the values $y_{ij}^{-0.67}$ and carrying out a grid multiplication process.

7.2.2.1.2 The transmission losses factor

It has been seen in section (6.5.4.3) that rainfall excess amounts generated at each cell reach the outlet reduced by the amount of transmission losses. Since the original formula estimates the reduction due to transmission losses at distances of mile multiples, an interpolated form is used to calculate the losses for any distance (see section 6.5.4.3). The interpolated form of the equation is a function of the initial rainfall excess amount and the distance travelled along the channel network from each cell to the outlet. Since the distance along the channel network is constant for each cell, a distributed layer representing the along-channel distances can be derived and used to create a transmission losses-factor layer based on the interpolated form of the transmission losses. The FLOWLENGTH function can be used to derive this layer by defining the cost grid as follows,

$c_{ij} = 1$ for channel cells,
$c_{ij} = 0$ for non-channel cells.

The convolution of this value will sum up the slope distance along the channel cells only and thus, a layer of the values of the along-channel distance for each cell is generated.

7.2.2.2 The Routing levels

The routing process is carried out at two steps: overland flow routing and channel flow routing. As discussed in section (6.5.4.1) the overland flow routing occurs at the sub-

watershed level, while the channel flow routing is concerned with routing the outflows of the sub-watersheds to the watershed outlet.

7.2.2.2.1 Overland flow routing

The aim of the overland flow routing process is to generate a hydrograph for each sub-watershed in the area. The procedure consists in generating two separate grids for each time step of computation, the time-of-flow grid and the discharge grid. The time-of-flow grid can be classified into isochrones and used, as a *zonal* grid, to calculate the accumulated discharge for each isochrone. A spatial merge between the two grids, the isochrone grid and the *zonal sum* grid, is required to combine the two attributes, time and discharge, for each cell. The combined grid represents the hydrograph generated from the rainfall excess of a given time step. Figure (7-2) illustrates the basic concept of the routing process. Besides the hydrograph elements of time and discharge that appear as attributes in the attribute table associated with the hydrograph grid, a raster map of the isochrone areas can be obtained. The hydrograph of a given rainfall event can be generated by shifting, in time, the hydrograph of a given input time step over that of the previous one and accumulating the discharges according to the required hydrograph time step. The amount of shift is equivalent to the time step of the input rainfall-excess amounts. This process is simulated by defining linear relationships between the tables of the individual time-step hydrographs. The hydrograph time step is set to an integer divisor of the input rainfall-excess time step.

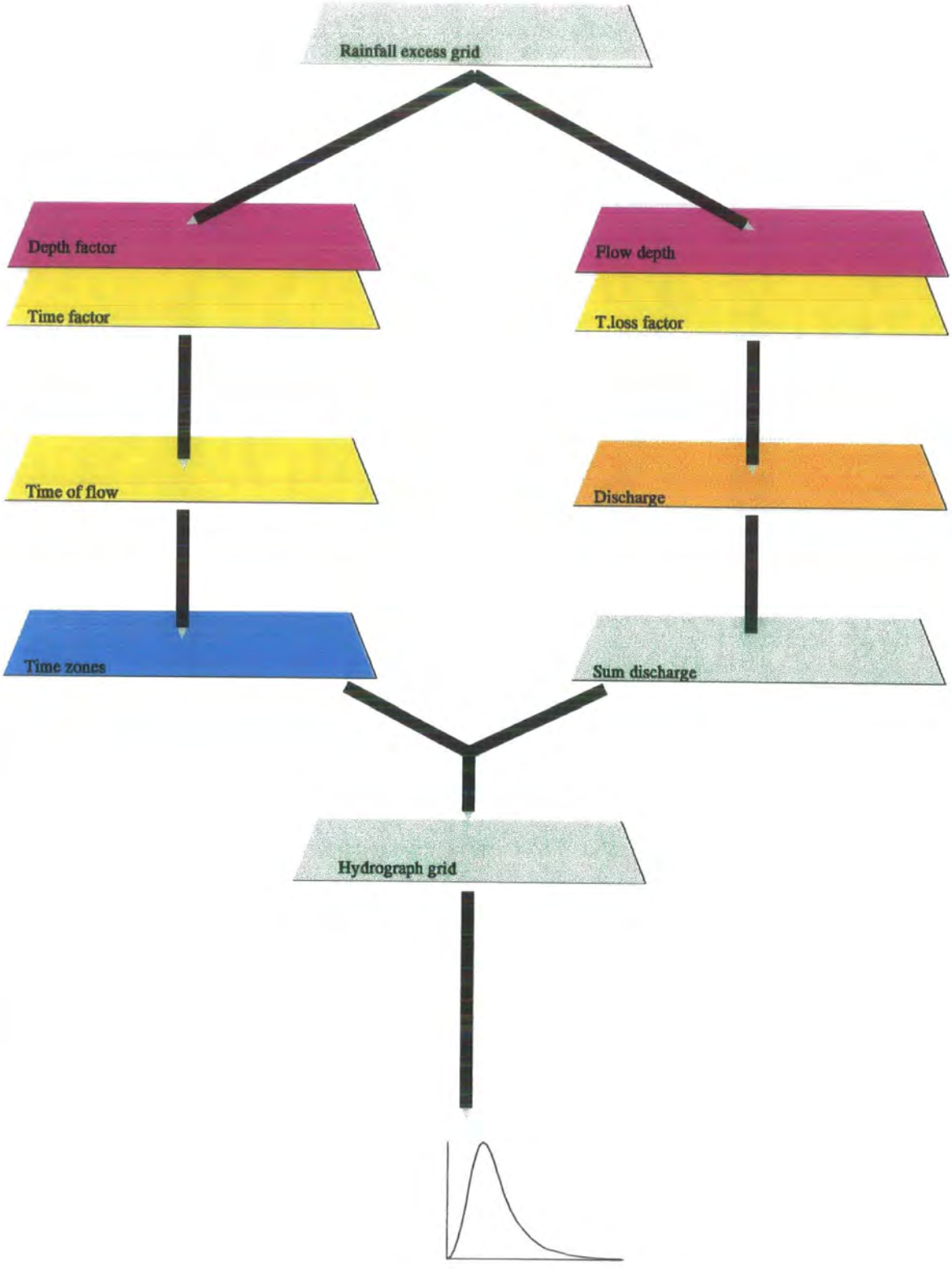

Figure (7 - 2) The basic procedure of the flow routing process

7.2.2.2.2 Channel flow routing

The overland flow routing process results in a hydrograph generated at the outlet of each sub-watershed in the area. These hydrographs are to be routed to the watershed outlet through the channel network. Before carrying out the channel routing process, the hydrographs of the upstream sub-watersheds that share a common outlet are combined in one node-hydrograph. The combined hydrograph will serve as the in-flow hydrographs for the downstream channel link associated with the node. The procedure used for generating the node-hydrographs consists of the following steps:

1. Generate a grid of the channel network nodes.
2. Include the node-id representing the sub-watershed outlet as an attribute of the sub-watershed grid.
3. The node-id item can be used to generate a grid representing the upstream area contributing flow to each node by selecting all the cells that share a common node-id.
4. The process of generating a hydrograph described in section (7.2.2.2.1) can then be applied to the node sub-watersheds to produce the required node hydrographs.

At this stage the routing process is abstracted as a set of node-hydrographs connected to the watershed outlet by a network of connected channel links. These hydrographs are routed to the watershed outlet as channel flows. The model assumptions related to the channel routing process could be summarised as follows:

1. The inflow hydrographs are routed independently from each other.
2. The velocity of flow through the channel links is constant for all links and is equal to $1\ m\ s^{-1}$.
3. The routing process is a pure translation process and the storage-discharge relationship is not simulated. This implies that transmission losses have no influence on the time of flow and their influence as losses of the routed flows only appears at the outlet.

4. The discharge amounts are reduced by the transmission loss-factor.

These assumptions, however, do not represent shortcomings of the model itself but rather are due to the availability of data and the objective of the research. From a functional point of view many of the above mentioned assumptions can be eliminated and a more realistic situation can be modelled. For example, the model structure allows for assigning different flow velocities for the channel sections according to their geometric shapes. Also, by manipulating the cell-based cost grid a storage-discharge relationship or a hydraulic routing procedure can be applied to the channel flow routing component and the convolution describing the channel response to this function can be performed using the FLOWLENGTH function.

The procedure for generating the watershed hydrograph from the node-hydrographs consists mainly in adding the time of flow along the channel from each node to the outlet to the node-hydrograph time. Since the channel flow velocity is assumed constant and equal to 1 ms^{-1}, the channel distance (in metres).gives the time of flow from each node to the outlet (in seconds). The discharge amounts at the watershed outlet are calculated from the node-hydrographs discharge values reduced by the transmission loss factor. Finally combining the time of flow and discharge grids generates the hydrograph at the watershed outlet.

7.3 Analysis of results and discussion

An important function of the hydrological model is to predict the watershed response under a given set of conditions. Models also serve to perform sensitivity analysis and calibration of the hydrological parameters involved. The Wadi Rajil model can only be expected to give a crude assessment of the hydrological parameters. This is mainly due to

two reasons. First, there are important hydrological parameters not simulated in the model. Secondly, the model has not been calibrated or tested against observed or verified measurements.

In the following sections the model is run under various hydrological conditions and the results are discussed. Since no runoff records are available, the discussions are basically based on comparative analysis of the model results with the results obtained from other approaches.

7.3.1 Generation of a unit hydrograph

In section (3.8.1.2) a method for generating a spatially distributed unit hydrograph was presented. The same approach can be applied to generate a 1-hour unit hydrograph using the Wadi Rajil model. The unit hydrograph can be generated by accumulating, on an hourly basis, the discharge amounts generated from 1 mm of rainfall excess regularly spread over the watershed area.

The model has been used to generate unit hydrographs under different combinations of flow velocity and transmission losses. The first hydrograph, shown in figure (7-3), was produced assuming fixed flow velocity and no transmission losses. These assumptions comply with the unit hydrograph theory, which assumes constant time base of the hydrograph and no abstractions of the routed amounts. The constant time base of the unit hydrograph implies that, for a given cell location, the time of travel to the watershed outlet, and hence the velocity of flow, is the same for all rainfall excess amounts (Maidment, 1993). The hydrograph has steep rising and falling limbs and a relatively short time of concentration of about 1.5 day. The isochrones shown in the figure exhibit distinct zones of relatively uniform shapes and regular distances from the outlet. Figure (7-4) shows a hydrograph generated assuming variable overland flow velocity. The hydrograph

has a steep rising limb but relatively longer recession period. The isochrones exhibit the effect of slope on the velocity of flow and hence the time of concentration. For example, the upper north west area has shorter time of concentration than areas to the north which are geographically closer to the outlet.

Comparisons between the unit hydrographs produced by the model and the SCS synthetic unit hydrograph described in section (3.8.1.1) are shown in figures (7-5) and (7-6). The unit hydrograph generated under fixed flow velocity and no transmission loss shows a relatively good fit, in terms of the peak flow and time to peak, (figure 7-5) with the SCS unit hydrograph. This implies that estimates of the discharge of Wadi Rajil based on the synthetic unit hydrograph approach may not include the influence of transmission losses.

If losses due to transmission represent a persistent property of the routed flows in the watershed then the unit hydrograph generated under the assumption of no transmission losses may not be representative to the watershed response. Instead, if transmission losses are applied to the 1 mm-depth of rainfall excess, then the resulting hydrograph can be considered as a representative unit hydrograph. This assumption is justified by the fact that transmission losses for each cell represent a constant reduction factor of the original cell flow and can be expressed by the following equation,

$$q_{ij} = k_{ij} * R_{ij}$$

where,

q_{ij} : the discharge at the outlet contributed by cell (i,j),

k_{ij} : the cell transmission loss factor,

R_{ij} : the initial cell flow.

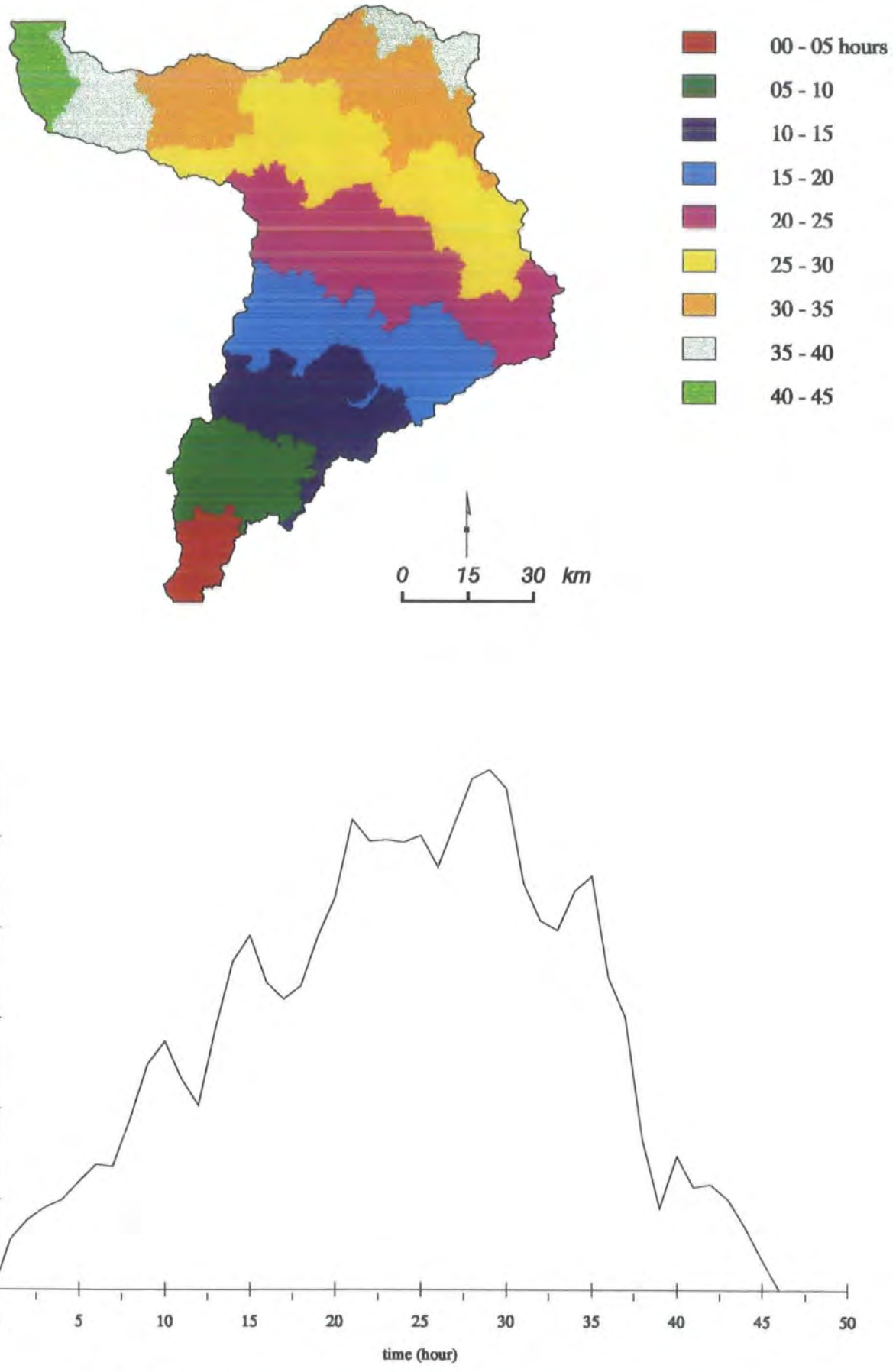

Figure (7 - 3) The isochrones and the unit hydrograph for conditions of fixed flow velocity and no transmission losses

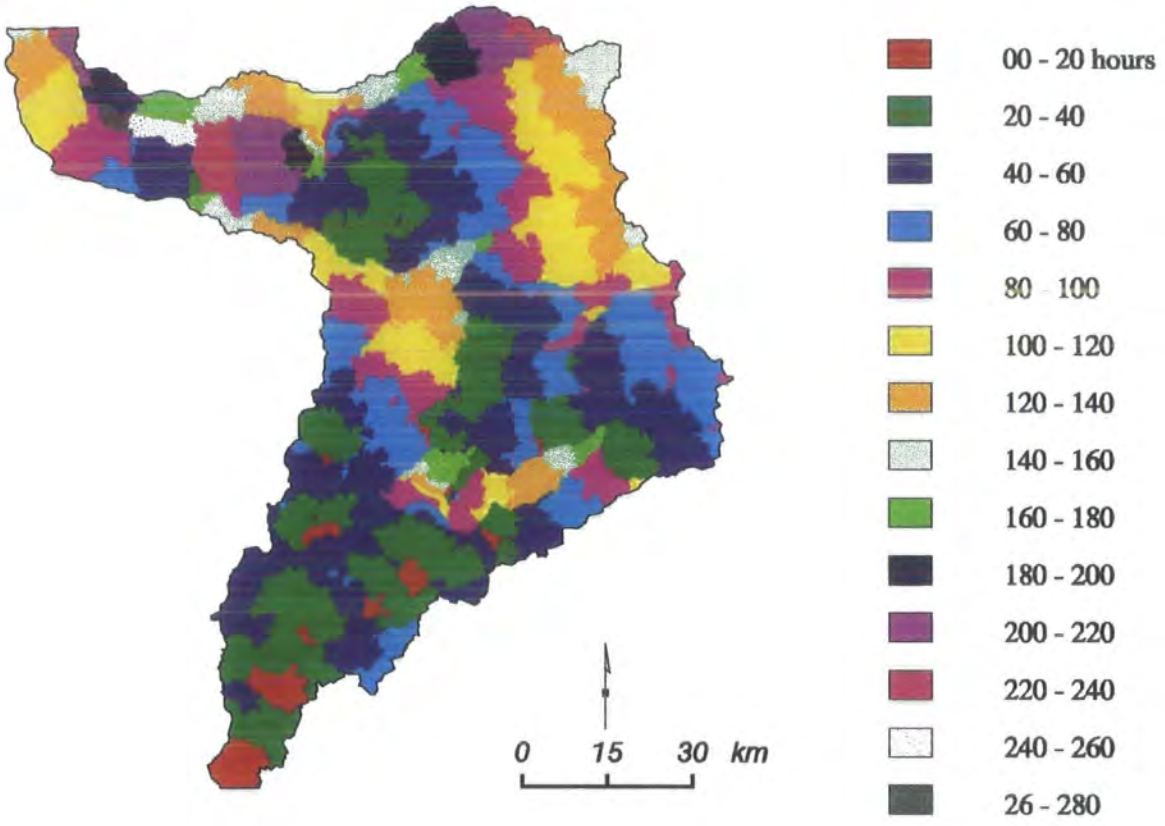

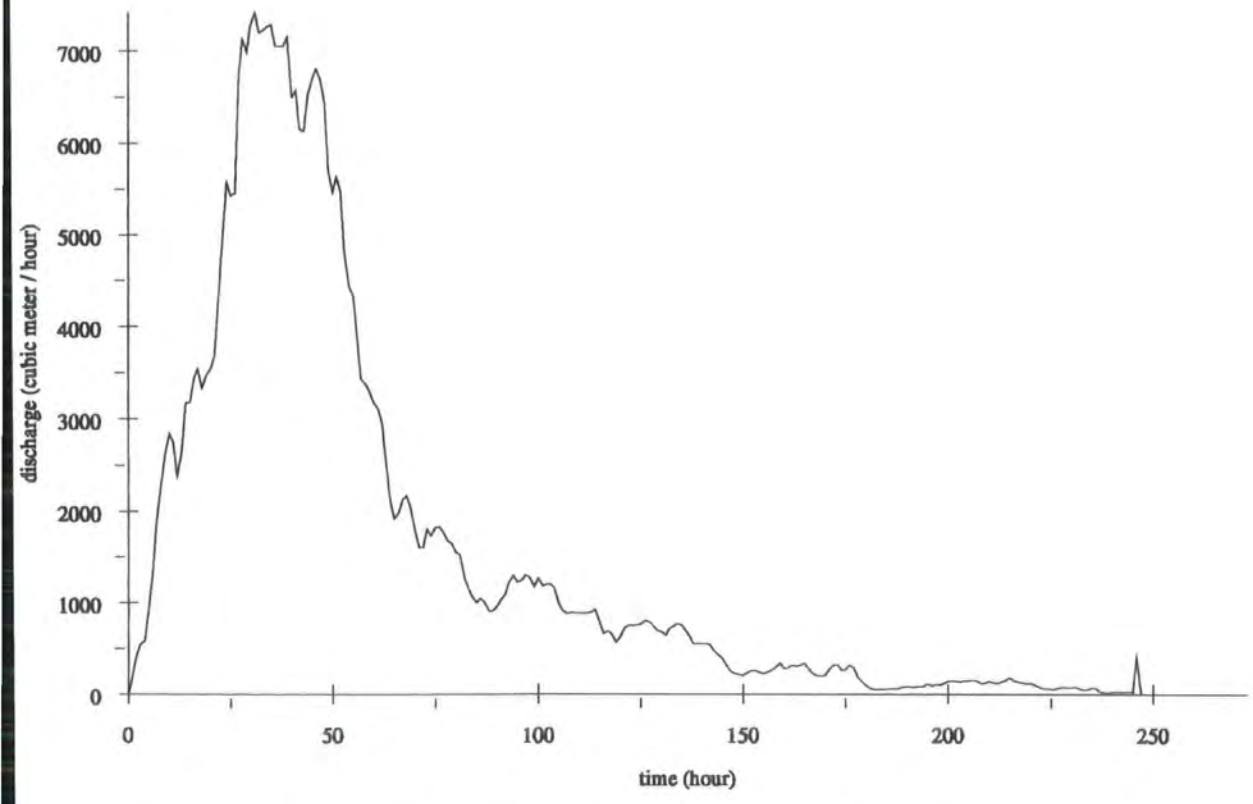

Figure (7 - 4) The isochrones and the unit hydrograph with variable flow velocity

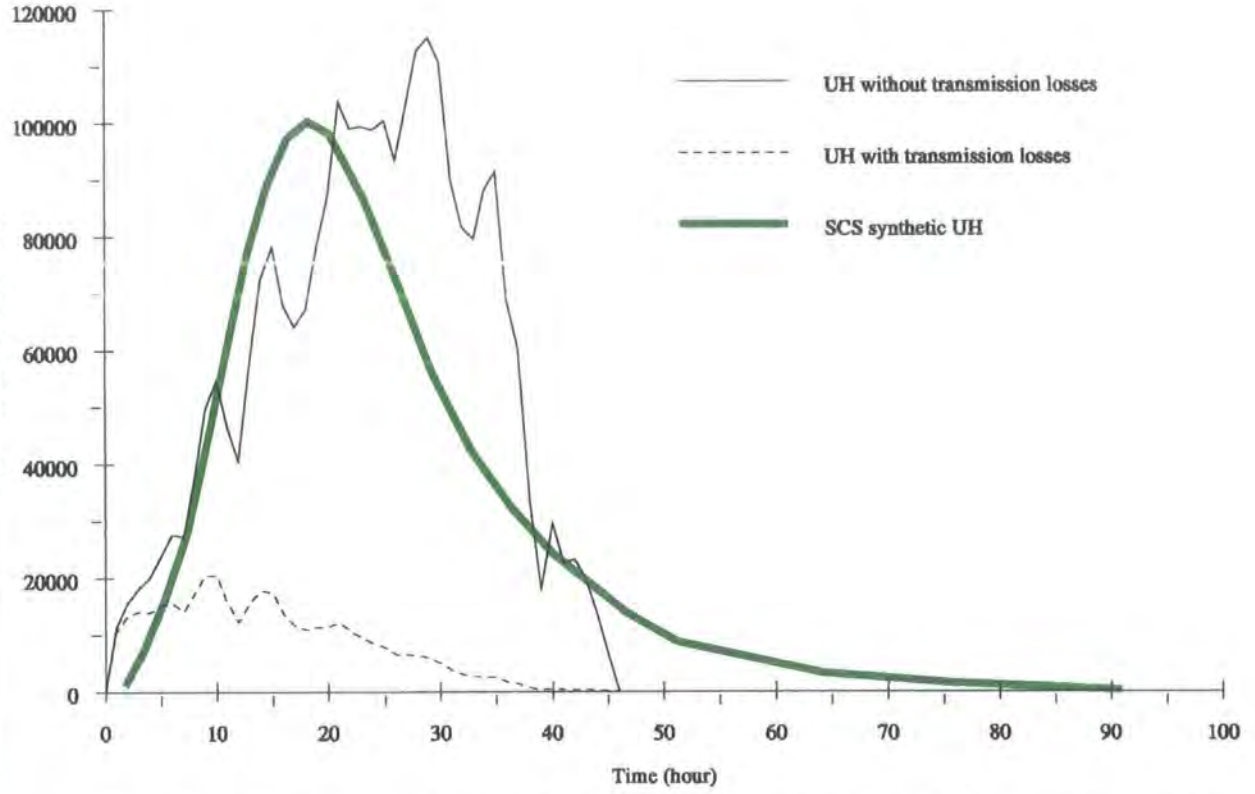

Figure (7 - 5) Comparison between the UH produced by the model (under constant flow velocity) and the SCS UH

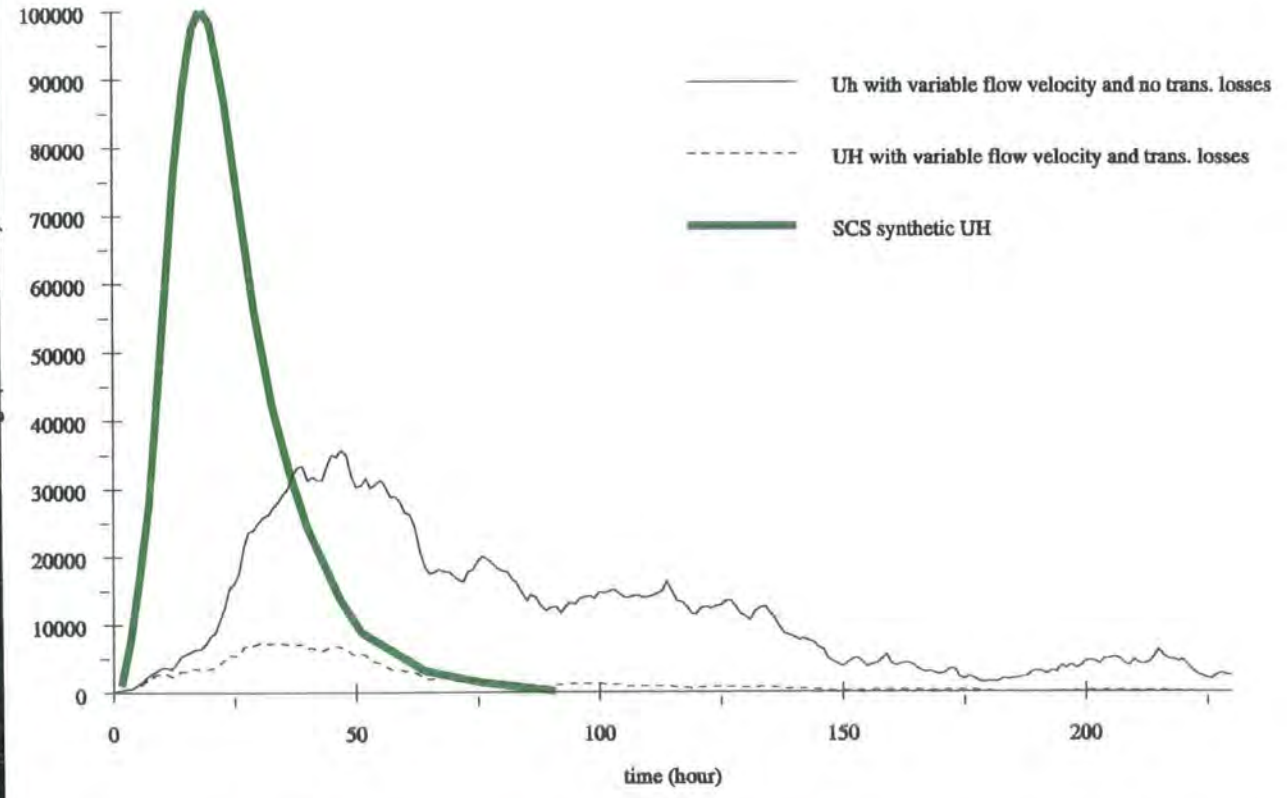

Figure (7 - 6) Comparison between the UH produced by the model (under variable flow velocity) and the SCS UH

7.3.2 Analysis of flood peak and flood volume

In this section the model is used to calculate the flood peak and flood volume of several simulated storms of different return periods. Table (7-1) shows the 24-hour rainfall of storms of 5, 10, 25 and 50 year-return periods produced from the intensity-duration-frequency curves for station F2. An hourly distribution of the rainfall of each storm is estimated using the mass curve described in section (3.2.4).

Table (7-1) 24-hour rainfall of 5, 10, 25, and 50 year-return period storms
(source: Sa'ad, 1986)

Return period (years)	24-hour rainfall (mm)
5	26
10	34
25	45
50	53

Hydrographs of the above simulated storms were generated with (figure 7-7) and without (figure 7-8) transmission losses. Tables (7-2) and (7-3) show comparisons between the model results an the results of other empirical studies described in section (3.6.3)

Table (7-2) Estimates of flood peaks ($m^3 s^{-1}$) of storms of different return periods

Study	5-year	10-year	25-year	50-year	mean annual flood $m^3 s^{-1}$
Ayed (1996)	-	18.0	185.6	440.0	146
Hydrosult (1990)	136	229	-	535	190
Wadi Rajil model (with trans. losses)	43	78.3	123	156.8	88
Wadi Rajil model (without trans. losses)	360.8	592.5	864.7	1087.7	522
Farquharson - Jordan					202
Farquharson - All arid region basins					184

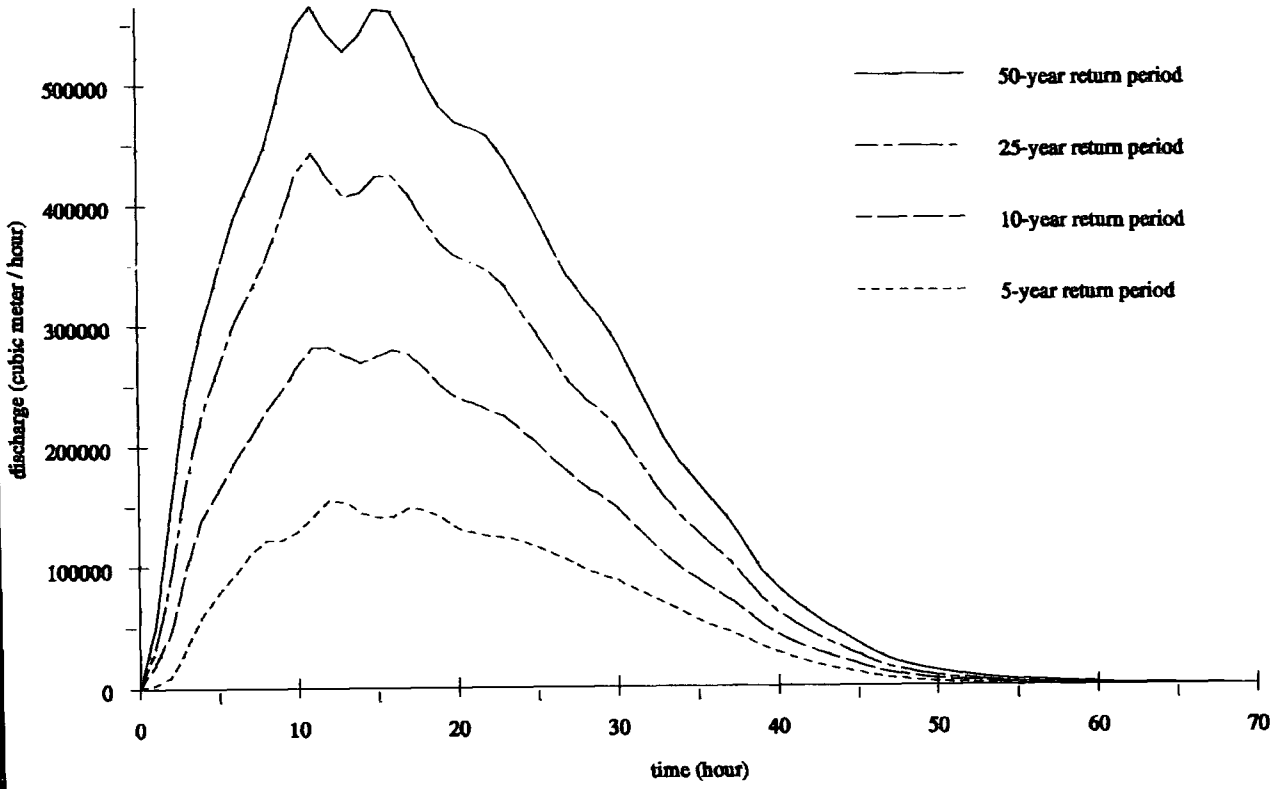

Figure (7 - 7) Hydrographs of simulated storms (with transmission losses)

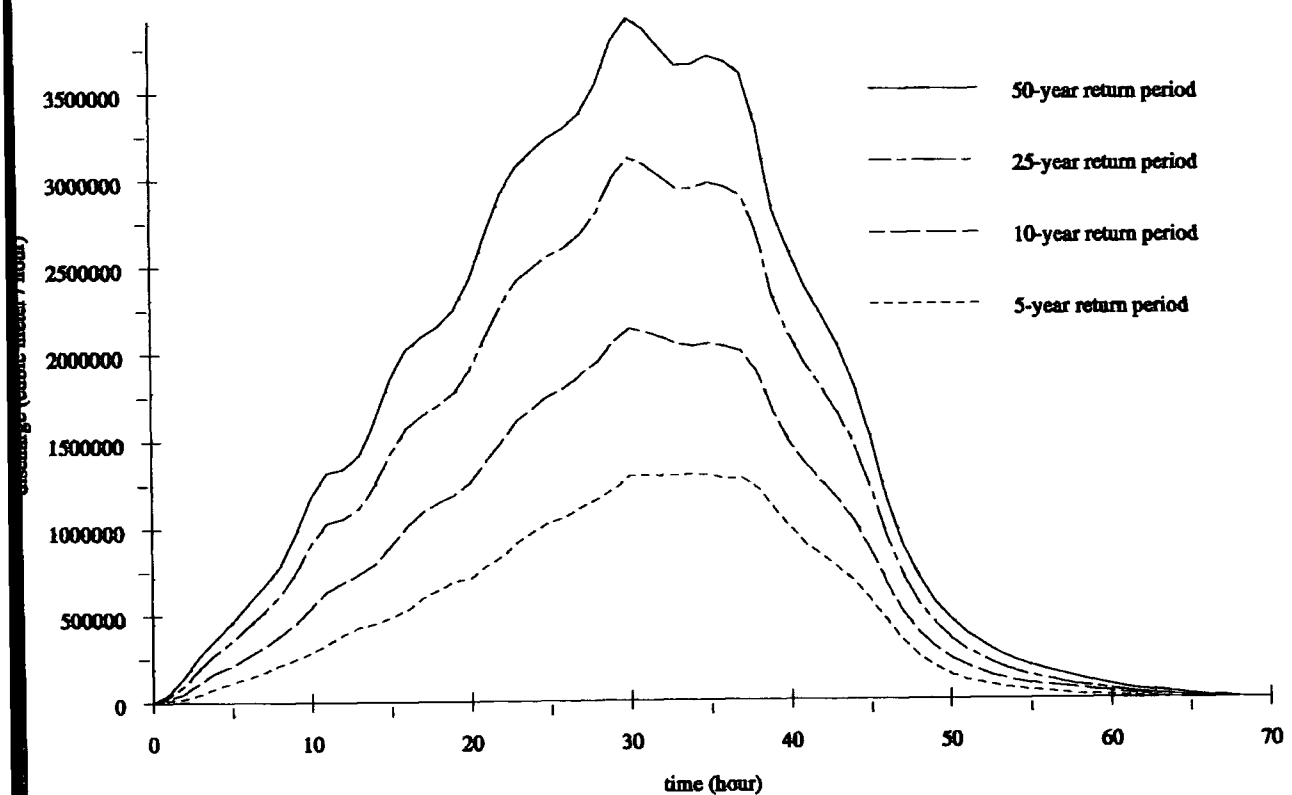

Figure (7 - 8) Hydrographs of simulated storms (with no transmission losses)

Table (7-2) shows also a comparison between the mean annual flood peak values, computed as a weighted average of the peak flow values of the storms of different return periods, and estimates of the mean annual flood values based on the study of Farquharson *et al* (1992) on the regional flood frequency analysis in arid catchments. The study of Farquharson *et al* (1992) relates the mean annual flood peak to the catchment area by the following regression equation

$$MAF = C \times AREA^{e}$$

where

MAF : mean annual flood $m^3 s^{-1}$,

C : constant. the value of which for Jordan is 6.83 and for all arid catchments is 1.87,

e : exponent. It's value for Jordan catchments is 0.427 and for all arid catchments is 0.578.

Table (7-3) Estimates of flood volumes (M m^3) of storms of different return periods

Study	5-year	10-year	25-year	50-year
Ayed (1996)	-	1.6	16.5	39.5
Hydrosult (1990)	16.8	28.2	-	54.7
Wadi Rajil model (with trans. losses)	3.95	7.26	10.96	14.44
Wadi Rajil model (without trans. losses)	34.85	57.75	85.0	107.22

It is seen from the tables that the values of flood peaks and flood volumes produced by the model assuming no transmission losses are significantly higher than the corresponding values of the other approaches, while the modelled values produced with transmission losses are much lower.

A further investigation of the results shows strong correlation between the model results and those of the Hydrosult (1990) study (figure 7-9). The relationships between the results of the two studies can be expressed by the following equations,

$$p_{m1} = 0.31 * p_D$$
$$p_{m2} = 2.42 * p_D$$
$$v_{m1} = 0.25 * v_D$$
$$v_{m2} = 2.02 * v_D$$

where,

p : flood peak,

v : flood volume,

$m1$: results of the model with transmission losses,

$m2$: results of the model with no transmission losses,

D :results of Hydrosult study (1990).

The above results indicate that the model simulates adequately the watershed response since the estimates of the Hydrosult (1990) study were based on indexes of the flood characteristics of other gauged sites in the area. The graphs show good correlation between the results and suggests the need to calibrate rather than change the model parameters.

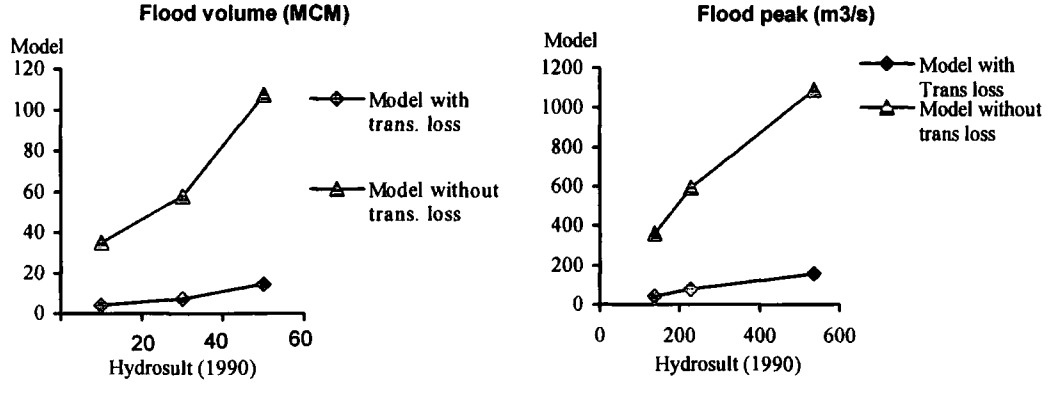

Figure (7-9) The relations between the results of the model and those of the Hydrosult (1990) study

7.3.3 Analysis of transmission losses

Transmission losses are modelled as functions of both the upstream flow volume and the channel length (see section 3.6). In this section an assessment of the influence of these two factors on transmission losses is investigated. The assessment may only be considered as indicative of the relative importance of the factors rather than an accurate quantitative assessment. This is mainly due to two reasons. First, the influence of antecedent moisture conditions on transmission losses is not considered. Secondly, the equation used was originally verified for transmission losses over short distances and its use for estimating losses at longer distances may give unpredictable results (Walters, 1990).

To test for the influence of the change in flow volume on transmission losses the hydrographs of the design storms of 5, 10, 25, and 50-year return periods are used (figures 7-7 and 7-8). Besides the significant influence on the peak flow and volume of flow transmission losses appear to reduce the time to peak and time of concentration of the hydrograph. This is mainly because the discharges contributed by the remote areas decrease significantly with the increase in distance away from the outlet. The ratio analysis of the flow peaks and volumes for the different storms (table 7-4) show that transmission losses maintain the same reduction factor for all flow volumes. This reduction factor is given by the following equation,

$$p_T = 0.13 * p$$
$$v_T = 0.13 * v$$

where,
p : flow peak,
v : flow volume,
T : index indicating that transmission losses are applied.

Table (7-4) Ratios between the flow peak and volume for the two transmission loss conditions

Return period of storm (year)	Ratio between peak flows (with trans. loss / without trans. loss)	Ratio between flow volumes (with trans. loss / without trans. loss)
5	0.12	0.11
10	0.13	0.13
25	0.14	0.13
50	0.14	0.13

The above results show that transmission losses occur at the same rate irrespective of the volume of flow. Eventually this is because the antecedent moisture conditions of the channels are not considered as a controlling factor in the transmission loss equation. Therefore, transmission losses occur always at the potential rate.

The effect of channel flow length has been investigated by calculating the hydrographs for a given storm (the storm of 10-year return period) at different channel flow lengths. The test was made by considering the channel flow lengths at Strahler orders greater than or equal to 1, 2, 3, and 4. Figure (7-10) shows the resultant hydrographs. Table (7-5) summarises the results of the hydrograph calculations.

Table (7-5) Transmission losses for different Strahler orders

Strahler order	Peak flow ($m^3 s^{-1}$)	Time to peak (hour)	Flow volume ($M m^3$)
> = 1	78.3	11	7.26
> = 2	80.02	11	7.46
> = 3	82.29	11	7.67
> = 4	100.0	12	10.08

Both the graphs and the table show that channels of Strahler orders 1 and 2 have very little influence, of about 5% only, on the transmission losses.

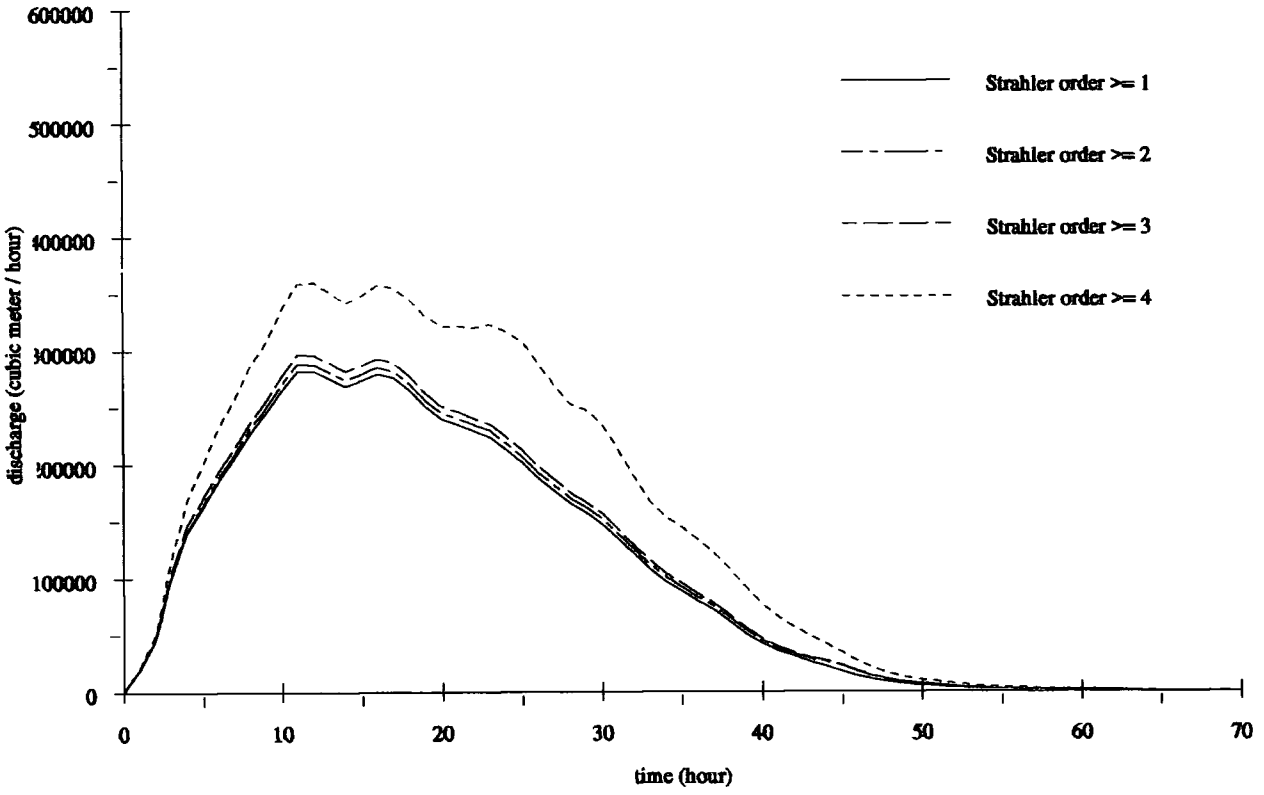

Figure (7 - 10) Transmission losses for different stream orders

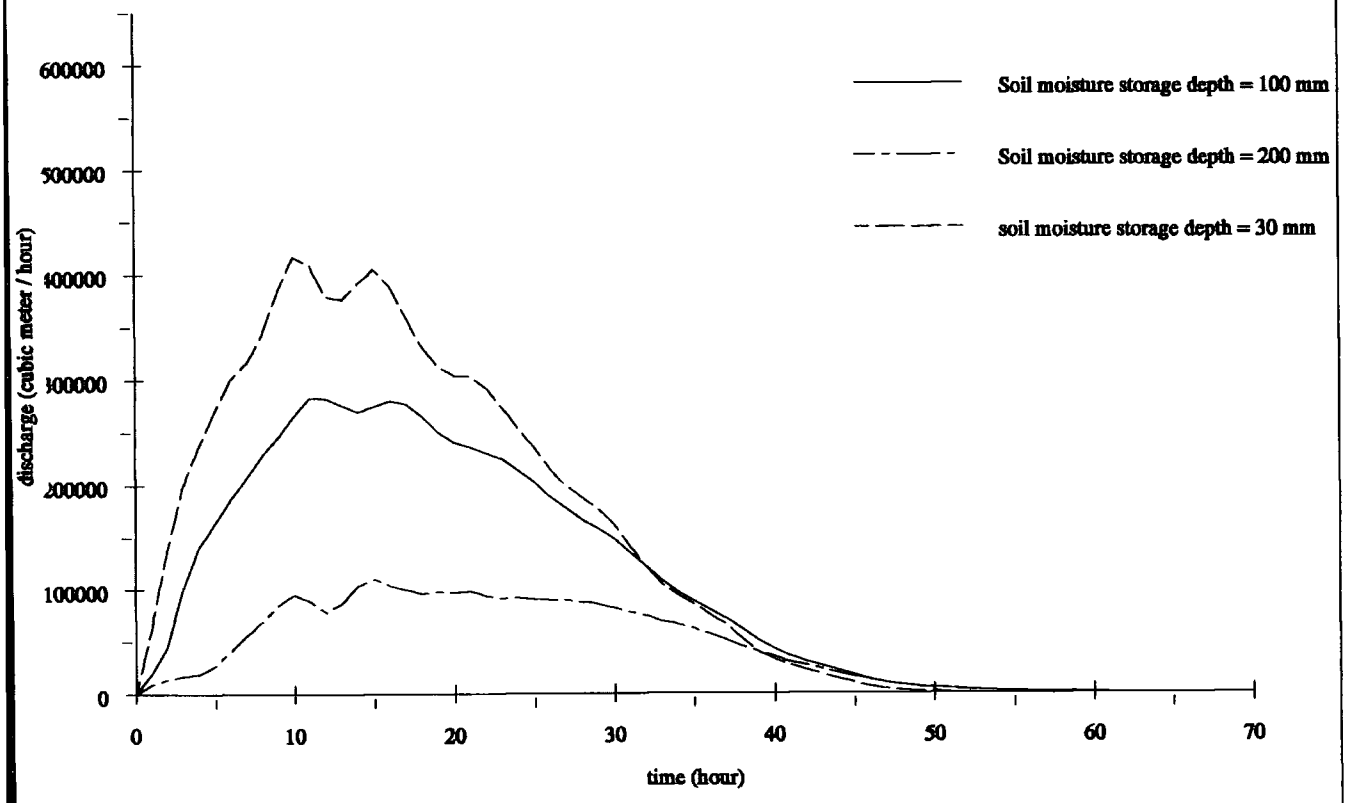

Figure (7 - 11) The influence of the soil water depth on the discharge

7.3.4 The influence of soil depth on the runoff hydrograph

In the model, the water holding capacity of the soil, expressed as depth in mm per 1 metre of soil profile, is the only parameter controlling infiltration. Since the rainfall excess is generated as infiltration excess, changes in the soil depth will directly affect the runoff generation produced in the watershed area, which results in changes of the shape of the output hydrograph.

To examine the influence of soil depth on the watershed hydrograph, soil depths of 3, 10, and 20 cm have been selected. Figure (7-11) shows the hydrographs corresponding to the three soil depths. The relationships between the flow peaks and flow volumes for the three soil depths appear to be approximately linear (figure 7-12). This result is expected since it derives directly from the linear structure of the runoff generation equations used in the model. However, it provides an indication of the functionality of the model.

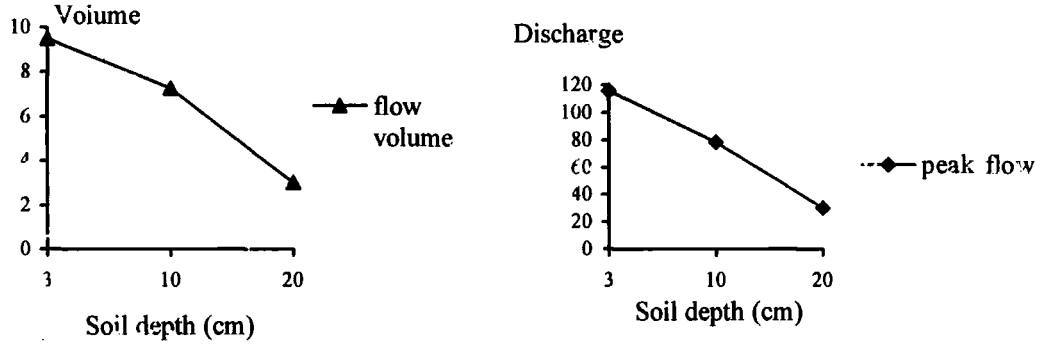

Figure (7-12) The influence of soil depth on the flow peak and flow volume

7.3.5 Analysis of the influence of rainfall distribution on the runoff hydrograph

This paragraph investigates the sensitivity of the watershed hydrological response to rainfall distribution. Due to the lack of adequate data on the spatial distribution of rainfall events in the area the approach used in this analysis is based on using the distribution of annual average rainfall as representative to events distribution. The test is carried out by

generating two hydrographs under two different patterns of rainfall distribution. For the first hydrograph, rainfall at station F1 is assumed to be uniformly distributed over the area. For the second hydrograph, the rainfall is assumed to be distributed according to Thiessen polygons. The polygons are weighted by the average annual rainfall in each polygon's area. The polygon corresponding to station F1 is given weight 1 and the other polygons' weights are adjusted accordingly (i.e. F4 = 1.62, F2 = F16 = H4 = 1, F13 = F17 = 0.93). Figure (7-14) shows the distribution of Thiessen polygons used and the rainfall weight of each polygon.

The assessment of the influence of the rainfall distribution is made by evaluating the effect on the hydrograph of the net change in rainfall resulting from the rainfall distribution. Since the rainfall of the uniform distribution has a weight of 1 over the whole area (the weight of station F1), the net change in rainfall for the variable distribution pattern can be calculated from the following table (table 7-6),

Table (7-6) Calculation of the net change in area rainfall for the variable rainfall distribution

Area	Rainfall weight	Area weight	Net change in rainfall	weighted rainfall change
1	1.62	0.06	+ 0.62	+0.0397
2	1.00	0.55	0.00	0.00
3	0.93	0.39	-0.07	-0.0273
Net change				+0.0124

The table shows that the distributed rainfall produces an increase of net rainfall over the watershed area. A 50-year return period storm distributed over 24 hourly steps is used for both rainfall distributions. Figure (7-13) shows the resulting hydrographs. The following table shows the amounts of flow peak and flow volume for both hydrographs (table 7-7). The hydrographs show that despite the net increase of rainfall within the watershed area, the hydrograph of the variable distribution of rainfall has a lower peak and volume.

Table (7-7) Peak flow and flow volume of the uniform and variable rainfall distribution hydrographs

Hydrograph type	Peak flow ($m^3 s^{-1}$)	Flow volume ($M m^3$)
Distributed rainfall	157	14.44
Uniform rainfall	172	15.00

The lower peak is mainly because the rainfall amount in the area closer to the watershed outlet has decreased. A slight influence of the increase of rainfall at area 1 appears near the end of the hydrograph.

The decrease in the volume of flow is mainly due to the influence of the distribution of rainfall over the watershed. Eventually, the net increase in the rainfall is attributed to the significant increase of rainfall in area 1, which is the farthest area from the outlet. Therefore, most of the increase of rainfall will be subject to high transmission losses and thus will not reach the outlet. On the other hand the rainfall of the variable distribution has decreased for the area closer to the outlet where the transmission losses are less important.

7.3.6 Analysis of the influence of flow velocity on the runoff hydrograph

In the previous application of the model the flow velocity has been considered constant for both the overland and channel flows. As discussed in section (7.2.2.1) the variable flow velocity depends on both the slope and the overland flow depth. Therefore, the overland flow velocity and consequently the isochrone areas change with overland flow depth. This is illustrated in the isochrone grids of different rainfall depths shown in figures (7-15) to (7-18). To investigate the effect of variable overland flow velocity on the output hydrograph, a 50-year return period storm hydrograph (figure 7-19), and a 25-year storm hydrograph are used (figure 7-20). The resulting hydrographs show that even for a 50-year return period storm the flow velocity is less than the assumed fixed flow velocity of

1 m s^{-1}.

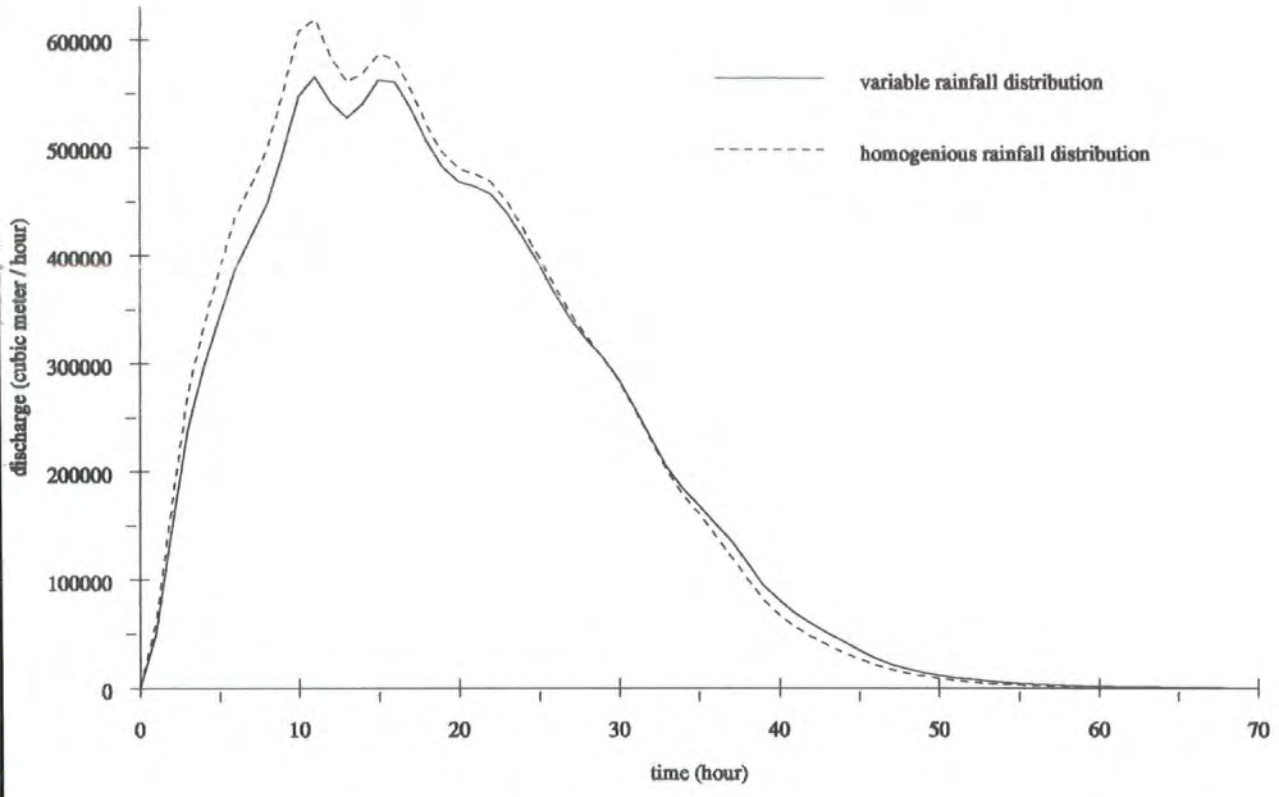

Figure (7 - 13) The effect of rainfall distribution on a 50-year return period storm hydrograph

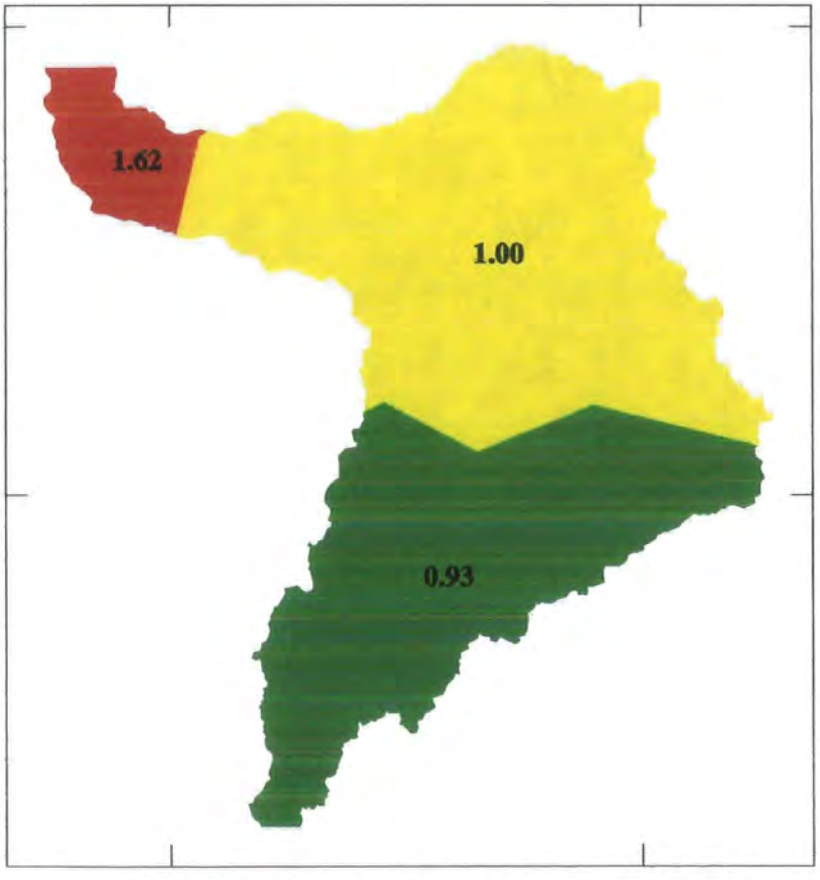

Figure (7 - 14) Area distribution of rainfall weighted according to the annual average

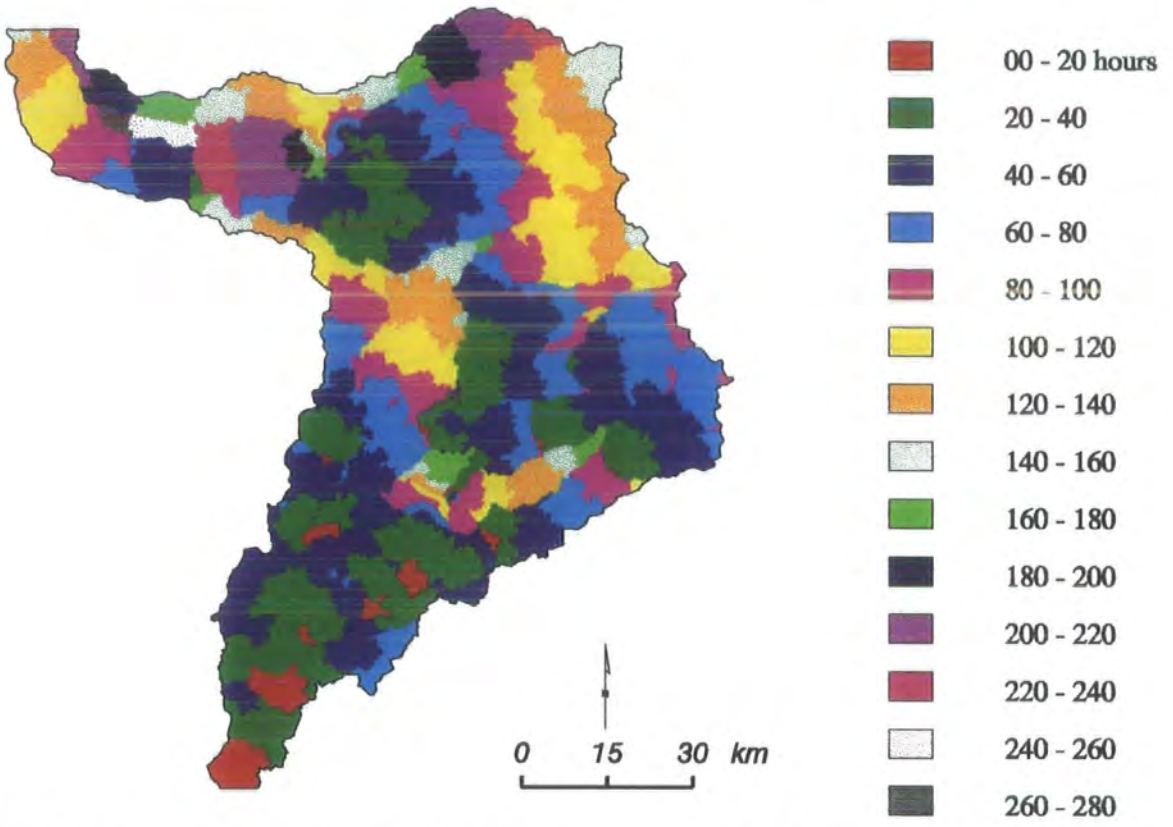

Figure (7 - 15) Time of concentration for 1 mm of rainfall excess with variable flow velocity

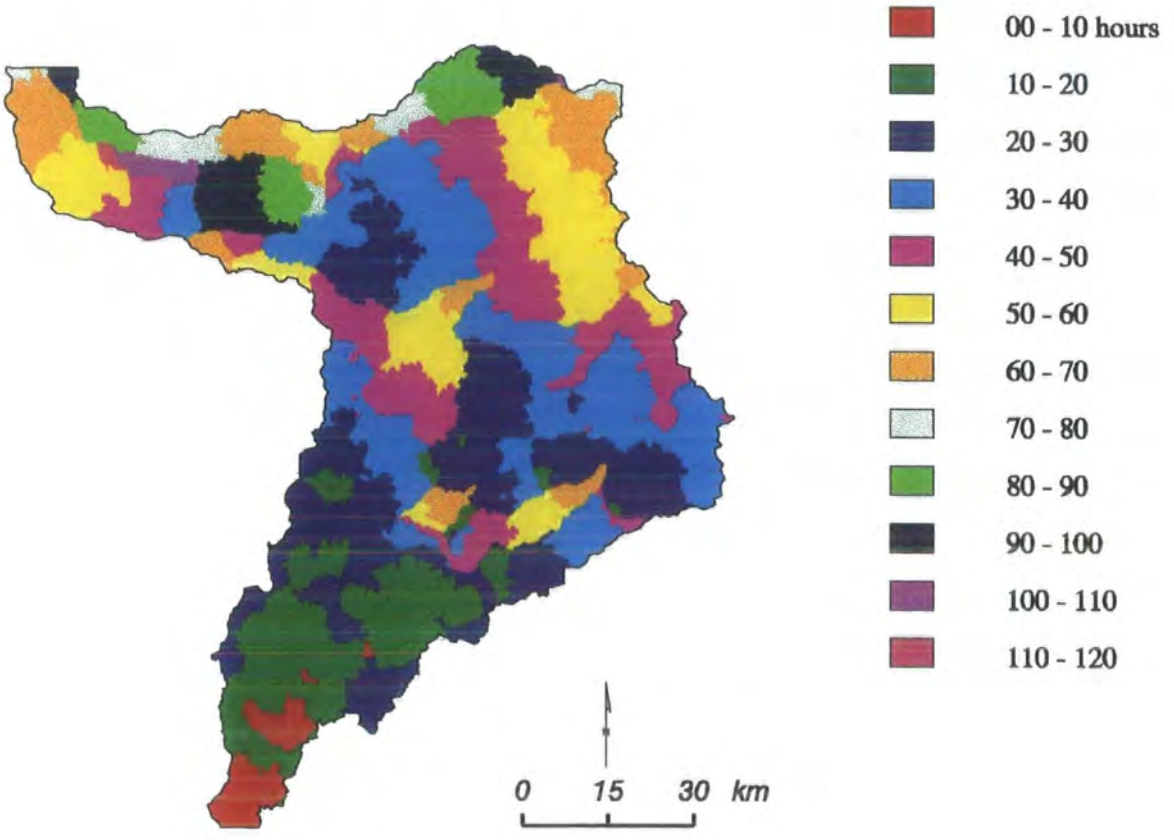

Figure (7 - 16) Time of concentration for 5 mm of rainfall excess with variable flow velocity

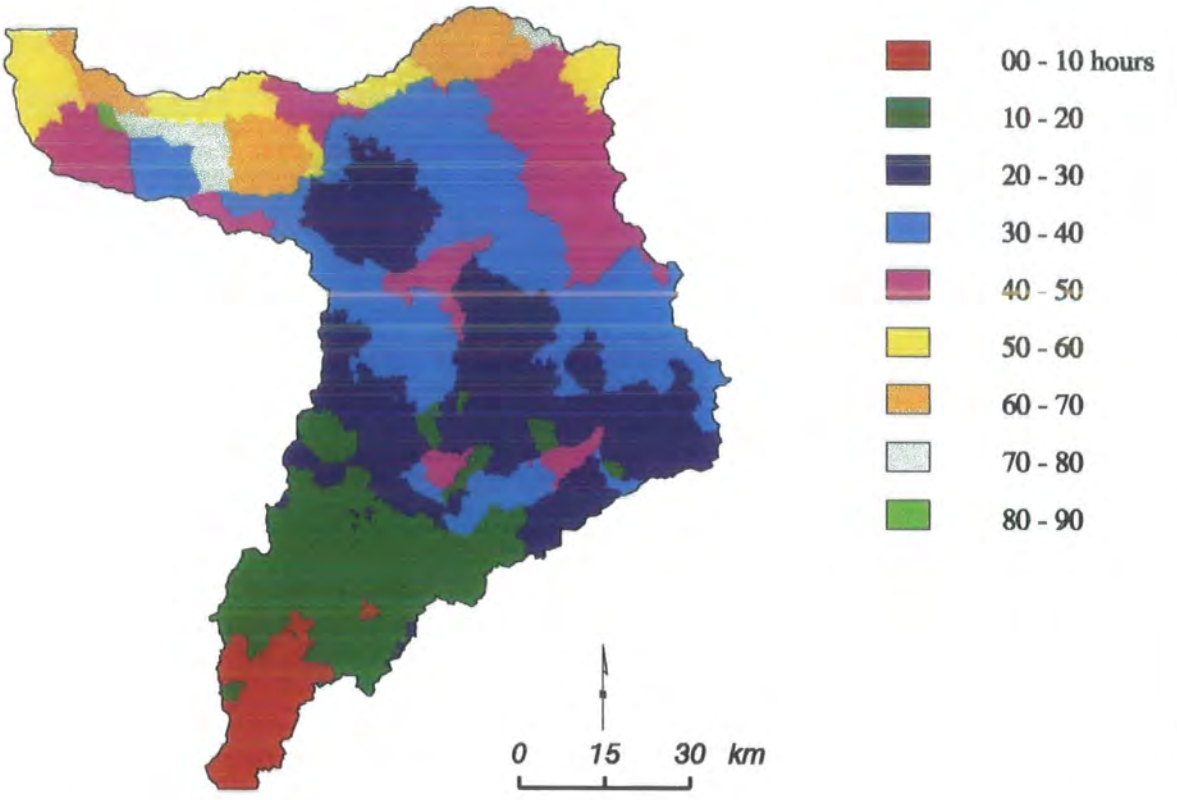

Figure (7 - 17) Time of concentration for 10 mm of rainfall excess with variable flow velocity

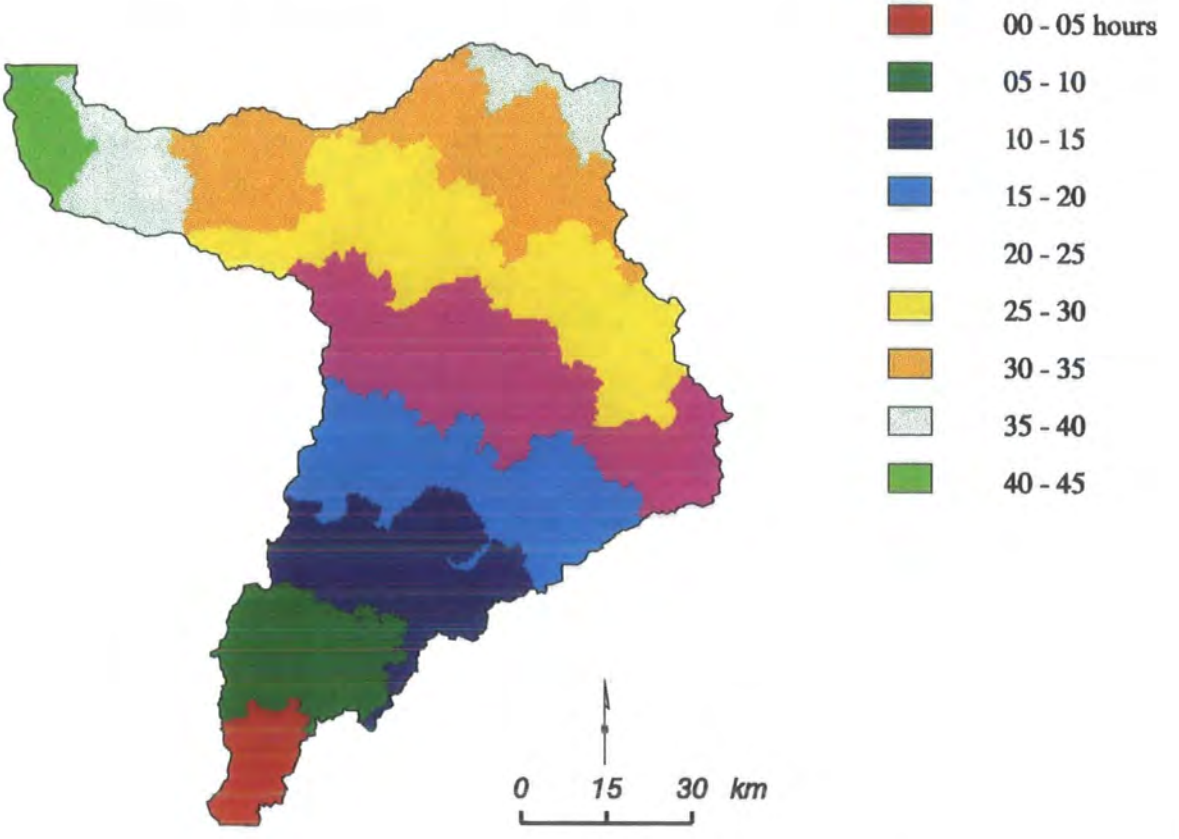

Figure (7 - 18) Time of concentration with fixed flow velocity

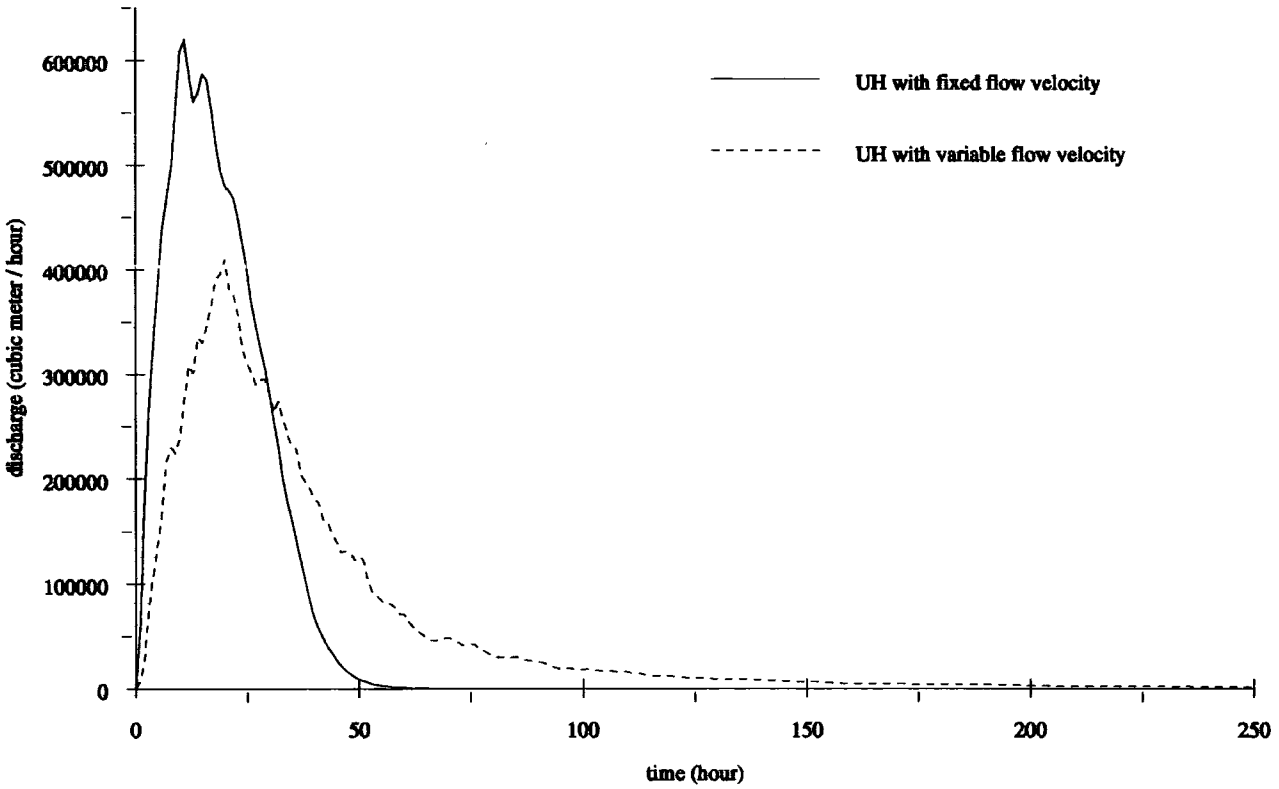

Figure (7 - 19) Comparison of the hydrographs at variable and fixed flow velocities for a 50-year return period storm

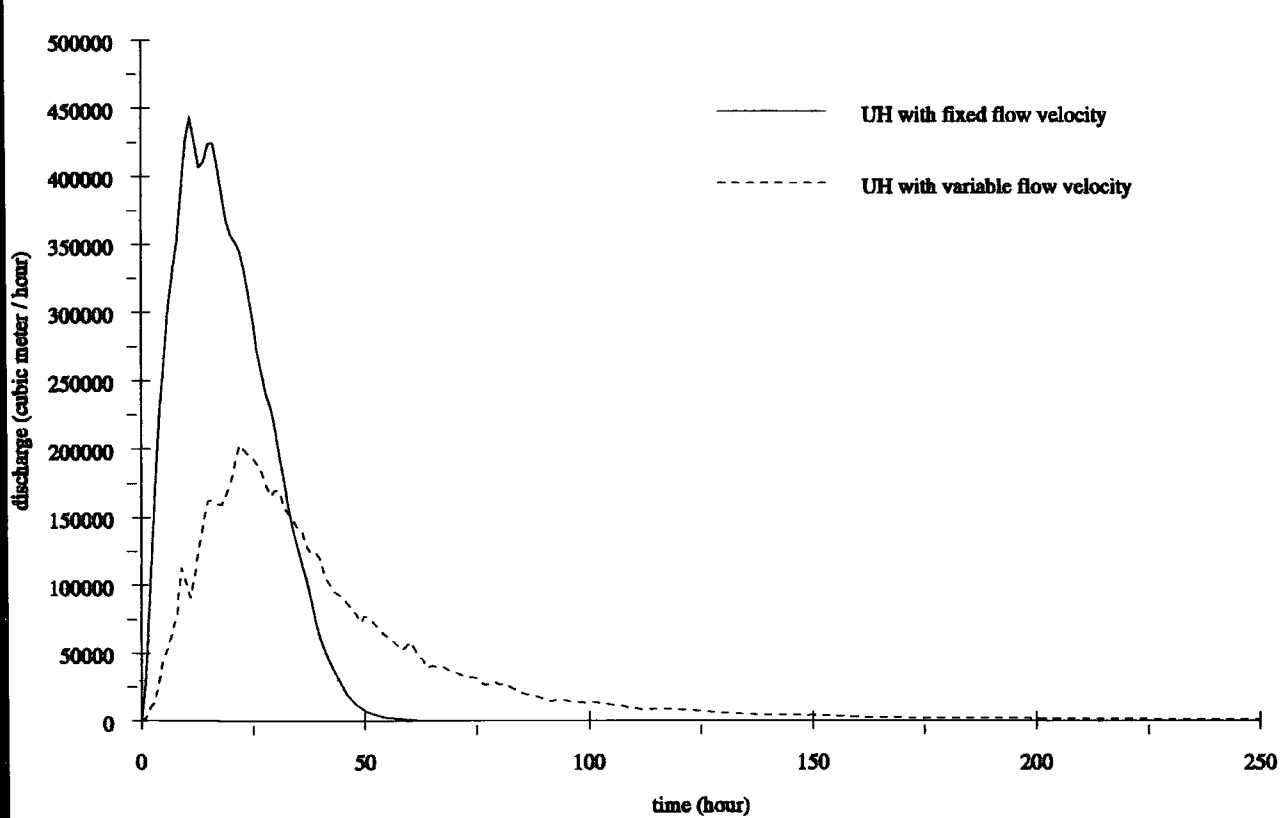

Figure (7 - 20) Comparison between the hydrographs at variable and fixed flow velocities for a 25-year return period storm

7.4 Summary

The computer form of the spatial model of Wadi Rajil consists of a program for calculating the rainfall excess amounts and a GIS procedure for routing the generated flows and deriving the hydrograph. The rainfall excess amounts are calculated by applying a sequence of abstractions to the input rainfall. The routing process is simulated as two separate grids representing the time of flow and discharge expected from each cell. The grid representing the time of flow is classified into isochrones according to the time step of the hydrograph. The total discharge of all the cells in each isochrone is computed. A spatial *combine* is performed to associate the total discharge of each isochrone to the time of concentration for that isochrone. This process results in a grid representing the hydrograph for one input time step. To generate the hydrograph for a given storm the hydrograph tables produced by the sequence of time-step rainfall amounts are convoluted using the database relate environment.

The performance of the model has been tested for simulated storms of different recurrence periods. The results show good correlation with a previous study on the area using local flood indexes. In addition, a unit hydrograph generated assuming no transmission losses has shown comparable fit with a unit hydrograph produced by the SCS synthetic method. Transmission losses have significant influence on the flow volume. The study also show that transmission losses from channel links of orders 1 and 2 are not very significant.

CHAPTER 8

CONCLUSIONS AND RECOMMENDATIONS

8.1 Conclusions

The main objective of the research has been to demonstrate GIS applications for surface water studies in the Jordan Badia region. Three typical GIS applications in hydrology have been presented. First, to build a digital elevation model and use it to extract hydrological information. Secondly, to develop a spatial database for surface hydrology. Thirdly, to build a distributed hydrological model using the database and GIS techniques. The major research findings relevant to each application are as follows.

8.1.1 Extracting hydrological information from the DEM

1. An accurate and sink free DEM is an essential requirement for extracting reliable hydrological features. The ARC/INFO TOPOGRID command provides a convenient interpolation method that is sensitive to surface drainage features. The command applies a drainage enforcement algorithm that attempts to open the flow path between the sinks by either filling the sinks to the level where the water flows out of it or clearing the saddle points that block the path. However, since the drainage enforcement process is controlled by tolerances set by the user, many sinks still exist in the DEM. These sinks need to be removed before attempting to use the DEM for extracting hydrological information.

Although the TOPOGRID command was originally designed to build DEMs from a relatively small but well selected number of points, its use with contour data has shown acceptable accuracy. An assessment of the absolute accuracy of the DEM using a large number of GPS field checked points has shown an average error of the same order as the error of the original contour data. This implies that no systematic error due to the interpolation method has been introduced.

2. One of the main research goals was to establish a channel drainage network that links the digitised drainage lines over the mud pan areas. The solution provided by the research has been to replace the topographic drainage network with a network extracted from the DEM. To maintain the density and locations of the topographic wadi lines, these lines were incorporated into the DEM by the drainage enforcement process performed by the TOPOGRID command. The drainage density of the extracted channel network for a number of threshold values was checked against the drainage density of the topographic wadis. The research has shown that a threshold value of 250 pixels produces a channel network of comparable drainage density.
3. Although the extracted network has the major advantage of connecting the drainage lines through the mud pan areas it presents two inconveniences. First, the relatively small threshold value may result in including very short links in the channel network. This has the effect of exaggerating the Strahler order of the links to which they join. Secondly, in the flat areas, two or more links may run parallel and very close to each other which results in having more than one link draining the same sub-watershed. Therefore, the extracted network needs to be manipulated to eliminate these links either manually or using GIS vector editing tools.

8.1.2 The database

1. The GIS was used to develop a database for storing, managing and analysing the relevant data. Both vector and raster data structures were used to represent the data layers in the database. The vector data structure is the most helpful for network analysis, the watershed query application, and overlay processes and in determination of the hydrologically similar units. On the other hand, the raster data structure is far more useful for the model simulation and computation.
2. The database layers are divided into two categories: basic layers, representing the original data sources and derived or processed layers produced to serve the GIS applications. The quality of the basic layers is controlled by the quality of the original data sources, while the quality of the derived layers is dependent on both their sources of information and the criteria used in their derivation. Generally, the layers based on the DEM including the channel drainage network, the slopes, the flow directions and sub-watersheds boundaries can be considered as reliable data. Other layers including the rainfall distribution, infiltration, and hydrological similar units are not fully validated.

8.1.3 The model

1. The raster data structure as well as the raster processing tools proved to be very useful in simulating the processes of a simplified distributed parameter hydrological model. The raster data structure enables performing a wide range of mathematical, logical, and combinatorial operators on any number of overlapping grid layers. This implies that complex model calculations can be carried out in a simple manner and at any resolution up to the cell level. On the other hand, efficient simulation of the routing process can be achieved using raster-processing functions. In this research the

following two raster functions have been extensively used to simulate the routing process,

1.1 The FLOWLENGTH function has been used to perform the convolution computations of the flow length and the time of concentration for each cell in the watershed area. The function can be used to carry out any sort of convolution along the direction of flow from each cell to the outlet.

1.2 The COMBINE function is very useful for the spatial merge of any number of grids. This function has been used to generate a hydrograph from the two grids of discharge and time of travel.

2. Since there are no discharge records are available, the model performance has been evaluated using simulated events. The model results were compared with the results of two empirical approaches using the same simulated events. Although there are significant differences between these results, the model calculations show good correlation with the results of one of the empirical approaches.

8.2 Recommendations

The database and the hydrological model presented in the research were developed using all the data that were available. If these applications are to be used for providing reliable and precise information the following recommendations are suggested:

1. Unless other more accurate and updated data are available, the basic layers need not be changed.
2. The watershed characteristics layers derived from the DEM need to be recreated if another DEM is used or if the cell size used in generating the DEM has to be changed.

3. The hydrological layers are dependent on certain assumptions. Therefore, these may need to be recreated if other assumptions prove to be more representative.
4. The hydrological model described in the research has not been tested against real or verified flow data. If this model is to be used for estimating the runoff of the watershed or any sub-watershed, calibration of the model results is required. The model performance can be verified either at the level of the individual hydrological processes involved, or as an overall rainfall-runoff model. It is suggested to test the model performance as a distributed model as part of the micro catchment studies proposed by Jolly (1996). On the other hand, the model can be calibrated as a rainfall-runoff model by selecting appropriate values, based on local data, for the model parameters of overland and channel flow velocities, soil depth, and transmission loss factor.

References

Abbott, M., Bathrust, J., Cunge, J., O'Connell, P. and Rasmussen, J. (1986a) An introduction to the European Hydrological System-Systeme Hydrologique Europeen, "SHE", 1 : history and philosophy of a physically-based, distributed modelling system. Journal of Hydrology, 87, 45-59.

Abbott, M., Bathrust, J., Cunge, J., O'Connell, P. and Rasmussen, J. (1986b) An introduction to the European Hydrological System-Systeme Hydrologique Europeen, "SHE", 2 : modelling system. Journal of Hydrology, 87, 61-77.

Abdulla, F. (1995) Regionalization of macroscale hydrological model. University of Washington, Department of Civil Engineering, Water Resources Series, technical report no. 144.

Abed, A. (1982) The geology of Jordan (*Arabic*). An-Nahda Al Islamiyyah Publications, Amman-Jordan.

Agrar und Hydrotechnik GMBH ESSEN. (1977) National water master plan of Jordan. Volume iii, surface water resources. Natural Resources Authority, Amman. 9-39.

Al-Homoud, A., Allison, R., El-Sallag, M., Khattari, S., Malkawi, O., Sunna, B., Tuffaha, S. and White, K. (1992) Geomorphology and physical resources. Report no. 1, JBRD, Amman-Jordan.

Ayed, R. (1996) Hydrological and hydrogeological study of the Azraq basin, Jordan. Unpublished PhD. Thesis, University of Baghdad. 37-85.

Ayyash, S. (1993) A development of water harvesting system at Safawi area in Northern Jordanian Badia. Unpublished M.Sc. Thesis, Jordan University of Science and Technology, Irbid.

Bathrust, J. (1986) Physically-based distributed modelling of an upland catchment using the Systeme Hydrologique Europeen. Journal of Hydrology, 87, 79-102.

Bedient, P., Huber, W. (1988) Hydrology and floodplain analysis. Addison-Wesley Publishing Company, Reading (Mass.).

Berndtsson, R. and Larson, M. (1987) Spatial variability of infiltration in a semi-arid environment. Journal of Hydrology, 90, 117-133.

Beven, K., Quinn, P.,Romanowicz, R., Freer, J., Fisher, J. and Lamb, R. (1995) Topmodel and Gridtab. 2nd Edition. CRES technical report, Lancaster University.

Burrough, P. (1990) Principles of Geographical Information Systems for land resources management. Clarendon press, Oxford.

Chairat, S. and Delleur, J. (1993) Integrating a physically based hydrological model with GRASS. In : *Applications of GIS in hydrology and water resources* (edited by Kovar, K. and Nachtnebel, H.) Proceedings of Vienna conf., April 1993. IAHS publ. no. 211. 127-140.

Christiaan, E. (1979) Water resources in the Arab Middle East and North Africa. Middle East and North African Studies Press. 6-7, 30-31.

Cooke, R., Warren, A. and Goudie, A. (1993) Desert geomorphology. UCL press limited, London.

Date, C. J. (1995) An introduction to database systems. Addison-Wesley Publishing Inc., Reading (Mass.).

Drayton, R., Wilde, B. and Harris, J. (1993) Geographical Information System approach to distributed modelling. In : *Terrain analysis and distributed modelling in hydrology* (edited by Beven, K. and Moore, I.). John Wiley & Sons, Chichester.193-199.

Environmental Systems Research Institute (1992) Understanding GIS, the ARC/INFO method. ESRI, California.

Environmental Systems Research Institute. (1996) Cell-based modelling with GRID. ESRI, California.

ERDAS. (1995) Field guide. 3rd edition. USA.

Farquharson, F., Meigh, J. and Sutcliffe, J. (1992) Regional flood frequency analysis in arid and semi arid areas. Journal of Hydrology, 138, 487-501.

Foth, H. (1984) Fundamentals of soil science. 7th edition. John Wiley & Sons, New York.

Francis, D. (1995) The creation of a digital elevation model of the Badia region of Jordan and the extraction of geomorphological information. Unpublished M.Sc. Thesis, University of Durham.

Furst, J, Girstmair, G. and Nachtnebel, H. (1993) Applications of GIS in decision support systems for groundwater management. In : *Applications of GIS in hydrology and water resources* (edited by Kovar, K. and Nachtenebel, H.) Proceedings of Vienna conf., April 1993. IAHS publ. no. 211. 13-21.

Grayson, R., Bioshl, G., Barling, R. and Moore, I. (1993) Process, scale and constraints to hydrological modelling in GIS. In : *Applications of GIS in hydrology and water resources* (edited by Kovar, K. and Nachtenebel, H.) Proceedings of Vienna conf., April 1993. IAHS publ. no. 211. 83-92.

Hunting Technical Services and Soil Survey and Land Research Centre. (1993) National soil map and land use project, the soil of Jordan. Volume 1. Ministry of Agriculture, Jordan.

Hutchinson, M. (1989) A new procedure for gridding elevation and stream line data with automatic removal of spurious pits. Journal of Hydrology, 106, 211-232.

Hydrosult Inc. (1990) Desert Dams. CIDA and Ministry of Water and Irrigation, Jordan.

Jolly, T. (1996) Surface water monitoring programme. Report to the Jordan Badia Research and Development Programme.

Jordan Badia Research and Development Programme (1995) Priority research themes and topics, 1996-1998 and beyond. JBRD, Amman-Jordan.

Jordan, P. (1977) Streamflow transmission losses in Western Kansas. Journal of Hydraulics Division, 103(8), 905-919.

Kemp, K. (1993) Environmental modelling and GIS : dealing with spatial continuity. In : *Applications of GIS in hydrology and water resources* (edited by Kovar, K. and Nachtenebel, H.) Proceedings of Vienna conf., April 1993. IAHS publ. no. 211. 107-115.

Maidment, D. (1993) Developing a spatially distributed unit hydrograph by using GIS. In : *Applications of GIS in hydrology and water resources* (edited by Kovar, K. and Nachtenebel, H.) Proceedings of Vienna conf., April 1993. IAHS publ. no. 211. 181-192.

Maidment, D. (1996) GIS and hydrologic modeling-an assessment of progress. *Internet : http://www.ce.utexas.ed...1/maidment/santafe.html.*

Manley, R. (1977) The soil moisture component of mathematical catchment simulation models. Journal of Hydrology, 35, 341-356.

Moore, I., Grayson, R. and Ladson, A. (1993) Digital terrain modelling: a review of hydrological, geomorphological and biological applications. In : *Terrain analysis and distributed modelling in hydrology* (edited by Beven, K. and Moore, I.). John Wiley & Sons, Chichester.7-30.

Morin, J. and Benyamini, Y. (1977) Rainfall infiltration into bare soils. Water Resources Research, Vol 13, No. 5, 813-817.

NIC, DLS and RJGC. (1997) National geographic information data dictionary. Release 1. *Internet : http://www.nic.gov.jo/geography/dictionary/contents.htm.*

Noble, P. (1994) Quantification of recharge to the Azraq Basin, North-East Badia, Jordan. Unpublished M.Sc. Thesis, University College London.

Olivera, F. and Maidment, D. (1996) Runoff computation using spatially distributed terrain parameters. *Internet : http://ciil.ce.utexas...dro/olivera/ASCECA1.HTM.*

Porter, J. and McMahon, T. (1971) A model for the simulation of streamflow data from climatic records. Journal of Hydrology, 13, 297-324.

Quinn, P., Beven, K., Chevallier, P. and Planchon, O. (1993) The prediction of hillslope flow paths for distributed hydrological modelling using digital terrain models. In : *Terrain analysis and distributed modelling in hydrology* (edited by Beven, K. and Moore, I.). John Wiley & Sons, Chichester. 63-83.

Raudkivi, A. (1979) An advanced introduction to hydrological processes and modelling. Pergamon Press, New York.

Sa'ad, A. (1986) Rainfall intensity-duration-frequency in Jordan. Water Authority, Professional paper No. 3.

Schaffer, U. (1995) Landsat Thematic Mapper imagery, the Cenozoic volcanic field of Jordan and Syria. Training course on using remote sensing data and GIS techniques in hydrology and hydrogeology, Amman-Jordan.

Schultz, G. (1993) Applications of GIS and remote sensing in hydrology. In : *Applications of GIS in hydrology and water resources* (edited by Kovar, K. and Nachtnebel, H.) Proceedings of Vienna conf., April 1993. IAHS publ. no. 211. 127-140.

Sharma, M., Gander, G. and Hunt, C. (1980) Spatial variability of infiltration in a watershed. Jounal of Hydrology, 45, 101-122.

Shaw, E. (1988) Hydrology in practice. 2nd edition. Van Nostrand Reinhold, UK.

Tarboton, D., Bras, L. and Rodriguez-Iturbe, I. (1993) On the extraction of channel networks from digital elevation data. In : *Terrain analysis and distributed modelling in hydrology* (edited by Beven, K. and Moore, I.). John Wiley & Sons, Chichester. 85-104.

Vann, J. (1971) A geography of landforms. W.M.C. Brown company, USA.

Viessman, W., Lewis, L. and Knapp, J. (1989) Introduction to hydrology. Harper Collins Publishers, New York.

Walters, M. (1990) Transmission losses in arid regions. Journal of Hydraulic Engineering, 116(1), 129-138.

Wanielista, M. (1990) Hydrology and water quality control. John Wiley & Sons, New York.

Warburton, J. (1997) Rapid assessment of surface water infiltration characteristics in the Northern Badia, Jordan. Department of Geography, University of Durham.

Wheater, H., Butler, A., Stewart, E. and Hamilton, G. (1991) A multivariate spatial-temporal model of rainfall in south west Saudi Arabia. I. Spatial rainfall characteristics and model formulation. Journal of Hydrology, 125, 175-199.

Wheater, H., Jolly, T. and Peach, D. (1995) A water resources simulation model for groundwater recharge studies : an application to Wadi Ghulaji, Sultanat of Oman. In : *Proceedings of the Sultanat of Oman international conference on water resources management in arid countries*, Mascat, March 1995.

White, K. (1996) Spectral reflectance characteristics of basalt surfaces, Eastern Badia of Jordan. In : *Remote sensing science and industry*. (edited by Donoghue, D. and Zong, Y.). Proceedings of the 22nd annual conf. of the Remote Sensing Society, University of Durham, September 1996.53-60

APPENDIX 1

The unitless hydrograph

(Source : Wanielista, 1990)

T / T_p	Q / Q_p
0.0	0.000
0.1	0.015
0.2	0.075
0.3	0.160
0.4	0.280
0.5	0.430
0.6	0.600
0.7	0.770
0.8	0.890
0.9	0.970
1.0	1.000
1.1	0.980
1.2	0.920
1.3	0.840
1.4	0.750
1.5	0.660
1.6	0.560
1.8	0.420
2.0	0.320
2.2	0.240
2.4	0.180
2.6	0.130
2.8	0.090
3.0	0.075
3.5	0.036
4.0	0.018
4.5	0.009
5.0	0.004

APPENDIX 2

Absolute accuracy test of the Digital Elevation Model of wadi Rajil

GPS height (m)	GPS - 20 metres	DEM height (m)	GPS - DEM
1114.5	1094.5	1094.8	-0.3
975.5	955.5	946.6	8.9
778.4	758.4	760	-1.6
761.8	741.8	747.6	-5.8
734.6	714.6	717.7	-3.1
736.6	716.6	722.2	-5.6
799.8	779.8	778.5	1.3
645	625	625.4	-0.4
827.1	807.1	802.7	4.4
784.8	764.8	765	-0.2
740.7	720.7	719.6	1.1
786.9	766.9	764.4	2.5
663.4	643.4	648.4	-5
721.1	701.1	701	0.1
650.5	630.5	629.3	1.2
650	630	629	1
652.9	632.9	636	-3.1
612.6	592.6	591.2	1.4
615	595	593.4	1.6
640.9	620.9	625.8	-4.9
942.7	922.7	921	1.7
972.9	952.9	951.6	1.3

The mean error = 0.16 m

Standard deviation = 3.5 m

APPENDIX 3

Attribute tables for the topographic layers

(Source : NIC, 1997)

Content

Contour

NAME	Contour		
TYPE	Line		
DATABASE	Topography		
DESCRIPTION	This layer contains contour lines		
USAGE	This layer represents the altimetric contour lines to be used in map production and the creation of digital terrain models and TIN's . These digital terrain models are used for terrain analysis and modelling.		
SOURCE	1. Digitizing the hard copy maps larger than 1/50000 scale		
	2. Direct survey		
	3. Photogrammetry		
	4. Remote sensing		
IMPORTANT ITEMS	Name	Description	Definition
	ID	Identification Number	Integer
	Elevation	Elevation Value in meter	Real
	Type	Type code	Integer
ANNOTATION	Elevation value for Index contours only		
LOOKUP TABLE	Type 1. Index 1. Normal 3. Supplementary		
SPECIAL CONSIDERATION	None		
KNOWN REDUNDANCY	None		
HIERARCHY	Not applicable		
HISTORY	There is no geometric history kept for this layer		
OWNER	RJGC		
UPDATE RIGHTS	RJGC		

Spot Height

NAME	Spot		
TYPE	Points		
DATABASE	Topography		
DESCRIPTION	This layer contains spot heights		
USAGE	This layer represents the altimetric points to be used in map production and the creation of digital terrain models and TIN's. These digital terrain models are used for terrain analysis and modelling.		
SOURCE	1. Digitizing the hard copy maps larger than 1/50000 scale 2. Direct survey		
IMPORTANT ITEMS	Name	Description	Definition
	ID	Identification Category Number	Integer
ANNOTATION	None		
LOOKUP TABLE	None		
SPECIAL CONSIDERATION	None		
KNOWN REDUNDANCY	None		
HIERARCHY	Not applicable		
HISTORY	There is no geometric history kept for this layer		
OWNER	RJGC		
UPDATE RIGHTS	RJGC		

Hydrography

NAME	HYDRO-LI		
TYPE	Line		
DATABASE	Thematic		
DESCRIPTION	This layer contains all natural and man made hydrographic features		
USAGE	This layer represents the base map for all hydrographic features and their attributes and used for water analysis and harvesting		
SOURCE	RJGC & Ministry of Water and Irrigation		
IMPORTANT ITEMS	Name	Description	Definition
	ID	Line-Id	Integer
	Name	Name	Character
	Type	Type code	Integer
	Use	Use code (General use)	Integer
	Volume	Flow volume (M3/hour)	Integer
	Date	Last maintenance date	Date
ANNOTATION	None		
LOOKUP TABLE	Type		
	1. Perennial		
	2. None Perennial (intermittent)		
	3. Canal		
	4. Limit of dam		
	5. Break water		
	6. Seawall		
	7. Rock		
	8. Coastline		
	9. Dam		
	10. Ditch		
	11 Levee		
	12. Wadi large outline		
	13. Wadi small centerline		
	99. Others		
	Use		
	1. Navigable		
	2. None Navigable		
	3. Abandoned		
	99. Others		

APPENDIX 4

Contingency table for the classified basalt formations

	Reference data			
Classified data	MOB	URC	AOB	FA2
MOB	2169	0	555	804
URC	0	1545	2660	0
AOB	79	0	2989	64
FA2	350	0	390	1331
AI	110	1	1325	26
AT	0	5	919	0
HAB	153	0	478	200
UM	7	0	350	173
UB	42	0	754	517
WMF	32	0	178	269
HN	4	0	476	14
SN	0	0	262	3
AZRAQ	186	1	1965	166
M	79	0	206	218
FA3	0	0	133	0
Alluvium	0	0	434	16
Farms	0	1	310	2
Column total	3211	1553	14384	3803

	Reference data			
Classified data	AI	AT	HAB	UM
MOB	32	0	203	6
URC	3	2	0	0
AOB	192	12	7	18
FA2	26	0	121	95
AI	1048	6	49	24
AT	3	946	3	11
HAB	61	0	127	59
UM	1	0	48	685
UB	2	4	43	262
WMF	2	0	75	426
HN	54	50	39	65
SN	0	34	0	330
AZRAQ	1	0	19	0
M	4	0	47	19
FA3	0	0	0	7
Alluvium	0	0	0	0
Farms	0	0	5	0
Column total	1429	1054	786	2007

	Reference data			
Classified data	UB	WMF	HN	SN
MOB	80	1	0	0
URC	0	0	0	0
AOB	52	2	16	47
FA2	78	25	0	0
AI	2	2	6	0
AT	0	0	87	29
HAB	23	26	5	0
UM	77	78	77	89
UB	626	10	666	116
WMF	38	520	1	0
HN	48	0	304	97
SN	88	0	133	2298
AZRAQ	0	0	0	0
M	1	4	0	0
FA3	18	0	2	357
Alluvium	1	0	0	0
Farms	1	0	1	0
Column total	1133	650	1298	3033

	Reference data			
Classified data	Azraq	M	FA3	Alluvium
MOB	157	21	0	0
URC	0	0	1	0
AOB	0	0	1	0
FA2	30	25	0	0
AI	0	0	0	0
AT	0	0	17	0
HAB	18	21	0	0
UM	0	4	3	2
UB	0	0	8	0
WMF	0	8	0	0
HN	0	0	3	0
SN	0	0	110	0
AZRAQ	1251	39	0	9
M	59	761	0	30
FA3	0	0	1342	0
Alluvium	26	43	0	407
Farms	0	0	0	0
Column total	1541	922	1485	448

	Reference data	
Classified data	Farms	Row total
MOB	0	4028
URC	0	4211
AOB	0	3479
FA2	0	2471
AI	0	2599
AT	0	2020
HAB	1	1172
UM	0	1594
UB	0	3050
WMF	0	1531
HN	0	1154
SN	0	3258
AZRAQ	0	3637
M	0	1428
FA3	0	1859
Alluvium	0	927
Farms	463	783
Column total	464	39201

APPENDIX 5

Soil layer attributes

(Source : Hunting, 1993)

Contents

SOIL PROFILE DESCRIPTION

INFORMATION ON THE SITE :

Profile No.: PS093

Series / Phase:		Had 5 / Gravelly
Soil Mapping Unit:		Level I:DUR (115)
Soil Classification:	USDA (1990):	Loamy-skeletal, mixed, hyperthermic Family of Typic Torrifluvents (KDDJ)
	ACSAD:	NFR t 2 a: Typic Torrifluvent
	FAO/UNESCO:	FL : Fluvisol
Author:		Suleiman Sawalha
Date of examination:		15/01/92
Location:		In Rijlat Mushawwah
Sample Area No.:		
Map sheet:		1:25000: 3550-IV-NE - 1:100000: 3550 - 1:250000: Beer
Coordinates:	Geographical:	37.63602 E/ 30.49971 N
	JTM:	561048 E/ 375056 N
Elevation:		668 m asl
Landform:	Position:	Wadi floor
	Land System:	13/9 (Ephemeral wadis draining to wadi Sirhan) -- 13.9.0 [GIS]
	Land Facet:	1 (Major wadis)
Microrelief:	Class:	Even (< 25 cm)
	Type:	Gullies
Slope:		Almost flat (1 %), concave to NE
Land Use:		3.3 Nat.grazing
Plant/Crop:		Kidad (20), Faras (20), Ajaram (20): 30 % groundcover
Climate:	Mean annual precipitation:	
	Mean annual temperature:	Air: 20.5° C / Soil (50cm): 23.4° C
	Soil moisture regime:	Aridic
	Precipitation zone:	0-50 mm p.a.
	Nearest raingauge:	Bayir (J 1)
Administrative unit/village:		(Ma'an Governorate)

GENERAL INFORMATION ON THE SOIL :

Geology:	Sedimentary chemic./organ. : Chert [tt2 LSt w/cherts,marls (Bender 1968)]
Parent Material:	Alluvium (fine-loamy texture)
Drainage: Surface Runoff:	Slow
Soil Drainage Class:	Well
Surface Cover:	Gravel (30 %)
Surface Feature:	Capping (30 %)
Soil Surface Conditions:	Dry / Hard
Erosion:	Moderate gully erosion
Soil Depth:	100 cm (Gravel/stones)
Diagnostic Horizon or Property:	-

PROFILE DESCRIPTION :

0 - 17 cm Reddish yellow (5YR 6/6) dry and yellowish red (5YR 5/6) moist; very gravelly sandy loam; weak medium subangular blocky breaking to weak fine subangular blocky ; dry slightly hard; moist very friable; non-sticky; non-plastic; common very fine (<0.5 mm) tubular pores; few very fine (<1 mm) fibrous roots; 50 % sub-rounded chert fine gravel (2-5 mm); moderate reaction to HCl; clear wavy boundary to:

17 - 28 cm Yellowish red (5YR 5/6) dry and yellowish red (5YR 4/8) moist; very gravelly sandy clayloam; weak medium subangular blocky breaking to weak fine subangular blocky ; dry moderately hard; moist friable; slightly sticky; non-plastic; common very fine (<0.5 mm) tubular pores; few very fine (<1 mm) fibrous roots; 45 % sub-rounded chert fine gravel (2-5 mm); moderate reaction to HCl; clear wavy boundary to:

28 - 43 cm Reddish yellow (5YR 6/6) dry and yellowish red (5YR 5/6) moist; extremely gravelly sandy loam; massive; dry soft; moist loose; slightly sticky; non-plastic; common very fine (<0.5 mm) tubular pores; 75 % sub-rounded chert gravel (5-20 mm); moderate reaction to HCl; clear smooth boundary to:

43 - 53 cm Reddish yellow (5YR 6/6) dry and yellowish red (5YR 5/6) moist; very gravelly sandy clayloam; weak medium subangular blocky breaking to weak fine subangular blocky ; dry slightly hard; moist very friable; slightly sticky; non-plastic; common very fine (<0.5 mm) tubular pores; few very fine (<1 mm) fibrous roots; 40 % sub-rounded chert fine gravel (2-5 mm); moderate reaction to HCl; clear smooth boundary to:

53 - 100 cm Yellowish red (5YR 5/6) dry and yellowish red (5YR 4/8) moist; extremely gravelly sandy loam; massive; dry soft; moist loose; slightly sticky; non-plastic; many very fine (<0.5 mm) tubular pores; 80 % sub-rounded chert coarse gravel (20-75 mm); moderate reaction to HCl.

100+ cm Gravel/stones

Note: Analytical analyses are available for horizons: 1 / 2 / 3 / 4
Outprint of JOSCIS - National Soil Map Project, SSLRC/HTS/MoA, Jordan (11/07/93)

PROFILE No: PS093 (1.analysis)

LAB No.	DEPTH	SAND	SILT	CLAY	SAND				GRA VEL	TXT.	PSC	BD	POR	PERM
					Coa-rse	Med	Fine	Very fine						
	cm	<-- 3A3 --> <-- % of < 2 mm -->							%	3A3	3A3	4A3a g/cm3		
175	0- 17	66.2	26.0	8.8	7.2	4.6	18.8	35.6		vfSL	M			
176	17- 28	69.8	17.2	13.0	17.3	13.2	22.0	17.3		SL	M			
177	28- 43	72.0	15.9	12.1	37.7	12.4	12.6	9.3		cSL	M			
178	43- 53	63.5	22.2	14.8	18.7	9.8	17.8	17.2		fSL	M			

DEPTH	MOISTURE 10 kPa	33 kPa	1500 kPa	pH Paste	EXTRACTABLE BASES Ca	Mg	Na	K	CEC	CEC/ clay	Na exch	ESP	ECe	SAT
cm				8C1	<-- 5B5a --> <-- meq / 100 g -->				5A10a	8A1a rat	8D1 meq/100g	5B6b	5D1b mS/cm	8A %
0- 17				8.0			0.3		3.4	0.38			1.6	21.6
17- 28				7.9			0.2		4.5	0.35			0.5	27.0
28- 43				8.0			0.2		4.1	0.34			0.6	22.1
43- 53				7.6			0.2		4.9	0.33			0.5	32.4

DEPTH	Ca CO3 tot	GYP-SUM	GYPS REQU	SOLUBLE CATIONS Ca	Mg	Na	K	SOLUBLE ANIONS Cl	SO4	CO3	HCO3	NO3
cm	6E1a %	6F1d %	6F5 t/ha	6N1b <-- meq / l -->	6O1b	6P1a	6Q1a	6K1d -->	6L1d	6I1a	6J1a	6N1a ppm
0- 17	37.5	1.7		4.5	1.8		0.6	6.6	7.0		2.4	33
17- 28	32.0	1.7		1.9	0.8		0.2	1.5	0.9		2.2	10
28- 43	42.0	2.1		1.8	0.8		0.2	2.7	1.5		2.0	7
43- 53	37.0	2.2		1.4	0.3		0.1	1.8	1.5		1.8	13

DEPTH	SALT tot	SAR	P total	P avail	N total	Org.C total	C/N	OM	MICRONUTRIENTS Cu	Zn	Fe	Mn	B
cm	8D5 %	5E	6S1a ppm	6S2 ppm	6B1a %	6A1d %		%	<-- ppm -->				
0- 17			1675	4.40	0.023	0.14	6.1	0.24					
17- 28													
28- 43													
43- 53													

APPENDIX 6

The continuity and momentum equations (source: Bedient and Huber, 1988)

1. Continuity equation

The general form of the continuity equation can be described as;

Inflow - Outflow = rate of change of storage

For a river element as shown in figure 1 below, the continuity equation is given by the following formula;

$$(Q - \frac{\partial Q}{\partial x}\frac{\Delta x}{2}dt + q\Delta x\Delta t) - (Q + \frac{\partial Q}{\partial x}\frac{\Delta x}{2}dt) = \frac{\partial A}{\partial t}\Delta x\Delta t$$

where

Q : discharge (m^3/s),
A : cross sectional area (m^2),
q : rate of lateral flow per unit length of channel

For a unit width the continuity equation becomes;

$$y\frac{\partial v}{\partial x} + v\frac{\partial y}{\partial x} + \frac{\partial y}{\partial t} = q$$

where v is the average flow velocity.

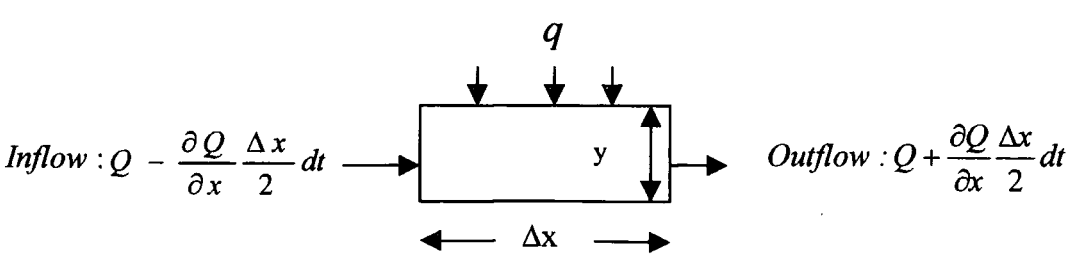

Figure 1

2. Momentum equation

The rate of change of momentum on a body is given by Newton's second low of motion as;

$$F = \frac{d}{dt}(mv)$$

where F is the resultant of all external forces acting on the body.

Forces acting on an element of length Δx of a river are as follows (figure 2);

- Hydrotstatic force F_p:

$$F_p = F_1 - F_2 = -\rho g \frac{\partial(\bar{y}A)}{\partial x}\Delta x$$

-Gravitational force F_g:

$$F_g = \rho g A S \Delta x$$

--Frictional force F_f:

$$F_f = \rho g A S_f \Delta x$$

where

$\bar{y}$: distance from the water surface to the centroid of pressure prism,

S : bed slope,

S_f : friction slope.

The rate of change of momentum is given by the following equation;

$$\frac{d(mv)}{dt} = m(\frac{dv}{dt}) + v\frac{dm}{dt}$$

$$= \rho A \Delta x(\frac{\partial v}{\partial t} + v\frac{\partial v}{\partial x}) + \rho q v \Delta x$$

Equating this to the sum of external forces results in the following general form of momentum equation;

$$\frac{\partial v}{\partial t} + v\frac{\partial v}{\partial x} + \frac{g}{A}\frac{\partial(\bar{y}A)}{\partial x} + \frac{vq}{A} = g(S - S_f)$$

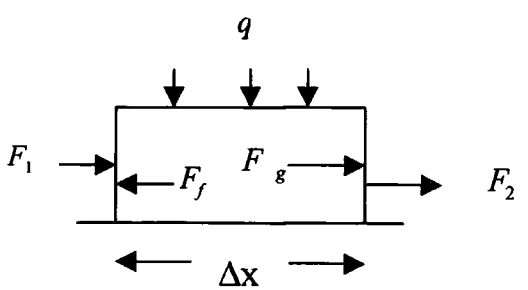

Figure 2